Development of novel polymeric materials for gene therapy and pH-sensitive drug delivery: modeling, synthesis, characterization, and analysis.

by

Brian Curtis Anderson

A dissertation submitted to the graduate faculty

in partial fulfillment of the requirements for the degree of

DOCTOR OF PHILOSOPHY

Major: Chemical Engineering

Program of Study Committee:
Surya K. Mallapragada, Major Professor
Valerie V. Sheares
Balaji Narasimhan
R. Dennis Vigil
Max D. Morris
Nita K. Pandit

Iowa State University

Ames, Iowa

2002

Graduate College
Iowa State University

This is to certify that the doctoral dissertation of

Brian Curtis Anderson

has met the dissertation requirements of Iowa State University

_____
Major Professor

_____
For the Major Program

TABLE OF CONTENTS

1

CHAPTER 1. Introduction

1.1 Organization

By definition, research is the investigation of the unknown. Usually this involves a goal, an end that is desired, although the verdict of this end is not known. This quest for something that has not been proven or even discovered is the beauty of research, especially in a university setting. Along with any unknown are twists and turns that were not anticipated. Some of these turns result in setbacks or disappointments, but some open up doors that no one knew existed. By exploring what is behind these doors, we find that there is an endless list of ideas that are just within our reach, some of which are both interesting and valuable and deserve further investigation.

The underlying theme of the following research is the use of polymeric materials in bioapplications. Chapters 2-5 either develop a fundamental understanding of current materials used for bioapplications or establish protocols and procedures used in characterizing and synthesizing novel materials. In chapters 6 and 7 these principles and procedures are applied to the development of materials to be used for gene therapy and drug delivery.

Chapter one is an introduction to the ideas that will be necessary to understand the subsequent chapters, as well as a literature review of these topics. Chapter two is a paper that has been published in the *Journal of Controlled Release* that examines the mechanism of drug release from a polymer gel, as well as experimental design suggestions for the evaluation of water soluble drug delivery systems. Chapter three is a paper that has been published in the *Journal of Pharmaceutical Sciences* that discusses the effect ionic salts have

on properties of the polymer systems examined in chapter two. Chapter four is a paper published in the Materials Research Society Fall 2000 Symposium Series dealing with the design and synthesis of a pH-sensitive polymeric drug delivery device. Chapter five is a paper that has been published in the journal *Biomaterials* proposing a novel polymer/metal composite for use as a biomaterial in hip arthroplasty surgery. Chapter six is a paper that will appear in an upcoming volume of the Journal *Biomaterials* dealing with the synthesis of a novel water soluble cationic polymer with possible applications in non-viral gene therapy. Chapter seven is a paper that has been submitted to *Macromolecules* discussing several novel block copolymers based on poly(ethylene glycol) and poly(diethylamino ethyl methacrylate) that possess both pH-sensitive and temperature sensitive properties. Chapter eight contains a summary of the research contained in chapters 2-7 and proposes future research for the gene therapy and drug delivery projects.

1.2 Polymeric Drug Delivery

Polymers exhibit many characteristics that make them very useful biomaterials in the field of drug delivery. The physical and chemical properties can be modified with such a dynamic range of characteristics that the applications of polymers for drug delivery are almost limitless. In order to understand the value of these properties, one must first attempt to understand the requirements of an effective drug delivery device.

A drug delivery device, for example a transdermal patch or slow-release gel tablet, administers bioactive molecules, drugs, or other medicinal chemicals in either a controlled or specifically modulated manner. These devices can deliver drugs in a much more controlled fashion than conventional administration methods, for example intravenous injection or consumption of a liquid dosage. These conventional methods require that the drug be manually administered roughly at the rate of consumption by the body in order to be effective. If a drug is introduced into the body, it begins to be consumed and excreted from the body by pathways intended for that very purpose, to remove foreign chemicals from the blood to protect the body from toxic chemical buildup (Patwardhan and Das, 1983). However, from a drug delivery standpoint this causes difficulties in maintaining a constant level of drug in the body. If the concentration of drug is not maintained in a specific window, it will either be toxic to the body or will be too low to be effective (Chien, 1984), (Figure 1a).
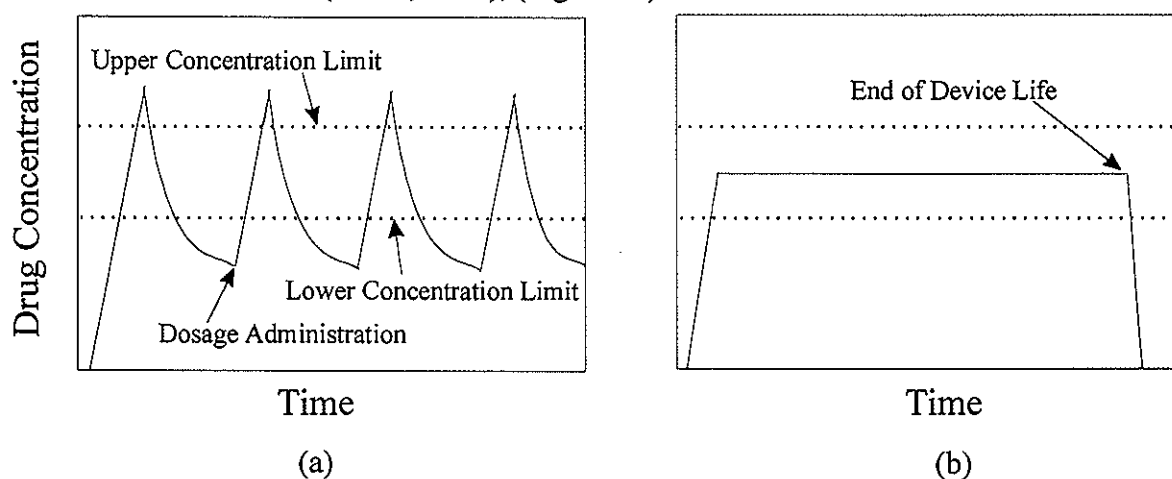
Figure 1- Drug concentrations in the body using (a) timed administration and (b) controlled release device

Controlled release delivery devices are designed to maintain the level of drug inside of this optimum therapeutic window by slowly releasing the drug at a rate sufficient to compete with the rate the drug is being consumed by the body (Figure 1b). There are several approaches to maintaining this constant delivery that are usually classified in the generic categories of reservoir devices and matrix devices.

In reservoir devices, a reservoir of drug is usually separated from the body by a thin polymeric membrane that allows release of the drug by diffusion to the bulk media, in this case the body (Figure 2). These devices are useful for many applications, but they do have drawbacks. The primary drawback is that the release relies on diffusive release of the drug, a mechanism that is proportional to the derivative of the concentration gradient between the reservoir and the body (Equation 1). In equation 1, $J[M\ L^{-2}\ T^{-1}]$ is the drug mass flux across the membrane, $D[L^2\ T^{-1}]$ is the diffusion coefficient of the drug across the membrane, and $\partial C/\partial x\ [M\ L^{-4}]$ is the concentration gradient across the membrane. In most cases the reservoir concentration cannot remain constant due to counter-diffusion of water into the device as the drug is released. As the concentration in the reservoir decreases, the release slows down. Simple differential equations can be solved to find that the release rate is actually a exponential function of time (Equation 2, Patwardhan and Das, 1984). This equation is for a spherical device with inner membrane diameter $a[L]$ and outer membrane diameter $b[L]$, a diffusion coefficient $D[L^2\ T^{-1}]$ and a partition coefficient $K[-]$. M_t/M_∞, or the fraction of mass released at time t, is a common way to express drug delivery as a function of time.
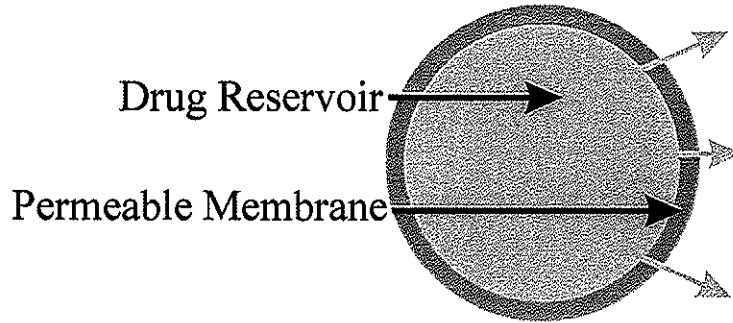
Figure 2 – Release from a membrane controlled release device

$$J = -D\frac{\partial C}{\partial x} \tag{1}$$

$$\frac{M_t}{M_\infty} = 1 - \exp\left(-\frac{3bDKt}{a^2(b-a)}\right) \tag{2}$$

Matrix devices, on the other hand, are composed of a drug trapped in a polymeric matrix that releases the drug as the matrix either erodes, swells, or dissolves. In erosion controlled matrix systems, the polymer used is typically a degradable polymer, for example a polyanhydride, that breaks down as water penetrates the device (Figure 3). The polymer is designed to optimize the rate of erosion at the interface and to degrade into biocompatible monomers or oligamers as the device erodes (Heller, 1984). In erodible matrix devices, when the device has been fully spent, the polymer can be removed from the body by natural filtration processes in the kidneys. The release from erosion controlled devices can be summarized by Equation 3 (Heller, 1984). In equation 3, k_o [M/L^2-T] is an erosion constant, C_o [M/L^3] is the initial drug loading, and a [L] is the dimensional thickness (radius or half-

height) and n is a constant that depends on the coordinate system (1,2, or 3 for Cartesian, cylindrical, and spherical respectively).

Erosion Controlled Device →

▲ Drug Molecule
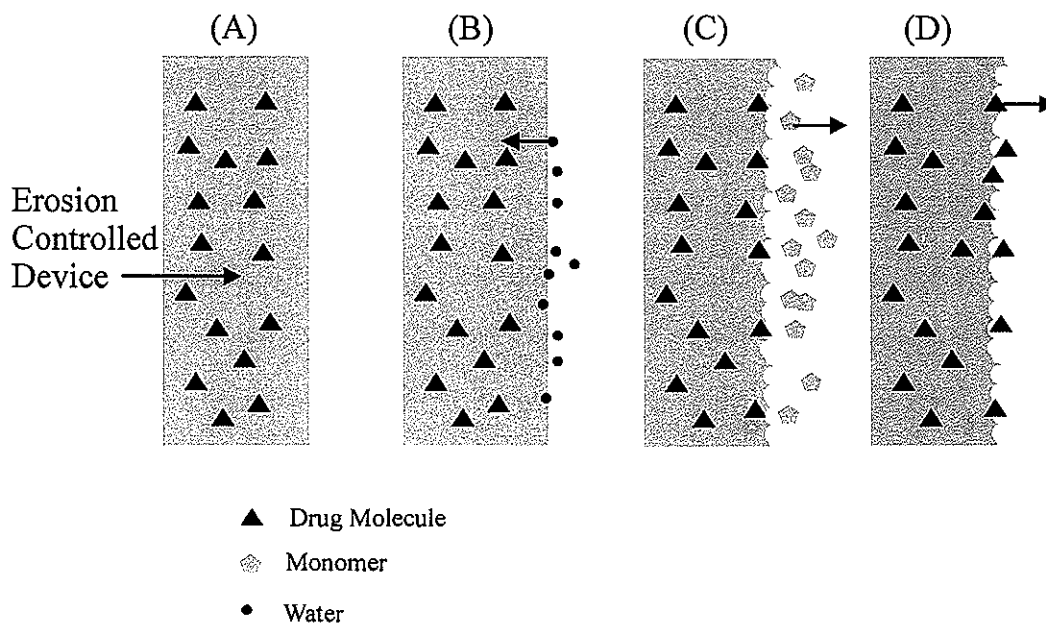
◉ Monomer

● Water

Figure 3 – Cartoon of an erodible maxtrix drug delivery device. (A) – Initial device, (B) – water penetrates the boundary of the device, (C) – Polymer degrades into monomeric state, (D) – Drug is released as polymer erodes at interface

$$\frac{M_t}{M_\infty} = 1 - \left[1 - \frac{k_o t}{C_o a}\right]^n \tag{3}$$

Swelling controlled devices rely on a similar mechanism to release drug at the rate of water penetration into the system. Before swelling, the diffusion rate of the drug is extremely slow and essentially does not occur. As water penetrates the material, typically a crosslinked hydrogel, the network swells and loosens the matrix to a point where the diffusion out of the material can occur (Ottenbrite and Fadeeva, 1994). This diffusion will predominately occur in the portion of the device that is swollen, so the interior drug remains trapped in the bulk of the device until water has penetrated deep enough to swell that section

of the device (Figure 4). Because swelling controlled devices are typically crosslinked, they remain in the body after release of all the drug and need to be removed. The exception to this is if the swelling device degrades on a time scale much longer than the life of the device, in which case it will eventually degrade and be removed naturally.
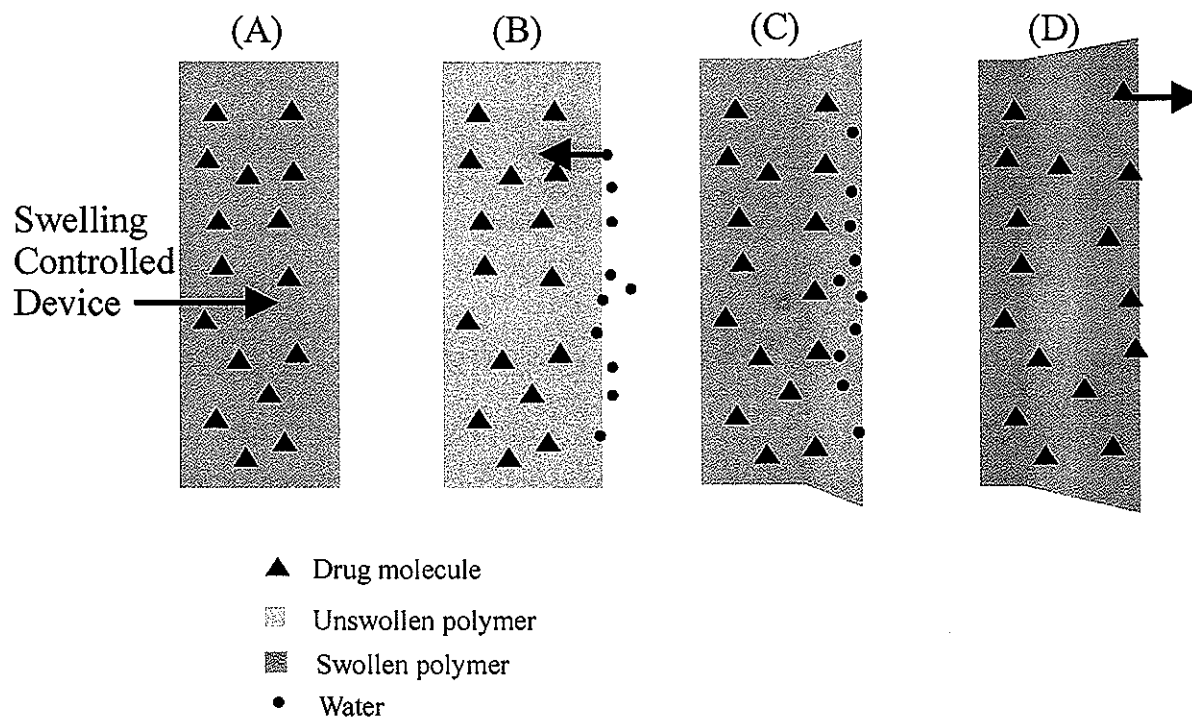
Figure 4 – Cartoon of drug release from a swelling controlled drug delivery device. (A) Initial device, (B) Water penetrates the unswollen polymer, (C) Polymer begins to swell due to the water, (D) Polymer swells enough to allow diffusion of the drug out of swollen portion of device. Unswollen portion retains drug.

Dissolution controlled devices are a combination of the previous two release mechanisms. These devices are controlled by the swelling of a polymer as water penetrates the bulk of the device, however they are made of water soluble polymers that will fully dissolve as the device is used (Figure 5). They are similar to erodible devices in this manner, however the polymers do not degrade into monomeric units, but rather are removed from the body in polymeric form. This places the restriction that the polymer chains must be small enough to be removed by the body by the kidneys, about 20 KDa.

(A)   (B)   (C)   (D)

Dissolution Controlled Device

▲ Drug molecule

▒ Unswollen polymer

▓ Swollen polymer

∿ Hydrated polymer molecule
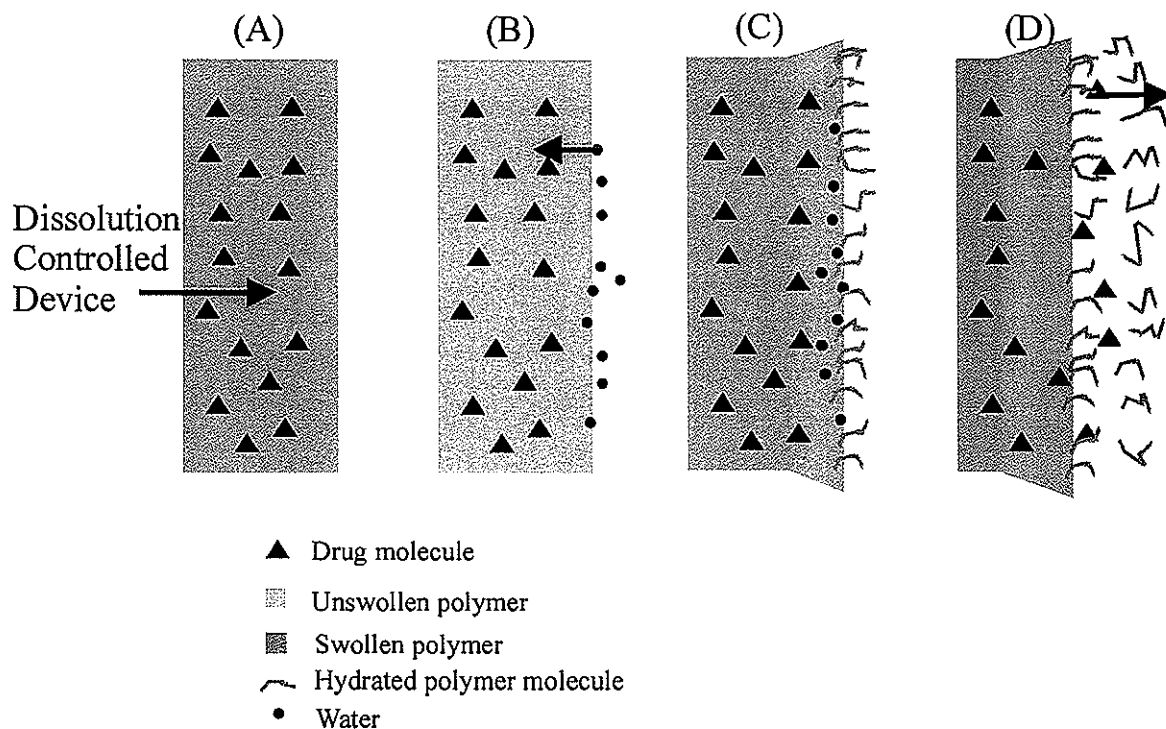
• Water

Figure 5 – Cartoon of drug delivery from a dissolution controlled drug delivery device. (A) – Initial device, (B) Water penetrates at the interface, (C) – Water swells the polymer and hydrates individual polymer chains. (D) As the polymer is hydrated, the polymer chains disentangle and leave the device, releasing drug trapped in the dissolving portion of the device.

With all of the above devices, the time scale of release can be varied greatly by modifying factors such as water solubility, degree of crosslinking for crosslinked devices, molecular weight of the polymers used, and nature of the degradation process. In addition, the devices can be customized to release under different pH, temperature, and other physical conditions based on the molecular structure of the polymer.

Controlled release devices have been constructed from many different polymeric materials for specific applications. The design of these devices can vary widely based on the nature of the application and the time scale on which the drug is to be administered. One class of materials that has been investigated for use as a dissolution controlled release device, Pluronic® polymers, will be discussed in the next section.

1.3 Properties of Pluronic® F127

Pluronic® polymers are a class of triblock copolymers of poly(ethylene oxide), PEO, and poly(propylene oxide), PEO, developed in the 1950s by BASF corporation. The molecular weights of both the PEO and PPO blocks can vary greatly, but the general structure is given as Figure 6. The combination of having both the hydrophilic PEO and the hydrophobic PPO as well as the interesting phase behavior of PEO give them a wide range of applications, for example industrially they are used in everything from cleaners to defoaming agents to mouthwash.

Poly(ethylene oxide)   Poly(propylene oxide)   Poly(ethylene oxide)

$$HO-[CH_2-CH_2-O]_n-[CH_2-CH-O]_m-[CH_2-CH_2-O]_n-H$$
$$CH_3$$
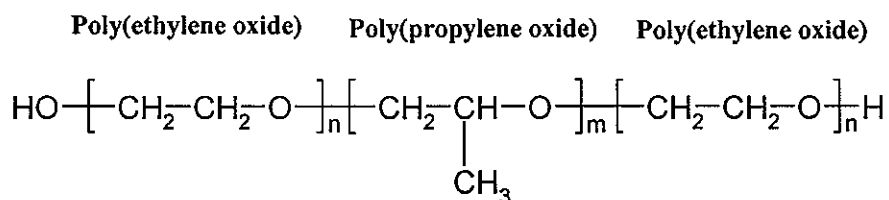
Figure 6 – General structure of Pluronic® polymers

The fact that this copolymer contains both hydrophilic and hydrophobic blocks gives rise to the formation of micelles under specific conditions. Under suitable conditions, the hydrophobic PPO center blocks aggregate together to form a stable lipophilic microphase surrounded by a hydrophilic halo of PEO (Figure 7). This phenomena has been studied by many researchers using a variety of techniques.
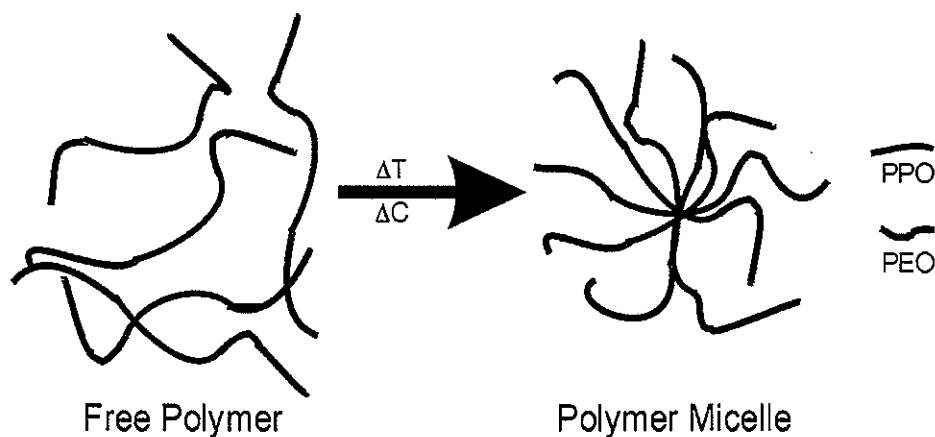
Figure 7 – Temperature and concentration induced micellization of Pluronic® polymers

Wanka et al. (1990) used light scattering, small angle neutron scattering (SANS), differential scanning calorimetry (DSC), as well as other techniques to characterize the temperature-concentration pairs that are required to induce micellization of selected Pluronic® analogs. Wanka et al. (1994) expanded on this information using SANS to create a phase diagram for the domain weight percent F127 (0, 100) and temperature (0, 100 °C). Alexandridis et al. (1994) studied the micellization phase transition for many Pluronic® analogs using a florescent probe.

Malmsten and Lindman (1992) carried out a nice analysis of the fraction of polymer molecules involved in micellization as a function of temperature using gel permeation chromatography (GPC). They found that because there were two distinct peaks detected by differential refractometry that the life of a polymer chain in a micelle is much longer than the length of the experiments, which was on the order of 2 hours. This is in contrast to some micellar aggregate systems of small molecular weight surfactants who have a residence time in the aggregate on the order of milliseconds.

One characteristic of Pluronic® micelles that is important for drug delivery is the micellar size. It is the size of the PPO core that determines the loading limit of some hydrophobic drugs. Wu et al. (1995) used SANS to determine this information as well as the aggregation number of the micelles at various temperatures for the Pluronic® analog L64. They found that there is a positive correlation between the aggregation number and the solution temperature for L64 with aggregation numbers on the order of 40-70. A similar correlation was found for core radius and temperature with core radii on the order of 4nm.

Some modeling work has been done that helps understand the microscale profile of a micellar aggregate. Hurter et al. (1993a,b) have used a statistical approach to evaluate the average concentration of PPO, PEO and water as a function of distance from the micelle core (Figure 8). A lipophilic molecule, naphthalene, was then included in the model to investigate the solubility of molecules that are not typically water soluble (Figure 9).

Other researchers have investigated this increase in solubility that arises from the PPO microphase at the core of each micelle. Lee et al. (1997) analyzed the increase in solubility of ibuprofen, a typically water insoluble drug, in the presence of micellar F127. The solubility of ibuprofen increased from 0.01 mg/ml in water to 6.3 mg/ml in 10 wt % F127. This characteristic of Pluronic® polymers has applications in drug delivery for the delivery of water-insoluble drugs.
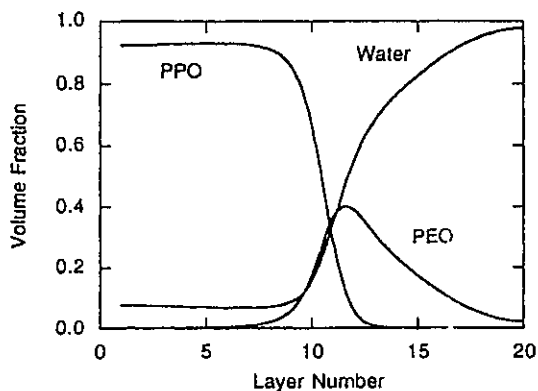
Figure 8 – concentration profiles of PPO, PEO and water in a Pluronic® micelle. Reprinted with permission from Hurter, Patricia N.; Scheutjens, Jan M. H. M.; Hatton, T. Alan. Molecular modeling of micelle formation and solubilization in block copolymer micelles. 1. A self-consistent mean-field lattice theory. *Macromolecules* 26(21), (1993) 5592-601. © 1993 American Chemical Society.
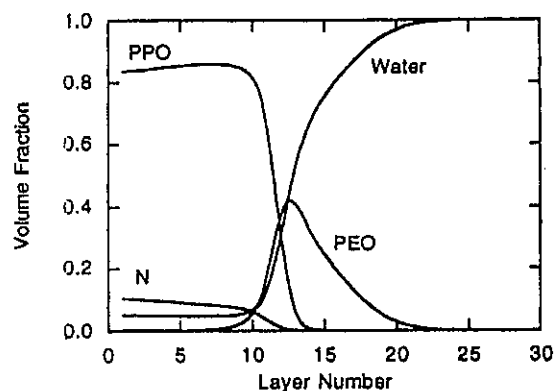
Figure 9 - concentration profiles of PPO, PEO naphthalene and water in a Pluronic® micelle. Reprinted with permission from Hurter, Patricia N.; Scheutjens, Jan M. H. M.; Hatton, T. Alan. Molecular modeling of micelle formation and solubilization in block copolymer micelles. 1. A self-consistent mean-field lattice theory. *Macromolecules* 26(21), (1993) 5592-601. © 1993 American Chemical Society.

The specific formulations of Pluronic® that are usually of interest in the field of drug delivery are Pluronic® F127 ($\overline{M}_n$ ~12600, 70% PEO by weight) and Pluronic® F68 ($\overline{M}_n$ ~8400, 80% PEO by weight). These formulations have a high enough overall molecular weight and a high enough percentage of PEO to undergo a thermoreversible gelation phase change at temperatures below body temperature. In cold aqueous solutions of high concentration, above about 20% w/w, the polymer chains are fully solvated and exist as free molecules. As discussed above, an elevated temperature induces a phase change into a solution of micellar aggregates, still in solution. Slightly above this temperature the micelles entangle forming a non-crosslinked gel. This temperature varies depending on the concentration of the solution, but for F127 the temperature is about 20°C for 20 w/w% solutions and about 10°C for 30 w/w% solutions. This phase change allows a semi-solid

matrix delivery device to be inserted in the body by sub-cutaneous or intramuscular injection at a depressed temperature, thus removing the need for surgery to implant the device (Figure 10).
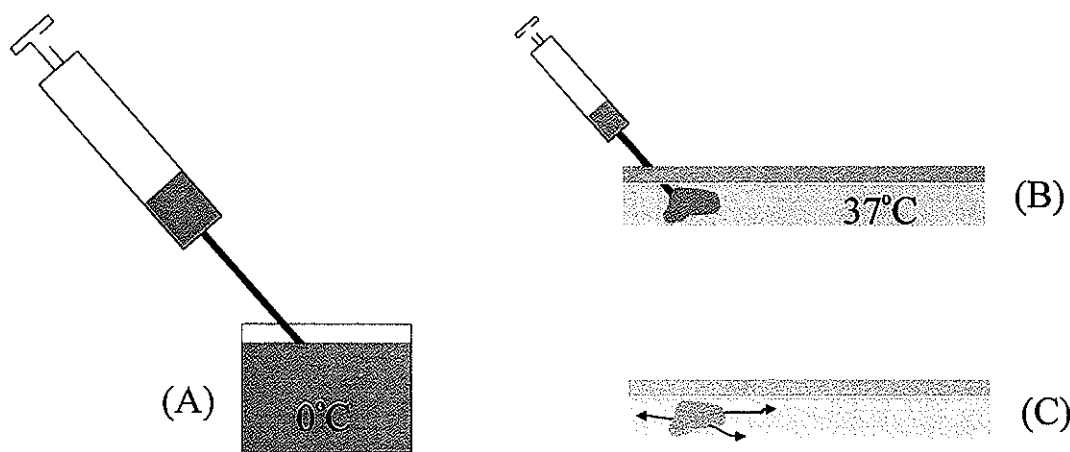
Figure 10 – Cartoon of a thermoreversible gel drug delivery device. (A) Loading of the drug/polymer solution as a liquid. (B) Sub- cutaneous injection and thermoreversible gelation. (C) Release of drug.

The thermodynamics of the sol to gel transition has been studied using a calorimetric method by Vadnere et al. (1984). The enthalpy of samples below and above the gel transition were measured and used as the enthalpy of gelation. A visual technique was used to determine where this gelation point was. Reproducible results were obtained that indicated from an enthalpic perspective, the Pluronic® systems did not favor the gel state. The entropic contribution to the free energy driving force for gelation, however, outweighs the increased enthalpy. It was also determined that because the PPO portion of the molecule has a much larger contribution to the increase in enthalpy and entropy, the ratio of PPO to PEO portions is important in determining the point at which gelation occurs.

Fourier transform infrared spectroscopy (FTIR) has also been used to evaluate the gelation properties of Pluroinc® F127. Cabana et al. (1997) used infrared spectroscopy to

investigate the hydrogen bonding between water and the aliphatic ether oxygen in the Pluronic® backbone during the gel phase transition. The C-O-C stretching frequency (1200-1000 cm^{-1}) was used to track the hydrogen bonding through the phase transition. It was determined by comparison to pure PPO and PEO spectra that in the absence of water, the block copolymer chains are crystalline, whereas in the hydrated state they are amorphous. It was also found that the hydrogen bonding in the gel state is weaker than in the solvated state as determined by a positive shift in the C-O-C stretching frequency upon gelation.

Yet another analytical tool that Cabana et al. (1997) used to characterize the sol to gel transition is differential scanning calorimetry (DSC). By detecting the small positive enthalpic change between the two states as the temperature is scanned from below the gel point to above, the gel point can be determined. The results of this study correlated well to their own rheological measurements for gel point as well as the measurements by Vadnere et al. (1984) for $\Delta H_{gelation}$.

The kinetics of the sol to gel transition have been studied using a pulse shearometer by Wang and Johnston (1991). This method of analysis measures the velocity of a propagating shear wave though a material. By this method, the shear modulus (G') could be measured as the gel transition occurred. One important finding of this study was that not only does the gelation temperature decrease with increasing Pluronic® F127 concentration in aqueous solution, in fact the rate of gelation also increases.

Some rather simple techniques have been implemented to study the gelation point of Pluronic® solutions based on inverting a container of the solution at different temperatures and noting the temperature at which the solution does not flow (Pandit and Kisaka, 1996). These measurements were in very good agreement with other more complicated methods.

Wanka et al. (1990), while investigating the micellization properties of Pluronic®
F127, had reported that solutions of F127 produced SANS signals that containing irregular
spikes in the scattering pattern of the neutrons when the sample was heated past its gelation
temperature. This is an indication that long range order is present in the system.

In addition to the effect of polymer concentration and temperature on gel formation,
research has been focused on detailing the effect salts have on the gelation transition and
resulting gel properties. Pandit and Kisaka (1996) found that the gelation point of Pluronic®
F127 was slightly reduced in the presence of some salts.

The use of Pluronic® polymer gels for drug delivery has been studied both *in vivo* and
in vitro. Although some of the *in vitro* tests show favorable data for the release rates of drugs
from Pluronic® gels, some of the methods and analyses are not sufficient to determine the
true release rate of the dissolution controlled system.

Gilbert et al. (1986) studied the release of drugs from Pluronic® F127 gels using a
membrane diffusion cell. In this type of setup, the gel is trapped behind a membrane and
allowed to release a trapped model drug through the membrane into a stirred bath. This setup
is not appropriate for this type of delivery device for two reasons. First, the release is not
diffusion controlled, but dissolution controlled. This setup does not allow the polymer to
freely dissolve, by trapping the polymer inside of a membrane covered chamber. Second,
water will diffuse through the membrane throughout the experiment, hydrating the gel at the
membrane interface more than the bulk gel. The release rate of these experiments will be
drastically different if the polymer concentration is lower, as diffusion coefficient is a
function of viscosity and the viscosity is a function of the polymer concentration. It is
impossible to determine, without complicated modeling of the water penetration and

simultaneous diffusion of the drug from the gel, the diffusion coefficient of the drug in a gel of a given polymer concentration. The polymer is only truly at the reported concentration at the beginning of the experiment, after which the diffusion of water reduces the polymer concentration at the liquid interface.

Chi and Jun (1989) improved on the measurement setup for release from dissolving Pluronic® gel systems by using a membraneless diffusion cell apparatus (Figure 11). Using a model to obtain the diffusion coefficient from the mass flux, the apparent diffusion coefficient was calculated. In this case, the gel was allowed to dissolve, but the effect of bath agitation was not taken into account. The apparatus in Figure 11 relies on an impeller to maintain a fully mixed receiving liquid. Our studies have indicated that the agitation rate in this type of a setup, especially when the impeller is so close to the soluble gel, strongly affects the dissolution of the device and thus the mass flux used in finding the diffusion coefficient. After only a few minutes of agitation, Pluronic® gels show signs of shear stress on the surface in a pattern consistent with the agitation of the bath (Figure 12). This stress increases the rate of dissolution and needs to be accounted for in an experimental setup such as the one used by Chi and Jun.

Safwat (1994) reverted back to a membrane diffusion cell to obtain data for the release of several drugs; progesterone, dexamethasone, ethinylestradiol, and α-methyldopa[MD]. Because of the use of a membrane diffusion type of setup, the release was reported as being linear when plotted versus $t^{1/2}$ and the release was said to be diffusion controlled. This was an acceptable analysis for the application of topical drug delivery, but could not be extended to internal use of the system.
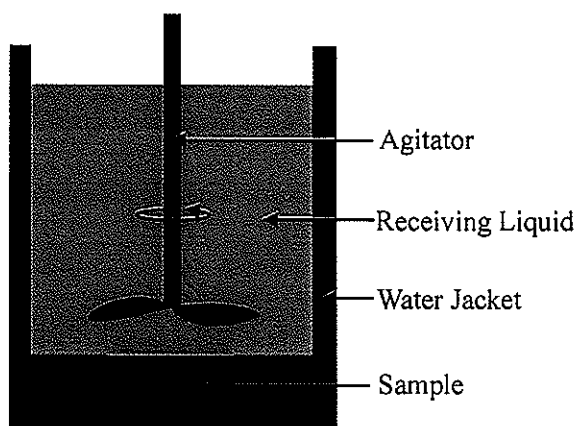
Figure 11– Membraneless diffusion cell
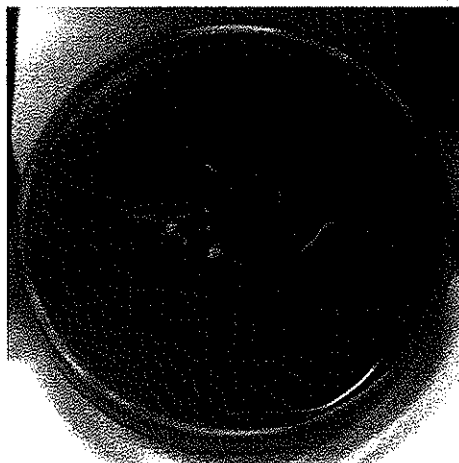
Figure 12 – Pluronic[®] gel subjected to sheer stress from agitation (20% F127 in water, 80 RMP agitation for 20 minutes)

Desai and Blanchard (1998) examined the use of Pluronic[®] F127 for ocular delivery of pilocarpine hydrochloride using an *in vitro* test method. Their method consisted of sample vials containing the polymer gel that had solidified on the bottom of the vial with a small amount of release medium, an artificial isotonic tear solution. The vials were rotated end-over-end and the medium was removed at set time intervals. The experimental setup in this case was appropriate, but the analysis ignored one important characteristic of Pluronic[®] polymer gels: water diffuses into the gel as the gel dissolves. We have measured this water uptake, and it is clearly not negligible. Desai and Blanchard weighed the polymer after each time interval to determine the mass loss from the polymer gel without taking the mass gain from water diffusion into account. The release rates of the drug using this experimental setup appear to be linear with time and increase with the addition of poly(ethylene glycol) and decrease with the addition of methylcellulose, poly(vinyl alcohol), and hydroxypropyl methylcellulose at concentrations less than 5%.

Other studies, like Yang et al. (1999), use membraneless diffusion setups similar to Chi and Jun, however the agitation was much slower, 20 RPM, and the agitation was well above the gel/water interface. The release from this setup was quite different from Chi and Jun and from studies carried out in our group (Moore et al., 2000) which is most likely an artifact of the neglected hydrodynamic effects.

As with the micellization and gelation properties, the effect of salt concentration on the drug delivery properties of Pluronic® gels has also been investigated. Pandit and Wang (1998) found that the release rate of propanolol was slowed by the presence of salts such as NaCl, Na_2SO_4, NaH_2PO_4, $CaCl_2$, and $MgSO_4$.

In vivo studies have been carried out to study intraperitoneal and intermuscular injections of Pluronic® F127. Jhonston et al. (1992) investigated interleukin-2 delivery from a Pluronic® F127 device that was inserted by intraperitoneal injection in rats. They found that the activity of interleukin-2 decreased only slightly when stored in Pluronic® F127 solutions at 4°C relative to a phosphate buffered saline solution for a period of 72 hours. They also found that the gels administered the drug in a controlled manner with no systemic side effects.

Bhardwaj and Blanchard (1996) studied the release of melanotan-I following intramuscular injection of guinea pigs. They found that the drug concentration in the blood following the injection of drug in a 25% F127 solution was approximately 0.7 mg/ml after 24. This compares to the same concentration after about 5 hours for an intramuscular injection of the drug dissolved in a phosphate buffer solution.

The above characterizations, *in vivo* studies and *in vitro* studies indicate that Pluronic analogs, specifically F127, have properties that make them ideal candidates for a controlled

release device. Their thermoreversible gelation phase change allows injectable administration of the device. The micellization properties lead to higher solubilities of hydrophobic drugs. The dissolution controlled release mechanism creates a near zero-order release under many conditions. However, the release mechanism is still not fully understood. In the experimental situations described above, it is not possible to discern diffusion driven release from dissolution controlled release if both mechanisms are happening simultaneously. In addition, the highly agitated systems might mask subtle contributions to the overall release kinetics made by diffusion controlled release. In chapter 2, a paper is presented that investigates the mechanism of the release from the Pluronic® gels to delineate. In chapter 3, a more detailed analysis of the effect that salts play on the parameters associated with the release is presented.

1.4 pH-Sensitive Drug Delivery

The application of polymeric materials to drug delivery is not limited to controlled release systems. In fact, one of the characteristics that make polymers useful delivery devices is their ability to include functionalities that exhibit different properties in different environments. These smart materials can release drugs at different rates depending on dynamic factors, for example pH, that either exist at different levels in different parts of the body or can be modulated based on other environmental factors. There are two main types of pH sensitive devices, devices that release their drug load at low pH levels and ones that release their drug load at high pH levels.

High pH releasing devices, usually consisting of a membrane or hydrogel with anionic character, serve two main functions in the delivery of drugs. Because of the high

acidity of the stomach and the slight alkalinity of the intestines, devices can be designed so

that drugs are not released until the device is in the intestines. Therefore the first function of

high pH release devices is to protect biomolecules from the harsh environment of the

stomach, a condition that might otherwise denature or degrade the molecule. The second

function is release of the drug in the intestine, where the absorption of the active ingredient

occurs at a rapid rate.

Low pH releasing devices are essentially the opposite of their high pH releasing

counterparts. They contain polymers with cationic character, making them release only

under acidic conditions (Figure 13).
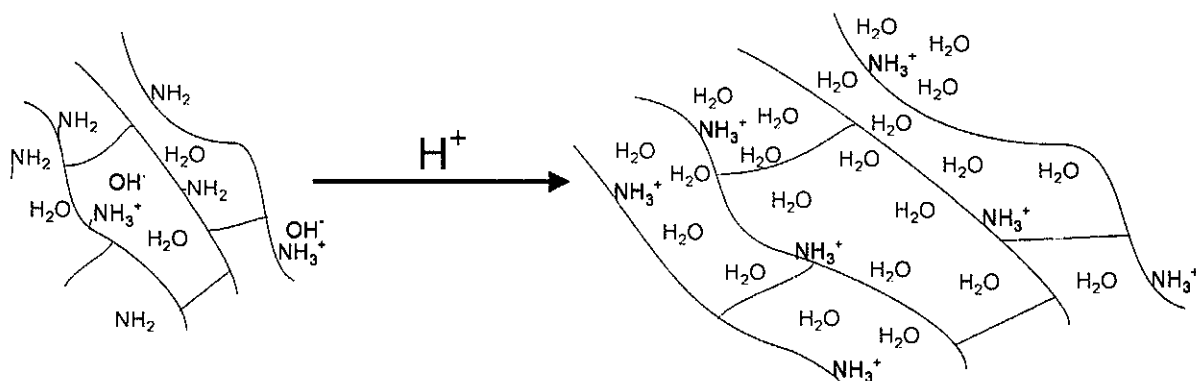
Figure 13 – Swelling of a crosslinked polymer with cationic character under acidic conditions

The most common application of this type of device is self regulating insulin release.

By the inclusion of the enzyme glucose oxidase in the matrix of a delivery device loaded

with insulin, glucose in the body can be enzymatically converted to gluconic acid. Because

the gluconic acid is acidic, the presence of glucose at a device interface causes protonation of

the cationic functional groups in this area. The protonated groups are now positively charged

and repel each other due to electrostatic repulsion. This repulsion results in swelling of the

device at the interface causing release of any molecules, in this case insulin, from the matrix. When the glucose levels in the body have subsided, the device does not undergo any further protonation and the swelling front does not continue to penetrate the device unless the glucose level surges again. An adequate device could self regulate the release of insulin for diabetics.

Over the past 20 years, there has been an extensive amount of research in this area. Most of the research has focused on crosslinked copolymer membranes consisting of a water soluble polymer, like poly(ethylene glycol) or a hydroxyalkyl methacrylate, and a pH sensitive polymer, like N,N-diethylaminoethyl methacrylate (DEAEM). Glucose oxidase (GluOx) was either chemically attached to the polymer backbone or physically trapped in the polymer matrix.

Horbett et al. (1983) prepared crosslinked membranes of DEAEM and 2-hydroxyethyl methacrylate (HEMA) initiated by irradiation and crosslinked with tetraethylene glycol dimethacrylate (TEGDMA). GluOx was physically trapped in the membrane matrix. The results of this study indicated that the swelling of this type of membrane was dramatically affected by the pH of the hydrating solution.

Ishihara, et al. (1984) produced membranes of another hydroxyalkyl methacrylate, hydroxypropyl methacrylate (HPMA), and DEAEM. The polymerization was thermally initiated and the GluOx was immobilized with ammonium persulfate. These membranes showed reversible swelling when the pH was cycled between 6.5 and 7.4. Although GluOx was present, no examination of the effect of glucose was tested.

Ishihara and Matsui (1986) later synthesized capsules using similar chemistry. Hydroxyethyl acrylate (HEA), DEAEM, and 4-trimethylsilylstyrene (TMS) were

polymerized using the initiator 2,2'-azobisisobutyronitrile. The TMS was needed for capsule formation. Their study presented results from an experiment where glucose was added to a diffusion cell in the presence of GluOx and insulin. The insulin permeating through the membrane was then measured. The results showed that there is a strong effect on membrane permeability when glucose is present.

Firestone and Siegel (1988) prepared a slightly different membrane using methyl methacrylate (MMA), DEAEM, and divinyl benzene (DVB) as the crosslinking agent. An important result from their experiments was that the polymer synthesized showed rapid swelling kinetics when cycled from a pH of 5.0 to a pH of 6.0. The deswelling and reswelling time was less than 20 minutes for repeated cycles between the two pH levels.

More recently, Schwarte, Podual, and Peppas (1998) produced crosslinked membranes of DEAEM and poly(ethyelene glycol) methacrylate (PEGMA) with TEGDMA as the crosslinking agent. The polymerization was initiated with ammonium persulfate and sodium metabisulfate, with GluOx chemically attached to the polymer backbone using acryloyl chloride. These membranes were tested for their swelling ability and response to oscillatory changes in pH. A 10:1 ratio of DEAEM to PEGMA was sufficient to produce dramatic swelling ratio differences below a pH of about 6.5.

Some research has also been focused on grafting polymers with ionic character onto a PEG or Pluronic® backbone. Most of this work, however, has been for polymers with anionic character for high pH releasing devices. Bromberg (1998 a,b) has grafted poly(acrylic acid) on a Pluronic® F127 backbone using radicalization of the F127 by ammonium persulfate. The radicals initiated the polymerization of acrylic acid. This led to polymers with a molecular weight between 10^6 and 10^7 consisting primarily of acrylic acid.

Hoffman et al. (1997) have grafted Pluronic® polymers onto poly(acrylic acid) backbones for extended release in delivery on mucosal surfaces.

Although much research has been focused on producing high pH releasing devices or crosslinked low pH releasing devices, not much work has been devoted to water soluble PEO-based low pH releasing devices. PEO-based polymers are highly biocompatible and exhibit unusual phase behavior because of the lower critical solution temperature of PEO. In chapter 4, a synthesis route for producing PEO based water soluble block copolymers with cationic character is presented. The end goal of this research will be to develop water soluble copolymers with cationic character that exhibit thermoreversible gelation behavior. Because of the need for a relatively monodisperse polymer as well as the goal of a block type copolymer, the synthesis route that was chosen is anionic polymerization.

1.5 Anionic Polymerization of Diethylaminoethyl Methacrylate

The process of converting a monomer into a polymer can be accomplished in many ways. However, all addition polymerizations consist of three main stages; initiation, propagation, and termination. There are many ways to chemically achieve initiation, but the one that will be focused on here is anionic initiation. In anionic initiation, an anionic molecule, for example an organic salt of an alkali earth metal, initiates either a ring opening or the formation of a carbanion where the monomer contains a double bond. A simplified pictorial description of this is shown in Figure 14. The carbanion then begins the stage of propagation, or the formation of the polymer.
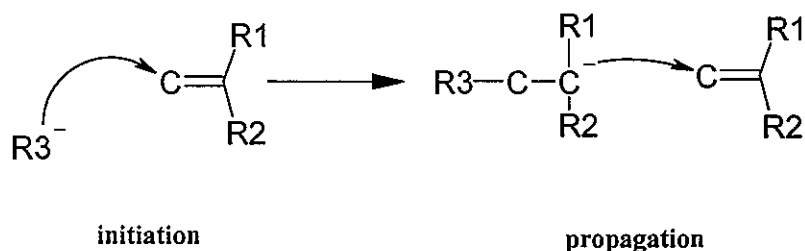
Figure 14 – Anionic polymerization of a 1,1-substituted ethylene.

The advantages of anionic polymerization over other methods of polymerization, for example free radical initiated, are that 1) the ion is a stable intermediate meaning the growing polymer chain is not quickly terminated when the monomer is fully consumed and 2) the growth kinetics are such that the polydispersity ($\overline{M}_w / \overline{M}_n$) of a polymer produced by anionic polymerization is quite low, often lower than 1.2. The first property of anionic polymerization is useful for this research because endcaps and blocks can easily be added to the end of a growing polymer. The second property is important in many specialty applications where the molecular weight plays an important role in the property determination of the polymer.

A polymer that has been studied for many pH-sensitive drug delivery devices is poly(2-(N,N-diethylaminoethyl methacrylate)), however this polymer is often incorporated in crosslinked poly(ethylene glycol) or poly(hydroxyalkyl methacrylate) membranes where free radical initiated polymerization is appropriate. In the case of the low molecular weight block copolymers this research aims to synthesize, an anionic initiated polymerization is the appropriate choice.

Nagasaki et al. (1997a) reported polymerization of 2-(N,N-diethylaminoethyl methacrylate) (DEAEM) and other semitelechelic functional poly(methacrylate)s using potassium alcoholates after earlier (1997b) reporting that the initiation of 2-(trialkylsiloxy)ethyl methacrylate (SEMA) could be achieved with potassium alcoholates. The coordination of the potassium with the acrylate oxygens and the oxygen in the slioxy group plays an important role in this polymerization (Figure 15a). Nagasaki et al. then used DEAEM as a model for other monomers that have a donor group in the same position as the siloxy oxygen (Figure 15b).
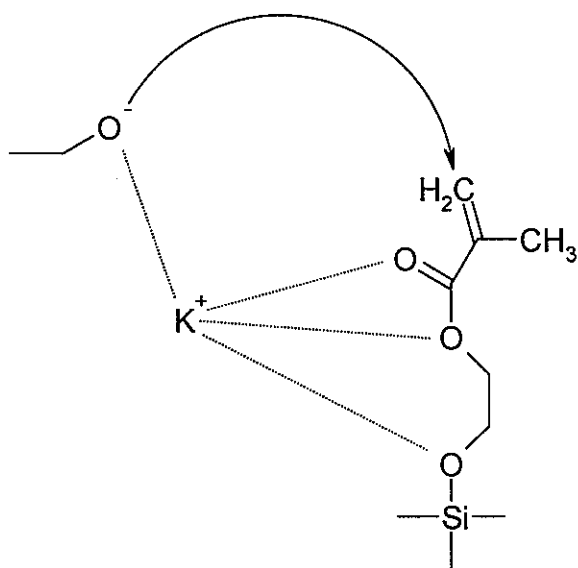
Figure 15a – Anionic initiation of 2-(trimethylsiloxy)ethyl methacrylate with potassium ethoxide
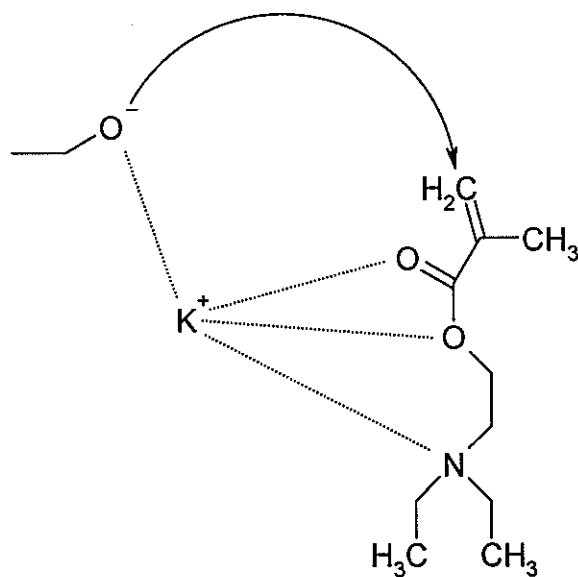
Figure 15b – Anionic initiation of 2-(N,N-diethylamino)ethyl methacrylate with potassium ethoxide

Lascalles et al. (1999) took the idea presented by Nagasaki et al. and extended the application to include larger alcoholates prepared by reaction of an alcohol with potassium hydride. The alcohols studied were allyl alcohol, di(ethylene glycol) vinyl ether and 4-

vinylbenzyl alcohol. The polymers produced by initiation of dimethylaminoethyl methacrylate (DMAEM) with these alcoholates were typically much higher molecular weight than their target with a polydispersity as low as 1.17 and as high as 1.34.

Shen et al. (2001) have recently expanded on the work of Nagasaki et al. and Lascalles et al. in an attempt to lower the polydispersity of the resulting polymer and bring the molecular weight more in line with the target molecular weight. By using a lithium amide instead of a potassium alcoxide, the polydispersity of the resultant polymers were reduced to as low as 1.03. The lithium amides were prepared by the reaction of a secondary amine with *sec*-butyllithium (sBuLi).

Due to the difficulties of a gas phase anionic polymerization of ethylene oxide, we have opted for a slightly different route that extends the work of Lascalles (1999) to include larger potassium alcoholate initiators like poly(ethylene glycol) and poly(ethylene glycol) methyl ether, whose alcohol terminating ends can be converted to the potassium salt using a similar route to Lascalles. The first stages of this work are presented in chapter 4.

1.6 Cytotoxicity Testing of Biomaterials

Thousands of new biomaterial devices enter the market every year. There are several steps that must be taken in order to ensure that the materials these devices are constructed from will be safe to humans. Usually the first, and simplest, of these tests is the evaluation of the material for cytotoxicity. If the material is toxic to living cells, it will probably elicit severe immune system defense responses if used internally. Even in cases of ocular or dermal contacting biomaterials, there is the need for a low or zero cytotoxic response on the cellular level. ASTM has developed a checklist of the tests that need to be performed before

a material is determined to be safe for human use. The extent and complexity of these tests varies from application to application, however the test for cellular cytotoxicity is required for all applications (ASTM, 2000a). It has been shown that *in vitro* testing for cytotoxicity can be more sensitive than *in vivo* testing (Brotzman et al., 2000), making it an obvious starting point for the testing of potential biomaterials.

In vitro cytotoxicity testing can be performed in one of three ways; agar diffusion (ASTM, 2000b), direct contact (ASTM, 2000c), or elution. The application of these three tests is determined by the nature of the material, i.e. which tests can physically be performed. For water soluble materials or materials with a natural leachability the elution test is the most sensitive test. In this test, the potential biomaterial is dissolved under sterile conditions into a growth medium. Cells, usually fibroblast cells due to their robustness and the ease at which they can be obtained, are grown to a confluent layer on a culture treated polystyrene substrate. The cells are then fed the media that has been contaminated with the dissolved biomaterial. The cells are evaluated after a period of 24 hours and examined for a cytotoxic response. The test is performed using appropriate positive and negative control chemicals. We have used such a test to compare the cytotoxocity of our polymeric materials for gene therapy and drug delivery applications with the appropriate controls. Agar diffusion testing is performed under similar conditions, with the exception that the cells are not in contact with the chemically tainted media. The cells and media are separated by a thin layer of agar.

For solid materials that are not soluble in aqueous growth media, a direct contact assay is performed. In this test, cells, again usually fibroblasts, are seeded on a polystyrene substrate and allowed to reach a near confluent level. The potential biomaterial is then placed on the cellular layer with adequate weight to prevent slippage. Growth media is then

added to the sample and the system is incubated for 24 hours. After this time, the cells are examined using light microscopy at the sample interface to determine if there has been a cytotoxic response. A cytotoxic response would consist of a thinned cellular layer, cell lysis, or cells detached from the polystyrene substrate (Figure 16). A negative control of ultra-high molecular weight polyethylene (UHMWPE) and a positive control of *cis*-polyisoprene are used for this test.
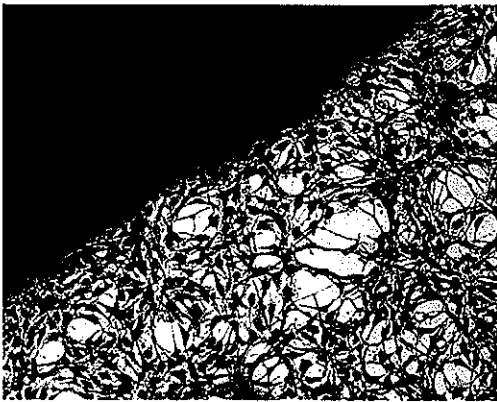
Figure 16a – Negative cytotoxic response. 3T3 mouse fibroblasts, 100x, stained with crystal violet. Ultra High Molecular Weight Polyethylene (UHMEPE) sample.
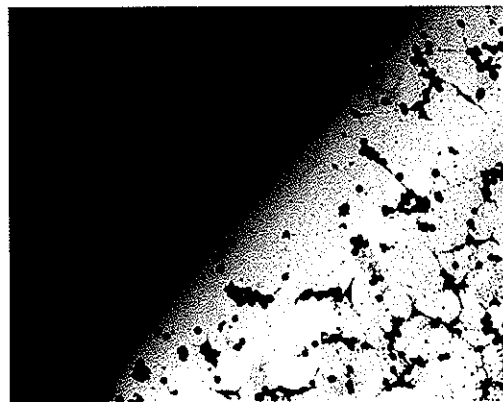
Figure 16b – Positive cytotoxic response. 3T3 mouse fibroblasts, 100x, stained with crystal violet. *Cis*-polyisoprene sample.

Assuming the materials have not failed these tests, more complicated tests like cellular adhesion (Hunter et al., 1995) and tests for cell functionality (Morrison et al., 1995) can be performed. The specific requirements for the agar diffusion, elution, and direct contact cytotoxicity tests are outlined by the ASTM (ASTM, 2000 b-d).

We have used this biocompatibility testing in order to investigate the use of a novel quasicrystal/ultrahigh molecular weight polyethylene composite for acetabular cup prosthetics. These prosthetic cups undergo large amounts of stress during their useful lifetime, usually resulting in high amounts of wear (Devane and Horne, 1999). The wear

debris that is caused by contact with prosthetic femoral head implants can lead to osteolysis and eventual device failure (Maloney et al., 1993). Osteolysis does not tend to occur in cases were there is not a high acetabular wear rate (Amstutz, et al., 1992). Quasicrystal/polymer composites have been studied in the chemistry department at Iowa State University and were found to have a much lower wear than their native polymer counterparts (Bloom et al., 2000). Because of this, the filled UHMWPE composites were investigated as an alternative to UHMWPE acetabular cup prosthetics. As a new biomaterial, these polymer composites were then tested for biocompatibility using the direct contact assay mentioned above. These results, as well as the mechanical properties of the filled polymer composites are presented in chapter 5.

1.7 References

Alexandridis, Paschalis; Holzwarth, Josef F.; Hatton, T. Alan. Micellization of Poly(ethylene oxide)-Poly(propylene oxide)-Poly(ethylene oxide) Triblock Copolymers in Aqueous Solutions: Thermodynamics of Copolymer Association. *Macromolecules*. 27, (1994) 2414-2425.

Amstutz H.C., Campbell P., Kossovsky N., Clarke I.C. Mechanism and clinical significance of wear debris-induced osteolysis. *Clin Orthop* 276 (1992) 7-18.

Bhardwaj, Renu; Blanchard, James. Controlled-Release Delivery System for the a-MSH Analog Melanotan-I Using Poloxamer 407. *Journal of Pharmaceutical Sciences*. 85(9), (1996) 915-919.

Bloom P.D., Baikerikar K.G., Otaigbe J.U., Sheares V.V. Development of novel polymer/quasicrystal composite materials. *J Mat Sci & Eng A*, 294-296, (2000) 156-159.

Bromberg, Lev. Polyether-Modified Poly(acrylic acid): Synthesis and Applications. *Ind. Eng. Chem. Res.* 37(11), (1998) 4267-4274.

Bromberg, Lev. Properties of Aqueous Solutions and Gels of Poly(ethylene oxide)-b-poly(propylene oxide)-b-poly(ethylene oxide)-g-poly(acrylic acid). J. Phys. Chem. B 102(52), (1998) 10736-10744.

Cabana, Alain; Ait-Kadi, Abdellatif; Juhasz, Julianna. Study of the Gelation Process of Polyethylene Oxide$_a$-Polypropylene Oxide$_b$-Polyethylene Oxide$_a$ Copolymer (Poloxamer 407) Aqueous Solutions. J. Colloid. Int. Sci. 190, (1997) 307-312.

Brotzman R.W., Aikens J., Batllo F., Kullberg M., Kritchevsky G. Nanomaterials and wear resistant polymers. Ceram Ind, 150, (2000) 39-43.

Chi, Sang C.; Jun, H. W. Release Rates of Ketoprofen from Poloxamer Gels in a Membraneless Diffusion Cell. J. Pharm. Sci. 80(3), (1991) 280-283.

Chien, Yie W. Novel Drug Delivery Systems: Fundamentals, Developmental Concepts, Biomedical Assessment. Marcel Dekker Inc, New York, (1984).

Desai, Suketu D.; Blanchard, James. In vitro Evaluation of Pluronic F127-Based Controlled-Release Ocular Delivery Systems for Pilocarpine. Jounal of Pharmaceutical Sciences. 87(2), (1998) 266-230.

Devane, Peter A; Horne, J. Geoffrey. Assessment of Polyethylene Wear in Total Hip Replacement. Clinical Orthopaedics and Related Research. 369, (1999) 59-72.

Gilbert, Julian C.; Hadgraft, Jonathan; Bye, Alan; Brookes, Leonard G. Drug Release From Pluronic F-127 Gels. Int. J. Pharm. 32, (1986) 233-228.

Heller, J. Use of enxymers and Bioerodible Polymers in Self-Regulated and Triggered Drug Delivery Systems. In Pulsed and Self-Regulated Drug Delivery, Kost Joseph Ed., CRC Press, Boca Raton, Florida, (1990) 93-108.

Hoffman, Allan S.; Chen, Guohua; Wu, Xiangdong; Ding, Zhongli; Kabra, Baghwati; Randeri, Kiran; Schiller, Matt; Ron, Eyal; Peppas, Nikolaos A.; Brazel, Christopher. Graft copolymers of PEO-PPO-PEO triblock polyethers on bioadhesive polymer backbones for use as drug delivery carriers. In Book of Abstracts, 213th ACS National Meeting, San Francisco, April 13-17. American Chemical Society, Washington, D. C., (1997) PMSE-167.

Horbett, Thomas A.; Kost, Joseph; Ratner, Buddy D. Swelling behavior of glucose sensitive membranes. Polym. Prepr. (Am. Chem. Soc., Div. Polym. Chem.) 24(1), (1983) 34-5.

Hunter, A.; Archer, C. W.; Walker P.S.; Blunn G.W. Attachment and proliferation of osteoblasts and fibroblasts on biomaterials for orthopaedic use. Biomaterials, 16(4), (1995) 287-296.

Hurter, Patricia N.; Scheutjens, Jan M. H. M.; Hatton, T. Alan. Molecular modeling of micelle formation and solubilization in block copolymer micelles. 1. A self-consistent mean-field lattice theory. *Macromolecules* 26(21), (1993) 5592-601.

Hurter, Patricia N.; Scheutjens, Jan M. H. M.; Hatton, T. Alan. Molecular modeling of micelle formation and solubilization in block copolymer micelles. 2. Lattice theory for monomers with internal degrees of freedom. *Macromolecules* 26(19), (1993) 5030-40.

Ishihara, Kazuhiko; Kobayashi, Mineko; Ishimaru, Naoshi; Shinohara, Isao. Glucose-induced permeation control of insulin through a complex membrane consisting of immobilized glucose oxidase and a polyamine. *Polym. J. (Tokyo)* 16(8), (1984) 625-31.

Ishihara, Kazuhiko; Matsui, Kiyohide. Glucose-responsive insulin release from polymer capsule. J. Polym. Sci., Part C: Polym. Lett. 24(8), (1986) 413-17.

Johnston, Thomas P.; Miller, Susan C. Inulin Disposition Following Intramuscular Administration of an Inulin/Poloxamer Gel Matrix. *J. Parenter. Sci. Technol.* 43(6), (1989) 280-285.

Lascelles, S. F.; Malet, F.; Mayada, R.; Billingham, N. C.; Armes, S. P. Latex Syntheses Using Novel Tertiary Amine Methacrylate-Based Macromonomers Prepared by Oxyanionic Polymerization. *Macromolecules* 32(8), (1999) 2462-2471.

Lee, Jang-Won; Park, Eun-Seok; Chi, Sang-Cheol. Solubilizaion of Ibuprofen in Aqueous Solution. *J. Kor. Pharm. Sci.* 27(4), (1997) 279-286.

Lijima, Michihiro; Nagasaki, Yukio; Kato, Masao; Kataoka, Kazunori. A potassium alcoholate-initiated polymerization of 2-(trialkylsiloxy)ethyl methacrylate. *Polymer* 38(5), (1997) 1197-1202.

Maloney WJ, Peters P, Engh CA, Chandler H. Severe osteolysis of the pelvis in association with acetabular replacement without cement. *J Bone Joint Surg* 75A, (1993) 1627-1635.

Malmsten, M.; Lindman, B. Self-assembly in aqueous block copolymer solutions. *Macromolecules.* 25, (1992) 5540-5445.

Moore, Theodore; Cray, Scott; Mallapragada, Surya; Pandt, Nivedita. Experimental Investigation and Mathematical Modeling of Pluronic® F127 Gel Dissolution: Drug Release in Stirred Systems. *Journal of Controlled Release.* 67, (2000) 191-202.

Morrison, G.; Macnair, R.; MacDonald, C.; Wykman, A.; Goldie, I., Grant, M.H.. *In vitro* biocompatibility testing of polymers for orthopaedic implants using cultured fibroblasts and osteoblasts. *Biomaterials*, 26(13), (1995) 987-992.

Nagasaki, Yukio; Sato, Yasuo; Kato, Masao. A novel synthesis of semitelechelic functional poly(methacrylate)s through an alcoholate-initiated polymerization. Synthesis of poly[2-(N,N-diethylaminoethyl) methacrylate] macromonomer. *Macromol. Rapid Commun.* 18(9), (1997) 827-835.

Ottenbrite, Raphael M; Fadeeva, Natalya. Polymer Systems for Biomedical Applications: An Overview. In Polymeric Drugs and Drug Administration, Ottenbrite, Raphael M., ed. American Chemical Society, Washington D.C. (1994) 1-13.

Pandit, Nivedita K.; Kisaka, Justin. Loss of Gelation Ability of Pluronic® F127 in the Presence of some Salts. *Int. J. Pharm.* 145, (1996) 129-136.

Pandit, Nivedita K.; Wang, Diana. Salt effects on the diffusion and release rate of propranolol from poloxamer 407 gels. *Int. J. Pharm.* 167(1-2), (1997) 183-189.

Patwardhan, S. A.; Das K. G. An overview of Controlled-Release Technology. In *Controlled Release Technology*. Das, K. G. ed. John Wiley & Sons, New York, (1993) 1-14.

Safwat, Salwa M.. Drug release from pluronic gels. *Bull. Pharm. Sci., Assiut Univ.* 17(1), (1994) 41-8.

Schwarte, Lisa M.; Peppas, Nikolaos A. Novel poly(ethylene glycol)-grafted, cationic hydrogels: preparation, characterization and diffusive properties. *Polymer* 39(24), (1998) 6057-6066.

Shen, Youqing; Zeng, Faquan; Zhu, Shiping; Pelton, Robert. Novel Cationic Macromonomers by Living Anionic Polymerization of (Dimethylamino)ethyl Methacrylate. *Macromolecules* 34(2), (2001) 144-150.

Standard practice for direct contact cell culture evaluation of materials for medical devices – Designation F813-83. In: The 2000 Annual Book of ASTM Standards, Philadelphia, (2000) 240-243.

Standard test method for agar diffusion cell culture screening for cytotoxicity – Designation F895-84. In: The 2000 Annual Book of ASTM Standards, Philadelphia, (2000) 254-257.

Standard practice selecting generic biological test methods for materials and devices – Designation F748-98. In: The 2000 Annual Book of ASTM Standards, Philadelphia, (2000) 209-215.

Wang, P; Johnston, T. P. Kinetics of Sol-to-Gel Transition for Poloxamer Polyols. *J. Appl. Polym. Sci.* 43, (1991) 283-292.

Wanka, G.; Hoffmann, H.; Ulbricht, W. The aggregation behavior of poly(oxyethylene)-poly(oxypropylene)-poly(oxyethylene) block copolymers in aqueous solution. *Colloid Polym. Sci.* 268(2), (1990) 101-17.

Wanka, G.; Hoffmann, H.; Ulbricht, W. Phase Diagrams and Aggregation Behavior of Poly(oxyethylene)-Poly(oxypropylene)-Poly(oxyethylene) Triblock Copolymers in Aqueous Solutions. *Macromolecules.* 27, (1994) 4115-4159.

Wu, Guangwei; Chu, Benjamin; Schneider, Dieter K. SANS Study of the Micellar Structure of PEO/PPO/PEO Aqueous Solution. *J. Phys. Chem.* 99(14), (1995) 5094-101.

Vadnere, Madhu; Amidon, Gordon; Lindenbaum, Siegfried; Haslam, John L. Thermodynamic Studies on the Gel-Sol Transition of Some Pluronic Polyols. *Int. J. Pharm.* 22, (1984) 207-218.

Yang, Lin; Talukdar, Suddha S.; Alexandridis, Paschalis. Controlled Drug Release from Poloxamer Formulations: Diffusion vs. Erosion Mechanism. *Polym. Prepr.* 40(1), (1999) 347-348.

CHAPTER 2. Understanding Drug Release from Poly(ethylene oxide)-*b*-poly(propylene oxide)-*b*-poly(ethylene oxide) Gels

A paper published in the Journal of Controlled Release[1]

Brian C. Anderson[2], Nita K. Pandit[3], Surya K. Mallapragada[2]

Abstract

Experimental and mathematical studies were performed to understand the release

mechanism of small molecular weight compounds from poly(ethylene oxide)-*b*-

poly(propylene oxide)-*b*-poly(ethylene oxide) polymer gels (trademarked Pluronic® by

BASF Corp.) of various concentrations. Studies of the diffusion coefficient of solutes in the

polymer gels were performed using a novel technique to predict movement of drugs within

the gel as release occurs. Studies were also performed to determine the diffusion coefficient

of water in the polymer gel, as it is this parameter that controls the dissolution rate of the

polymer, and in turn, the drug release rate. A model was formulated and solved numerically

to determine the controlling release mechanism. By parameter modification, this algorithm

for determining the overall mass of drug released from a drug loaded gel can be used for a

number of drugs and for a wide range of initial polymer concentrations. Drug release data

were obtained with a novel experimental setup and were used to verify the accuracy of the

overall solution of the model. The results of the model indicate that although the rate of

polymer dissolution ultimately controls the drug release, about 5% of the release is due to

---

diffusion at the gel/liquid interface, giving rise to a slightly non-linear release. It was also found that agitation speed greatly affects the dissolution rate of these polymer gels.

Introduction

Many drug delivery systems have been developed to achieve zero order release kinetics, so that the drug is delivered at the same rate over the release life of the system. Recent trends have been to develop and characterize novel systems that go beyond zero order release kinetics and have other characteristics that make the delivery device preferential to other choices of delivery methods. One such system that has been extensively studied is the thermoreversible non-crosslinked hydrogel created by aqueous solutions of poly(ethylene oxide)-*b*-poly(propylene oxide)-*b*-poly(ethylene oxide) (Trade named Pluronic® by BASF and also known as Poloxamer).

These polymers, specifically analogs that have a high PEO content, seem to have the desirable property of zero order release kinetics for geometries where the surface area is not changing and have other properties that can be exploited to make them successful drug delivery devices [1-5]. At low temperatures (~0°C), the polymeric solution containing the drug to be released is a liquid that can be injected into the body via a syringe. At a higher temperature (slightly above 5°C for the particular concentrations and polymer compositions studied), the polymers in solution form micelles with the hydrophobic poly(propylene oxide) (PPO) forming a core that is surrounded by the hydrophilic poly(ethylene oxide) (PEO) [6-18]. This formation of a two-phase mixture (aqueous phase and micellar microphase) allows

³ Department of Pharmacy, Drake University, Des Moines, IA, 50311

hydrophobic drugs to be dissolved in higher concentrations than would normally be achieved in a pure aqueous solution [19-24]. This effect becomes quite important for relatively water-insoluble drugs like ibuprofen [19] with a water solubility of approximately .01 mg/ml. [25] As the temperature of this micellar solution increases to body temperature upon sub-cutaneous or intramuscular injection, the micelles begin to entangle with other micelles provided the molecular weight of the polymer and the ratio of PEO/PPO is high enough. For the particular Pluronic® formulation we investigated, F127 (70% ethylene oxide, $\overline{M_n}$ = 12,600), this concentration is about 20% w/w at 37°C. The entangled micelles form a gel inside the body, thereby eliminating the need for surgery to implant the device. The properties of this gelation process have been extensively studied [26-29]. Once in the body, the gel begins to draw water from its surroundings and dissolve, causing drug release that is dependent on the dissolution of the gel, which is a zero order process.

There has been some research on the drug delivery properties of this polymer, but most either do not address the actual drug release mechanism or use empirical methods to determine the mechanism [30-34]. In addition, most studies use an experimental setup that is stirred in such a way that the agitation rate influences the release rate by adding shear on the gel/liquid surface [30,32,34]. In other cases, experimental setups were used where the gel was trapped by a membrane [31,33]. A model has been developed to predict gel dissolution rates at high agitation rates, but fails under low agitation rates [34]. Models also exist for polymer dissolution controlled release systems that provide insight into the mechanics of the dissolution but do not address the effect of agitation on the dissolution process. [35-40] We investigated the characteristics of the drug release of small molecular weight molecules *in vitro* to determine the effects of drug diffusion and polymer dissolution by formulation of a

model that numerically solves mass transport equations governing the system. The experimental setup was constructed in such a way so that there is not an added effect of agitation rate due to shear forces. This leads to an understanding of the parameters needed to control the release of drugs from Pluronic® gels and provides insight into possible limitations of this device. It is also thought that this reflects the conditions seen in the human body more accurately.

Materials and Methods

Chemicals- Culture tested Pluronic® F127 was obtained from Sigma Corp. (St. Louis, MO) and used with no purification for all studies. Solutions were made from the F127 by dissolution in ultrapure water at 2°C until no solids were visible. The dyes Nile Blue Chloride (NBCl, visible absorbance maximum at 636 nm, MW=375.0), toluidine blue O (TBO, visible absorbance maximum at 626 nm, MW=305.0), and chromotrope 2R (C2R, visible absorbance maximum at 508 nm, MW=468.37) and the drug metronadiazole (MNZ, UV absorbance maximum at 319 nm, MW=171.2) were also obtained from Sigma and was used for the release and diffusion studies. These chemicals were chosen because of their specific water solubility and small molecular weight, as this was the focus of this study. The low water solubility of NBCl and TBO was focused on because of the benefit that Pluronics® add to delivering drugs that normally are not soluble in aqueous solutions. C2R was used to verify the application to more water soluble drugs.

Methods- *Overall Approach* – In order to model the drug release from Pluronic[®] gels

in a manner that would enable prediction of release rates for different drug and polymer

compositions, several aspects need to be investigated. The solubility of the drug in Pluronic[®]

formulations, the diffusion rate of drugs within the gel, and the diffusion rate of water into

the gel are all important parameters needed for the model that were measured. This

information was then used to numerically solve the moving boundary problem that represents

the dissolving polymer gel. A schematic representation of the overall physics of the situation

is given as Fig. 1. This representation predicts that there will be a period of time (t=0 to

t=t_{qss}) where the drug release will be controlled by Fickian diffusion of the drug. In this step

the diffusion of drug from the gel is important. The faster the diffusion, the more drug can be

released at this time and vice-versa. After t_{qss}, the controlling factor for the release is the rate

of polymer dissolution, which is controlled by the diffusion coefficient of water in the gel.

Both of these diffusional properties appear to be important.

Preparation of Gels – The polymer gels were prepared by adding a mass of the solid

polymer to an appropriate amount of ultrapure water. The polymer/water mixture was then

cooled to ~2°C until all the solids were dissolved, usually for 24-48 hours depending on the

concentration of solids and the total mass of sample.

Drug Diffusion within the Polymer Gel - In order to assess the diffusion coefficient of

a solute through a polymer hydrogel, a thin film of the material is often tested in a membrane

diffusion cell to obtain the solute diffusion coefficient. In the case of a non-crosslinked water

soluble hydrogel this does not work because an equilibrium swollen state does not exist.

Therefore a novel image analysis based technique was developed. A gel, free of drug, was

placed in the bottom half of a square glass vial and allowed to reach equilibrium at 37°C.

This gel was prepared by dissolution of the solid polymer in 2°C water for 48 hours. Another formulation with the same polymer concentration was loaded with the dye toluidine blue O. This dye was chosen because its molecular weight is comparable to the drugs that are of interest in this study, and the brilliant blue color is easy to analyze using image analysis. The gel loaded with dye was then filled in the remaining half of the vial and also maintained at 37°C. At set time points, the vial was placed into an apparatus that had been fabricated to allow light from a halogen lamp to enter from the back of the vial and pass through the gel normal to the front of a SLR camera (Cannon T60) equipped with a macro lens (Fig. 2). These photos were digitized and analyzed using the imaging software ImagePro for Windows. Using a non-linear calibration curve made from known concentrations of dye, the images were converted to concentrations, and a concentration profile for the dye was obtained. These data were fit to the solution of unsteady state Fickian diffusion into a semi-infinite slab in one Cartesian dimension to obtain an estimate for the diffusion coefficient of the small molecular weight solute. The semi-infinite model was used, because the dye was not allowed to reach the finite end of the vial. Three samples were tested for gel concentrations of 20% and 30% w/w, and the experiment was repeated for the dye Nile Blue Chloride.

Diffusion of Water into the Polymer Gel - To obtain data for the diffusion coefficient of water into the Pluronic® gel, a simple system was set up. A 25 ml syringe (2.18 cm ID) had the tapered tip removed, leaving a cylinder with a plunger. To this, 10-15 g of gel at various polymer concentrations were added and allowed to reach equilibrium at 37°C, with the polymer/air interface remaining flat. The syringe was then inverted and submerged in water at 37°C, allowing water to diffuse into the gel (Fig. 3). After a given amount of time,

the syringe was removed from the water and the gel was extruded onto a glass plate after noting the height change in the gel. A metal gel-cutting device was fabricated consisting of thin stainless steel plates spaced at 0.25 cm intervals that can slice through the gel and separate 0.25 cm sections in one cut. Samples from these sections were placed into small containers and weighed. The samples were dried at 37°C under atmospheric conditions for 24 hours and then under vacuum for 6 hours until only the solids were left, and weighed again. This information was then used to calculate the final water concentration of each slice. All measurements were performed in triplicate. The averaged curves were fit to a diffusion equation for Fickian diffusion for a moving boundary problem in one dimension to obtain the value for diffusion coefficient. Interfacial velocities were measured between subsequent time intervals ignoring the first time step. This was done because there is an initial unsteady state that needs to be accounted for, after which a quasi-steady state has formed and subsequent intervals should have the same interfacial velocities.

Overall Drug Release from the Polymer Gel - Measurements of the total mass of drug released from a gel initially loaded with a drug or dye was obtained by placing the loaded gel into a petri dish (7.2 cm ID) fitted with a metal apparatus holding the dish inverted 10 cm above the surface the apparatus rests on (Fig. 4). This setup was placed in a 1000 ml beaker with 700 ml of water that was arranged in a 37°C water bath with a water heater/circulator (Neslab EX-111). After a set amount of time, either the gel was removed from solution and weighed if dissolution data were needed, or a small sample of the receiving water was taken if only release data were needed. The gel was dried and weighed to analyze the amount of total gel and solids lost during that time period. Samples from the 700 ml of water were then analyzed by UV/visible spectrophotometry for drug concentration, allowing for the mass of

solute released to be calculated. This experiment was also performed in a United States Pharmacopoeia approved dissolution apparatus (Hanson Scientific, CA) with the samples held upright under agitation speeds of 20, 40, and 60 RPM as well as under unstirred static conditions where the gel was not inverted. The inverted method was studied because of the ability to use the fully mixed assumption under conditions of no stirring without disturbing the surface of the gel enough to need to take the fluid dynamics of the situation into account. It was seen that visible deformations on the surface were produced under any agitation due to the shear on the gel surface. It appears that the slightly increased density caused by the gel dissolution is enough to cause gentle mixing when the higher density region is above the bulk water. Without inversion, the higher density liquid created as the gel dissolves stays just above the gel surface and prevents further gel from dissolving. Our studies found that there is a marked effect on the release rate as a function of agitation rate when the gels were not inverted and were subjected to any agitation.

Results and Discussion

Diffusion Coefficients in Polymer Gel - *Small Molecule Solute Diffusion* - The diffusion coefficient of TBO and NBCl in Pluronic® gels at 20% and 30% w/w was found to be the same with a value of approximately 3×10^{-7} cm^2/s. This value was used for modeling all drugs and dyes in this molecular weight range. A more accurate value is not essential, because the diffusion of the drug within the gel is so slow compared to the dissolution of the polymer. The non-linearity of the calibration curve contributes to the spread in the value obtained for the diffusion coefficient.

Water Diffusion into the Pluronic® Gel - The method used for this experiment yielded very reproducible results that fit Fickian models for diffusion with a moving boundary quite well. The model the data were fit to was for a moving boundary with Fickian diffusion, given as Eq. 1 with boundary conditions Eqs. 2 and 3. The solution of this equation with the appropriate boundary conditions is given as Eq. 4. In this equation D_w is the diffusion coefficient of water inside the gel, v_I is the velocity of the moving interface, x is the distance from the interface, C is the concentration of water in the gel, C_o is the initial concentration of water in the gel, and C^* is the interfacial water concentration. Fig. 5 is a sample of collected experimental data and the model fit of Eq. 4 from one of the initial polymer concentrations with error bars representing standard deviations. This simple model fit yielded a value for the diffusion coefficient and a profile for the gel concentration near the interface as the gel is dissolving. By noting the distance the gel had moved from its initial interface, a value for the interfacial velocity was measured and plotted as a function of polymer concentration in Fig. 6. The comparison of diffusion coefficients and interfacial velocities are given as a function of polymer concentration in Table 1.

$$-v_I \frac{\partial C}{\partial x} = \frac{\partial}{\partial x}\left(D_w \frac{\partial C}{\partial x}\right) \tag{1}$$

$$\textit{Boundary Conditions} : C\big|_{x=0} = \text{constant} = C_I \tag{2}$$

$$\frac{\partial C}{\partial x}\bigg|_{x=\infty} = 0 \tag{3}$$

$$C(x) = (C_i - C_o)\exp\left(\frac{-v_I}{D_w}x\right) + C_o \tag{4}$$

Modeling the Overall Drug Release - To model the drug release, the following

assumptions were made: (i) the bulk liquid surrounding the gel is pure water, (ii) the drug can

freely diffuse out of the gel at the interface based on Fickian diffusion through a thin film

into the bulk, (iii) the drug diffusion coefficient through this thin film can be estimated by the

Stokes-Einstein equation, and (iv) the dissolution of the polymer gel and drug diffusion at the

surface occur concurrently. These assumptions seem valid because (i) the concentrations of

solute and polymer in the receiving water are low, (ii) there is nothing that would stop drug

diffusion from occurring at the interface, (iii) the drug diffusion is taking place in a low

viscosity liquid and the Stokes-Einstein equation is valid for diffusion in dilute solutions and

would be a good estimate, and (iv) dissolution will not stop the drug diffusion due to a

concentration gradient. These assumptions were implemented with the boundary conditions

and initial conditions of continuous flux at the interface (equal to the flux determined from

diffusion through the thin film), zero flux at great distances from the interface, and a

homogeneous starting condition. A numeric solution of Equation 2 was found using the

FORTRAN subroutine DO3PCF written by the Numerical Algorithms Group. In eq. 5 and

the boundary/initial conditions in Eqs. 6-8 D is the diffusion coefficient for Fickian diffusion,

C is the drug or dye concentration, D_{gel} is the diffusion coefficient of the drug or dye inside

the gel, $C_{surface}$ is the interfacial concentration of drug or dye, $\delta_{diffusion}$ is the diffusional

boundary layer, and D_{water} is the diffusion coefficient of the drug or dye in water. This

equation was solved in small time increments with the given boundary conditions until the

time t_{qss}, when the interface of the gel begins to dissolve. The boundary conditions used are

simply steady Fickian diffusion at the interface across a thin boundary layer, a solid

boundary at a long distance from the interface, and a homogeneous initial starting

concentration. At each time step up until this point, the amount of drug released was recorded. A flowchart of this algorithm is given as Fig. 7.

$$\frac{\partial C}{\partial t} = D \frac{\partial^2 C}{\partial x^2} \tag{5}$$

$$\text{Boundary Conditions:} \left. \frac{\partial C}{\partial x} \right|_{x=0} = \frac{C_{surface} D_{water}}{\delta_{diffusion} D_{gel}} \tag{6}$$

$$\left. \frac{\partial C}{\partial x} \right|_{x=\infty} = 0 \tag{7}$$

$$\text{Initial Condition} \quad C_{t=o} = C_o \tag{8}$$

To account for the steadily dissolving boundary, at each time step after t_{qss} the amount of drug released is assumed to be due to both diffusion and the dissolving polymer. To achieve this, the time steps and spatial mesh points were set up so that each mesh point is the amount that the boundary would move in one time step. After each time step the drug that was released due to diffusion was calculated, but then the spatial ordinate was re-scaled by moving the entire concentration profile over by one spatial mesh point. The amount of drug that was trapped in that distance of one mesh point was then calculated and attributed to dissolution based release. This process was then repeated for the remaining time of interest. An estimation of the diffusion coefficient of the solute molecule was obtained using the Stokes-Einstein equation and the initial flux of drug from a loaded gel was used to estimate the thickness of a resistance layer at the gel-water interface.

Data were obtained to compare experimental results with the numerical predictions from the model. The value used for tqss was 2.5 min and was found experimentally by measuring the weight change of dried gels as a function of time. There was a distinct point at 2.5 minutes where the weight change switched from zero to a constant value. Most of the data obtained were from the dyes TBO blue and NBCl due to ease of measurement in the

visible wavelengths. Fig. 8 compares the results from these release experiments to the numerical solution to Eq. 5 with good agreement. Data for another solute, C2R, were also collected at 30% initial polymer concentration and TBO at 22% initial polymer concentration. The comparison of the C2R (30% gel) and TBO (22% gel) data and the model is given in Fig. 9. For the 30% gels, approximately 5% of the release was due to diffusion at the interface while the remainder was due to trapped molecules being released when the gel dissolves. The 22% gel produced a more linear profile with only about 2.5% of the release attributed to the diffusion and the interface due to the increased dissolution rate.

To assess the validity of using the inverted spatial orientation in these experiments, more experiments were performed with the more commonly used setups. The release measurements were made in the same manner, but the dishes of gels were placed upright, and the receiving medium, the bulk water, was stirred at various rates. Measurements of amount of gel dissolved and amount of drug released were taken for 20, 40, 60 and 80 RPM agitation rates in the stirred USP approved dissolution apparatus. The rate of release was determined for each of these speeds. A plot of agitation rate versus both fraction gel dissolved and fraction of drug released plotted along with the data obtained for the inverted static gel setup indicates that the inverted method achieves a release rate slightly less than that of the agitated system under 20 RMP agitation (Fig. 10). Visual inspection of the gels after being subjected to agitated conditions also indicated problems with using a fully agitated system. The surfaces were visibly stressed with swirled patterns forming at the surface in the direction of water movement. This shows that a drug release model either must contain a term that accounts for the fluid dynamic surface effects, or a setup that does not disturb the surface needs to be used. The latter was chosen because of its obvious simplicity compared to

incorporating fluid dynamics. An analysis of the effect of fluid dynamics on surfaces for non-eroding surfaces has been presented by Levich, and the situation is even more complex for eroding surfaces [41]. Studies were also performed where the receiving water was not agitated, and the gel was not inverted. A thick layer of dissolved gel formed above the gel greatly slowing diffusion. The release rates for this setup were an order of magnitude slower with a purely Fickian release profile and were decided to not be indicative of the characteristics of a biological system (Fig. 11). In order to maintain this dissolved layer, the gel has to be perfectly upright with a one-dimensional interface and with no agitation at all, which would not be the case in the body.

Conclusions

The conclusion drawn from this research was that although the rate of dissolution of the Pluronic® gel is actually the controlling factor in the drug release, it is not the only effect. Because the interface is eroding at a constant rate, the surface concentration of drug is held relatively constant and drug diffuses out at a constant rate. More concentrated gels dissolve at a slower rate than less concentrated ones because of the decreased water diffusion coefficient for the rate of water diffusing into the gel. The measurement technique described here allows for a simple and accurate method of diffusion coefficient measurement for a quickly dissolving hydrogel. The measurement of diffusion rate from these gels are greatly influenced by high rates of agitation, which should be avoided by a setup such as described here. When designing controlled release devices using Pluronic® hydrogels, the relative rates

of drug and water diffusion is a factor that changes the way in which the drug is released into the body.

Although these results are interesting, they are still not a perfect model for *in vivo* use. In an *in vivo* situation, the diffusion at the interface would most likely not occur into pure bulk water. There are tissues and other fluids that would impede both the release of drug and dissolution of polymer. However, this model does provide a relative comparison between different Pluronic® devices and gives insight on how to control the release rates of drugs from these devices.

Acknowledgements

References

[1] Johnston, Thomas P.; Miller, Susan C. Inulin Disposition Following Intramuscular Administration of an Inulin/Poloxamer Gel Matrix. *J. Parenter. Sci. Technol.* 43(6), (1989) 280-285.

[2] Bhardwaj, Renu; Blanchard, James. Controlled-Release Delivery System for the a-MSH Analog Melanotan-I Using Poloxamer 407. *Journal of Pharmaceutical Sciences.* 85(9), (1996) 915-919.

[3] Desai, Suketu D.; Blanchard, James. *In Vitro* Evaluation of Pluronic F127-Based Controlled-Release Ocular Delivery Systems for Pilocarpine. *Jounal of Pharmaceutical Sciences.* 87(2), (1998) 266-230.

[4] Johnston, Thomas P.; Punjabi, Monika A.; Froelich, Christopher J. Sustained Delivery of Interleukin-2 from a Poloxamer 407 Gel Matrix Following Intraperitonal Injection in Mice. *Pharmaceutical Research*. 9(3), (1992) 425-433.

[5] Neal, Jonathan C.; Stolink, Snow; Schacht, Etienne; Kenawy, El Rafaie; Garnett, Martin C.; Davis, Stanley S.; Illum, Lisbeth. *In Vitro* Displacement by Rat Serem of Adsorbed Radiolabeled Poloxamer and Poloxamine Copolymers from Model and Biodegradable Nanospheres. *Journal of Pharmaceutical Sciences*. 87(10), (1998) 1242-1248.

[6] Wanka, G.; Hoffmann, H.; Ulbricht, W. Phase Diagrams and Aggregation Behavior of Poly(oxyethylene)-Poly(oxypropylene)-Poly(oxyethylene) Triblock Copolymers in Aqueous Solutions. *Macromolecules*. 27, (1994) 4115-4159.

[7] Armstrong, Jonathan K.; Parsonage, John; Chowdhry, Babur; Leharne, Stephan; Mitchell, John; Beezer, Anthony; Lohner, Karl; Laggner, Peter. Scanning Densitometric and Calorimetric Studies of Poly(ethylene oxide)/Poly(propylene oxide)/Poly(ethylene oxide) Triblock Copolymers (Poloxamers) in Dilute Aqueous Solution. *Journal of Physical Chemistry*. 97, (1993) 3904-3909.

[8] Chu, Benjamin. Structure and Dynamics of Block Copolymer Colloids. *Langmuir*. 11, (1995) 414-421.

[9] Tanodekaew, Siriporn; Deng, Nan-Jie; Smith, Sibyl; Yang, Yung-Wei; Attwood, David; Booth, Colin. Micellation and Gelation of block-Copoly(oxyethylene/oxybutylene) in Aqueous Solutions. *J. Phys. Chem.* 97, (1993) 11847-11852.

[10] Alexandridis, Paschalis; Holzwarth, Josef F.; Hatton, T. Alan. Micellization of Poly(ethylene oxide)-Poly(propylene oxide)-Poly(ethylene oxide) Triblock Copolymers in Aqueous Solutions: Thermodynamics of Copolymer Association. *Macromolecules*. 27, (1994) 2414-2425.

[11] Beezer, A. E.; Loh, W.; Mitchell, J. C.; Rowall, P. G.; Smith, D. O.; Tute, M. S.; Armstrong, J. K.; Chowdhry, B. Z.; Leharne, S. A.; Eagland, D.; Crowther, N. J. An Investication of Dilute Aqueous Phase Behavior of Poly(oxyethylene)+Poly(oxypropylene)+Poly(oxyethylene) Block Copolymers. *Langmuir*. 10, (1994) 4001-4005.

[12] Wanka, G.; Hoffmann, H.; Ulbricht, W. Phase Diagrams and Aggregation Behavior of Poly(oxyethylene)-Poly(oxypropylene)-Poly(oxyethylene) Triblock Copolymers in Aqueous Solutions. *Macromolecules*. 27, (1994) 4115-4159.

[13] Mortensen, Kell; Brown, Wyn; Jorgensen, Erling. Phase Behavior of Poly(proplene oxide)- Poly(ethylene oxide)-Poly(propylene oxide) Triblock Coploymer Melt and Aqueous Solutions. *Macromolecules*. 27, (1994) 5654-5666.

[14] Zhou, Zukang; Chu, Benjamin. Phase Behavior and Associatin Properties of Poly(oxypropylene)-Poly(oxyethylene)-Poly(oxypropylene) Triblock Copolymer in Aqueous Solution. *Macromolecules*. 27, (1994) 2025-2033.

[15] Mortesen, K. Phase Behaviour of Poly(ethylene oxide)-Poly(propylene oxide)-Poly(ethylene oxide) Triblock-Copolymer Dissolved in Water. *Europhys. Lett.* 19(7), (1992) 599-604.

[16] Kabanov, Alexander V.; Nazarova, Irina R.; Astafieva, Irena V.; Batrakova, Elena V.; Alakhov, Valery Yu.; Yaroslavov, Alexander A.; Kabanov, Victor A. Micelle Formation and Solubilization of Florescent Probes in Poly(oxyethylene-b-oxypropylene-b-oxyethylene) Solutions. *Macromolecules*. 28, (1995) 2303-2314.

[17] Nagarajan, R.; Ganesh, K. Block Coploymer Self-Assembly in Selective Solvents: Spherical Micelles with Segregated Cores. *J. Chem. Phys.* 90(10), (1989) 5843-5856

[18] Wanka, G.; Hoffmann, H.; Ulbricht, W. The Aggregation Behavior of Poly-(Oxyethylene)-Poly-(Oxypropylene)-Poly-(Oxyethylene)-Block-Copolymers in Aqueous Solution. *Colloid Poly. Sci.* 268, (1990) 101-117.

[19] Lee, Jang-Won; Park, Eun-Seok; Chi, Sang-Cheol. Solubilizaion of Ibuprofen in Aqueous Solution. *J. Kor. Pharm. Sci.* 27(4), (1997) 279-286.

[20] Hurter, Particia; Hatton, T. Alan. Solubilization of Polycyclic Aromatic Hydrocarbons by Poly(ethylene oxide-propylene oxide) Block Copolymer Micelles: Effects of Polymer Structure. *Langmuir*. (1992) 8, 1291-1299.

[21] Jafert, Chad T; Van Hoof, Patricia L.; Heath, Janice. Solubilization of Non-Polar Compounds by Non-Ionic Micelles. *Wat. Res.* 28(5), (1994) 1009-1017.

[22] Mailk-Nubarov, N. S.; Kozlov, M. Yu. Evaluation of Partition Coefficients of Low Molecular Weight Solutes Between Water and Micelles of Block Copolymer of Ethylene Oxide based on Dialysis Kinetics and Fluorescence Spectroscopy. *Colloid. Polym. Sci.* 276, (1998) 381-387.

[23] Saettone, Marco F.; Giannaccini, Boris; Delmonte, Giuseppe; Campigli, Vincenzo; Tota, Giovanni; Marca, Filippo. Solubilization of Tropicamide by Poloxamers: Physicochemical Data and Activity Data in Rabbits and Humans. *Int. J. Pharm.* 43, (1988) 67-76.

[24] Krishna, Aravind K; Flanagain, Douglas R. Micellar Solubilization of a New Antimalarial Drug, β-Arteether. *J. Pharm. Sci.* 78(7), (1989) 574-576.

[25] Fini, Adamo; Laus, Michele; Orienti, Isabella; Zecchi, Vittorio. Dissolution and partition thermodynamic functions of some nonsteroidal anti-inflammatory drugs. *J. Pharm. Sci.* 75(1), (1986) 23-5.

[26] Cabana, Alain; Ait-Kadi, Abdellatif; Juhasz, Julianna. Study of the Gelation Process of Polyethylene Oxide$_a$-Polypropylene Oxide$_b$-Polyethylene Oxide$_a$ Copolymer (Poloxamer 407) Aqueous Solutions. *J. Colloid. Int. Sci.* 190, (1997) 307-312.

[27] Vadnere, Madhu; Amidon, Gordon; Lindenbaum, Siegfried; Haslam, John L. Thermodynamic Studies on the Gel-Sol Transition of Some Pluronic Polyols. *Int. J. Pharm.* 22, (1984) 207-218.

[28] Wang, P; Johnston, T. P. Kinetics of Sol-to-Gel Transition for Poloxamer Polyols. *J. Appl. Polym. Sci.* 43, (1991) 283-292.

[29] Pandit, Nivedita K.; Kisaka, Justin. Loss of Gelation Ability of Pluronic® F127 in the Presence of some Salts. *Int. J. Pharm.* 145, (1996) 129-136.

[30] Chi, Sang C.; Jun, H. W. Release Rates of Ketoprofen from Poloxamer Gels in a Membraneless Diffusion Cell. *J. Pharm. Sci.* 80(3), (1991) 280-283.

[31] Safwat, Salwa M. Drug Release From Pluronic Gels. *Bull. Pharm. Sci.* 17(1), (1994) 41-48.

[32] Yang, Lin; Talukdar, Suddha S.; Alexandridis, Paschalis. Controlled Drug Release from Poloxamer Formulations: Diffusion vs. Erosion Mechanism. *Polym. Prepr.* 40(1), (1999) 347-348.

[33] Gilbert, Julian C.; Hadgraft, Jonathan; Bye, Alan; Brookes, Leonard G. Drug Release From Pluronic F-127 Gels. *Int. J. Pharm.* 32, (1986) 233-228.

[34] Moore, Theodore; Cray, Scott; Mallapragada, Surya; Pandt, Nivedita. Experimental Investigation and Mathematical Modeling of Pluronic® F127 Gel Dissolution: Drug Release in Stirred Systems. *Journal of Controlled Release.* 67, (2000) 191-202.

[35] Narasimhan, Balaji; Peppas, Nikolaos A. Molecular Analysis of Drug Delivery Systems Controlled by Dissolution of the Polymer Carrier. *J. Pharm. Sci.* 86(3), (1987) 297-304.

[36] Ju, Robert T. C.; Nixon, Phillip R.; Patel, Mahesh V. Drug Release from Hydrophobic Matrices. 1. New Scaling Laws for Predicting Polymer and Drug Release Based on the Polymer Disentanglement Concentration and the Diffusion Later. *J. Pharm. Sci.* 84(12), (1995) 1455-1463.

[37] Ju, Robert T. C.; Nixon, Phillip R.; Patel, Mahesh V. Drug Release from Hydrophobic Matrices. 2. A Mathematical Model Based on the Polymer Disentanglement Concentration and the Diffusion Layer. *J. Pharm. Sci.* 84(12), (1995) 1464-1477.

[38] Lee, Ping I.; Peppas, Nikolaos A. Prediction of Polymer Dissolution in Swellable Controlled-Release Systems. *J. Controlled Release.* 6, (1987) 207-215.

[39] Grassi, Mario; Lapasin, Romano; Pricl, Sabrina; Colombo, Italo. Apparent Non-Fickian Release from a Scleroglucan Gel Matrix. *Chem. Eng. Commun.* 155, (1997) 89-112.

[40] Edwards, David A.; Cohen, Donald S. A Mathematical Model for a Dissolving Polymer. *AIChE Journal.* 41(11), (1995) 2345-2355.

[41] Levich, V. G. *Physicochemical Hydrodynamics.* Prentice Hall, Inc., Englewood, New Jersey, 1962.

Table 1 – Water diffusion coefficients and interfacial velocities for some initial polymer concentrations

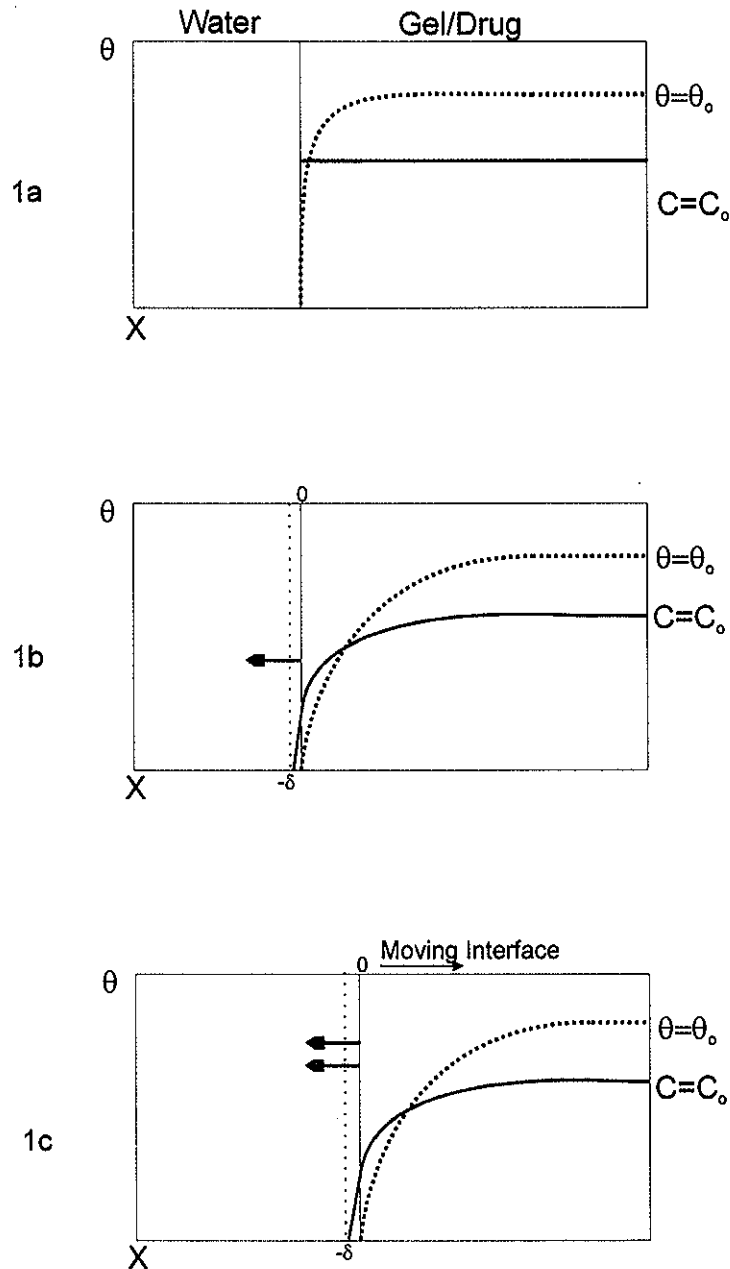| Gel Concentration (wt%)	D_w (cm^2/s)	v_I (cm/hour)
24	4.3	0.045
27	3.4	0.033
30	2.3	0.029

Figure 1 - Schematic depicting the physical situation of gel dissolution / drug release (θ-polymer concentration —— , C-Drug concentration - - - -, - release of drug/polymer into bluk water). 1a. ($t=0^+$) – Water begins to diffuse into gel. 1b. ($t<t_{qss}$) – Water continues to diffuse into gel lowering polymer concentration, drug diffuses out into bulk water. 1c. ($t>t_{qss}$) – Polymer concentration has achieved steady profile and moves right at constant velocity, drug continues to diffuse out at a rate based on $C(x=0)$ and $dC/dt(x=0)$.

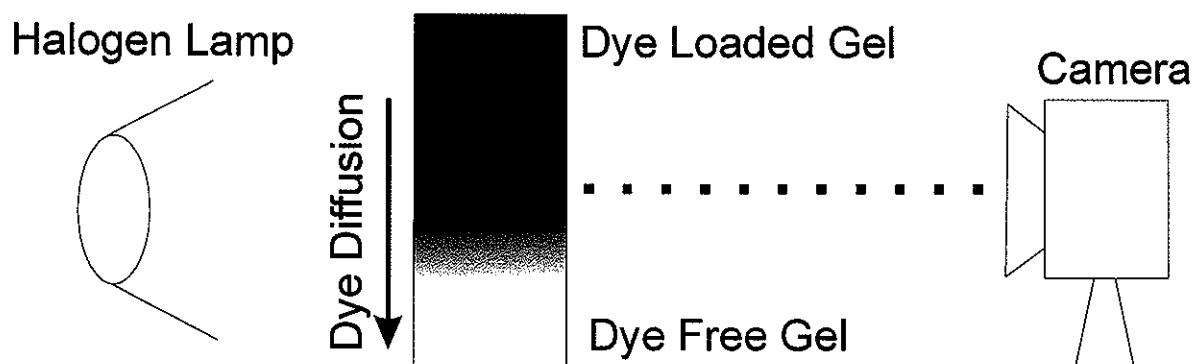**Figure 2** – Setup used for visually analyzing the diffusion rate of molecules through the Pluronic® gel.
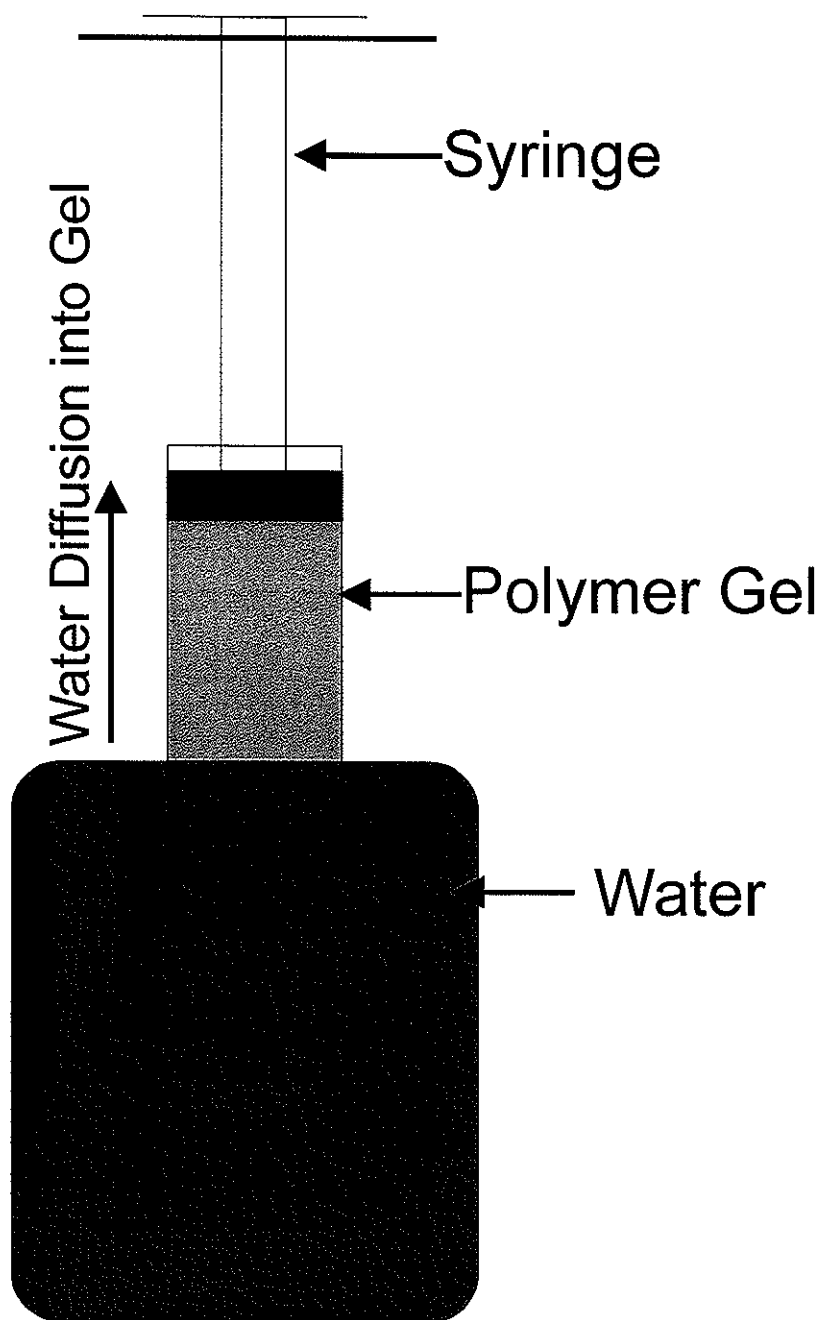
Figure 3 – Setup used for determining the diffusion coefficient of water in gel.

Top View

Legs

Petri dish with gel -
(gel exposed)

Steel holding plates

Side View

Steel holding plates

Petri dish with gel -
(gel exposed)

Legs
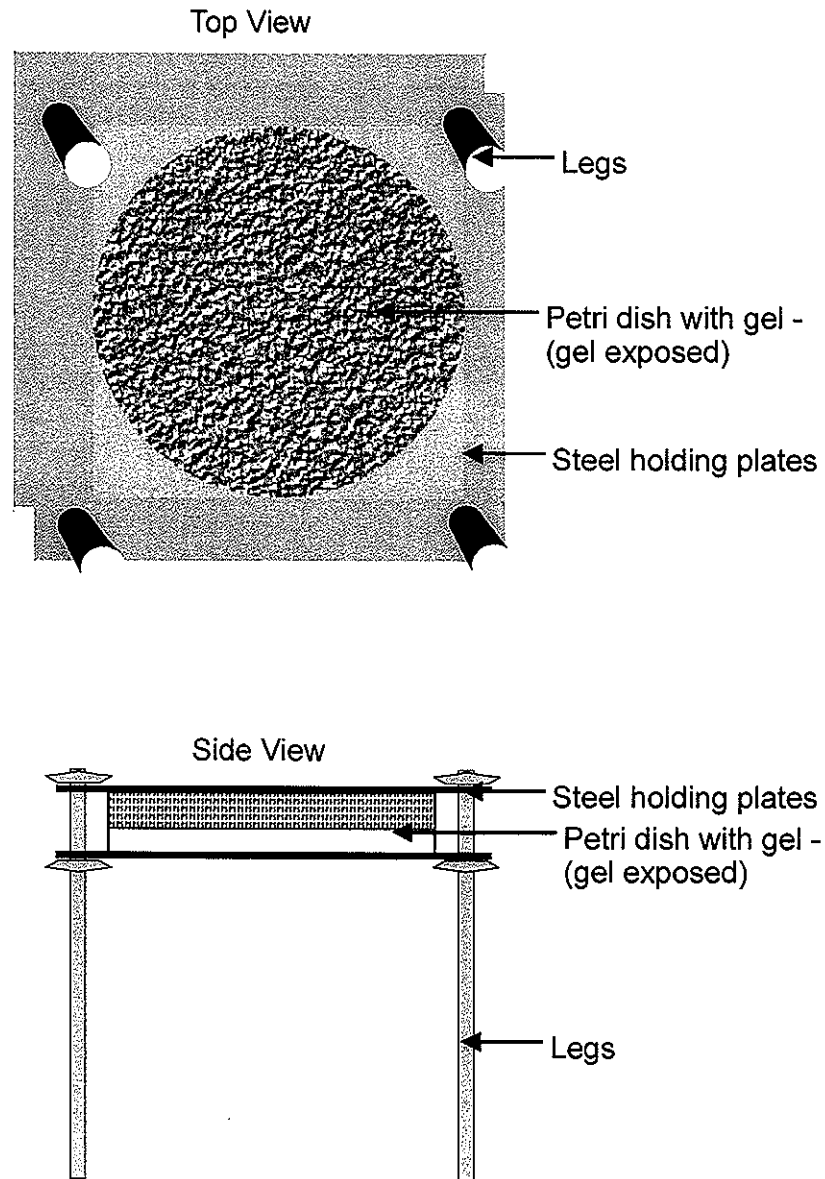
Figure 4 – Schematic of inverted gel holder.
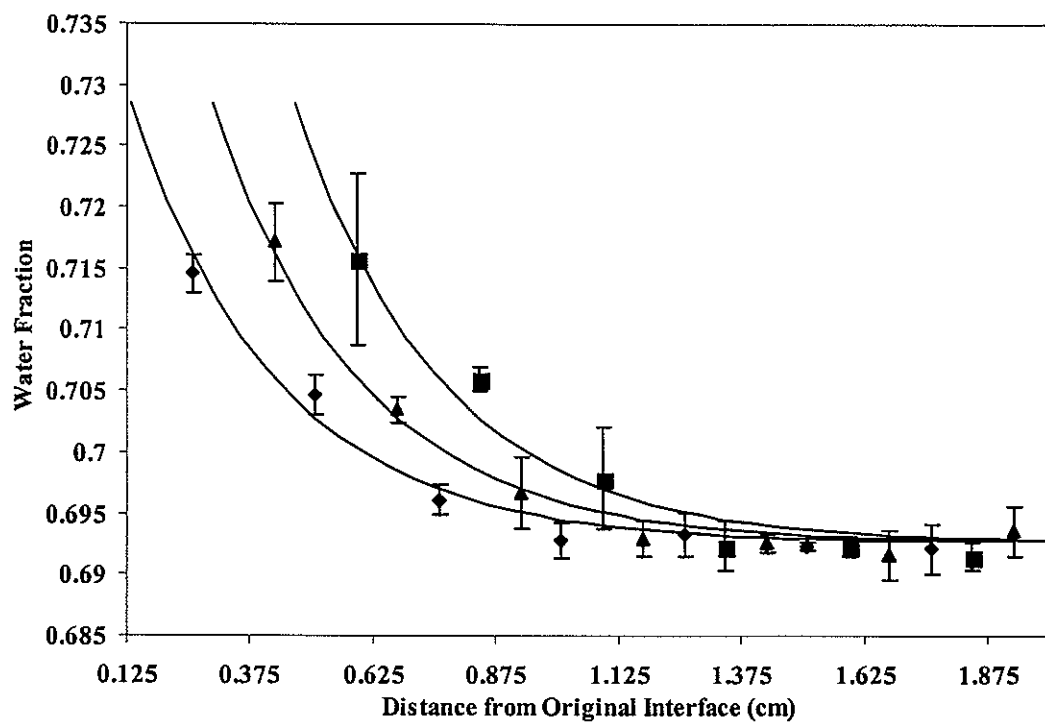
Figure 5 – Comparison of water diffusion data to Fickian diffusion model – 30% w/w Pluronic® F127. The data points represent water fraction remaining after (♦-1 hour, ▲-2 hours, ■-3 hours) and the lines represent the Fickian diffusion model.
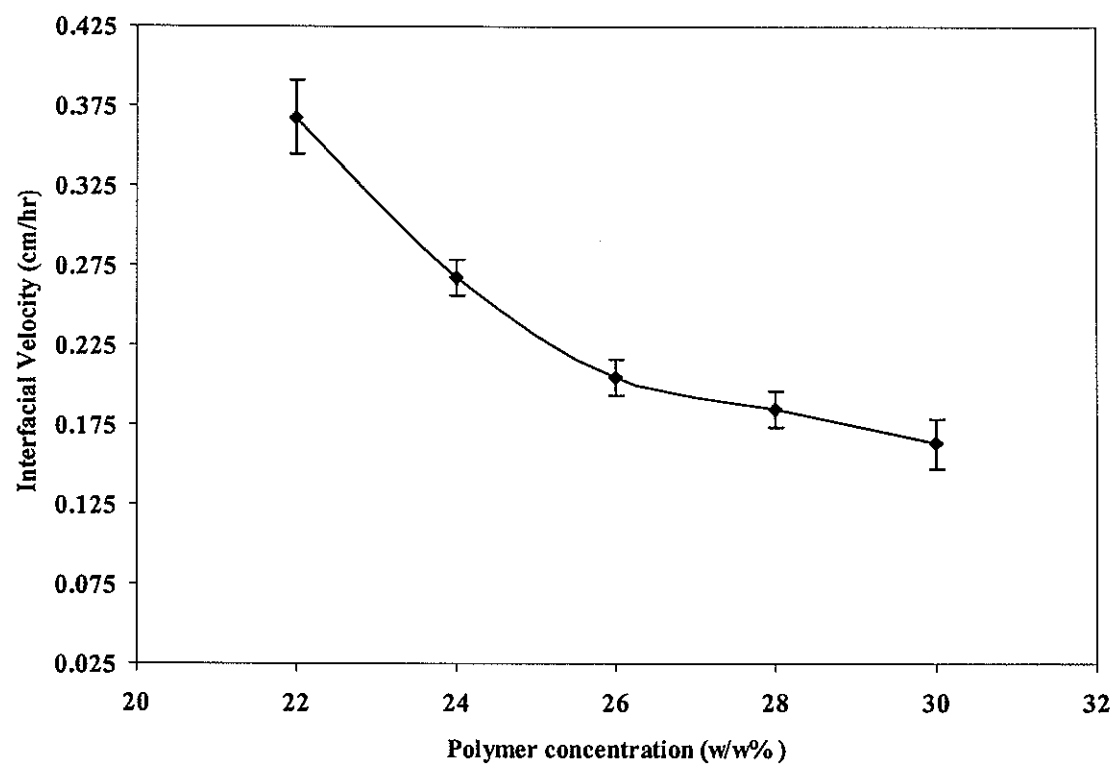
Figure 6 – Plot of interfacial velocity versus polymer concentration
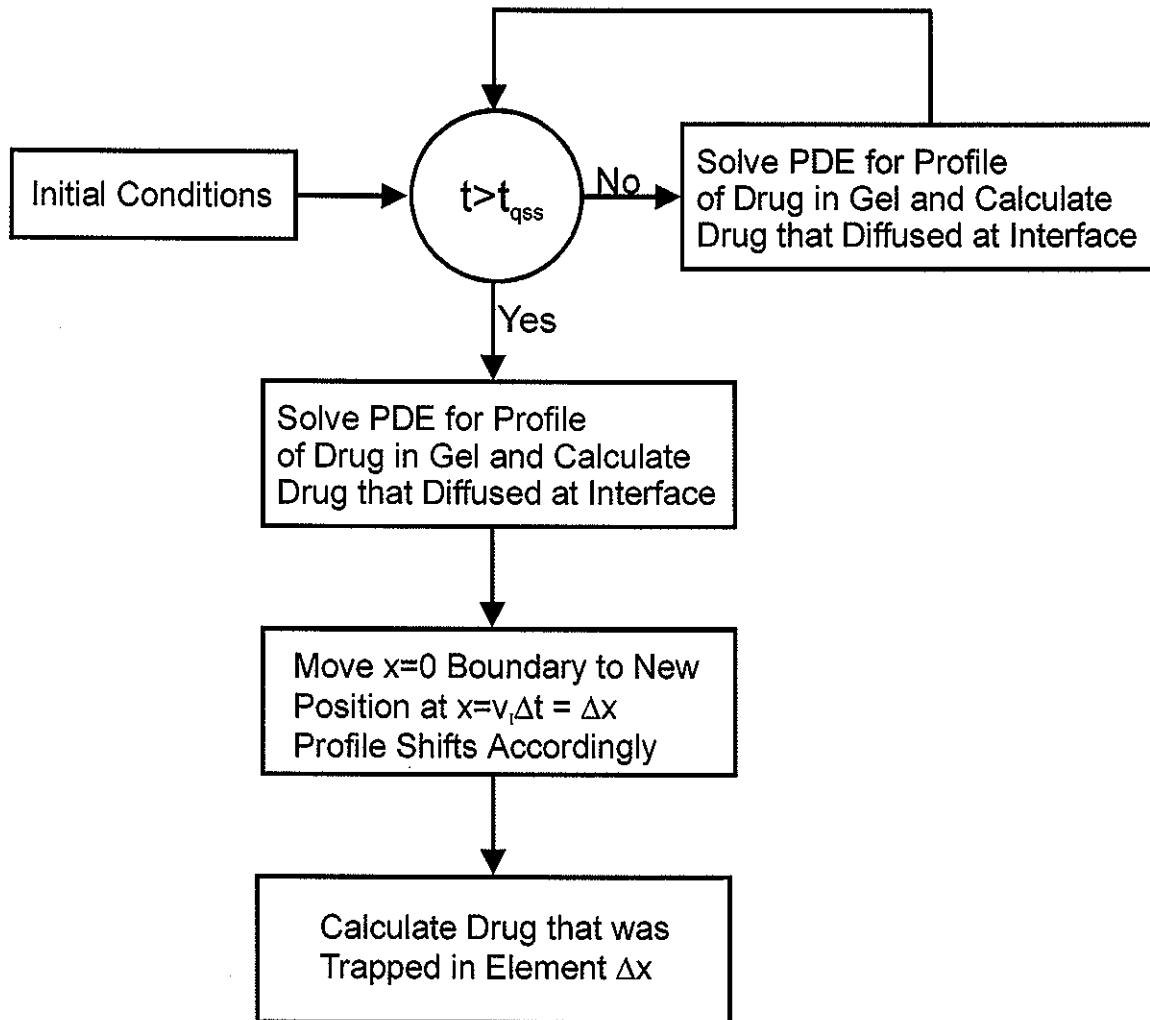
Figure 7 – Algorithm for numerically solving dissolution/diffusion problem
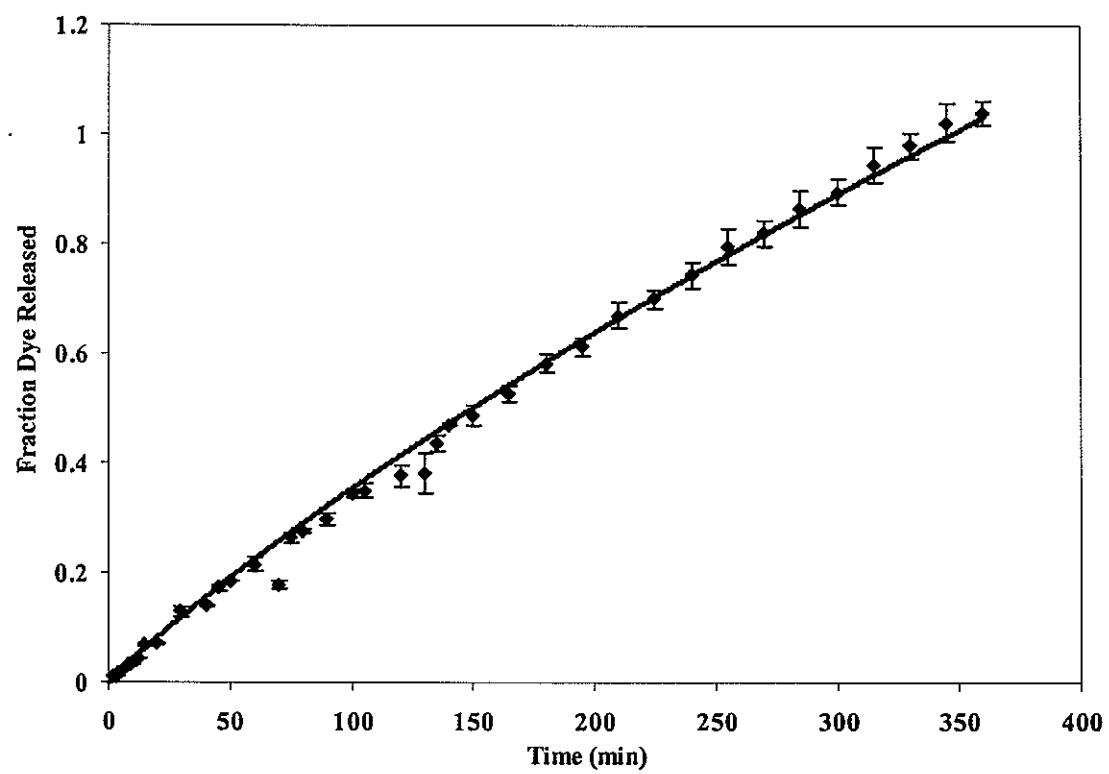
Figure 8 – Comparison of model to release data for toluidine blue O and nile blue chloride from 30% w/w Pluronic[®] F127 in water. The line represents the model.
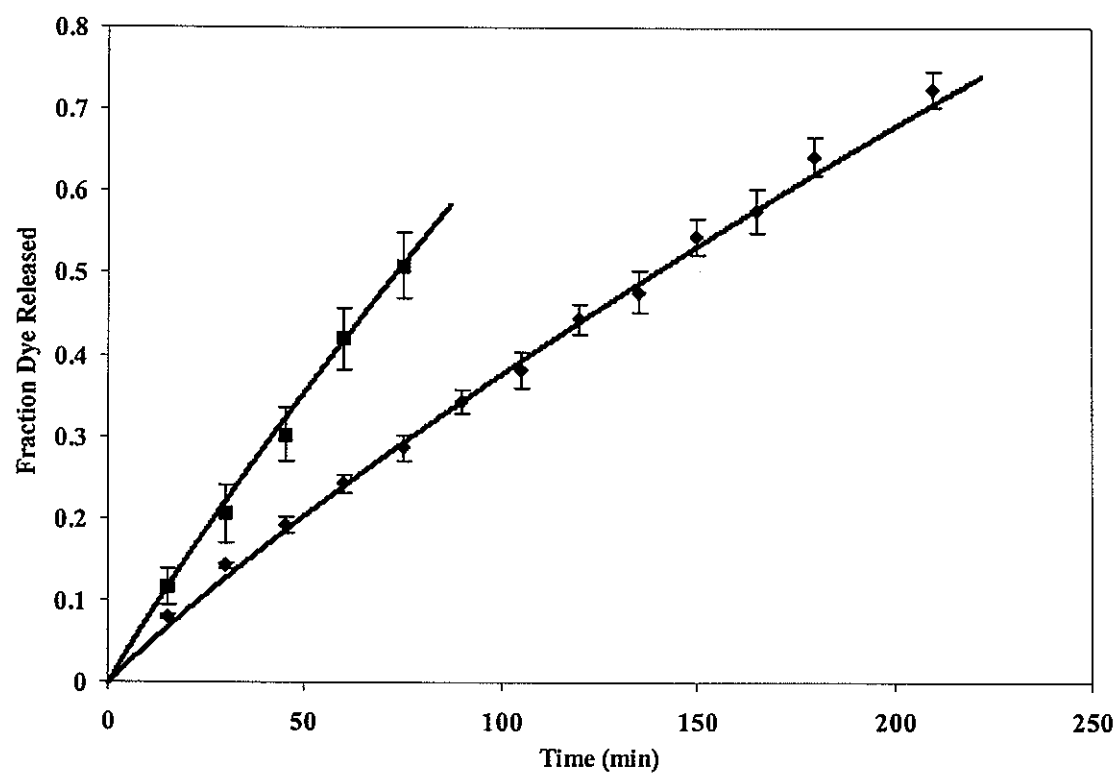
Figure 9 – Comparison of model to release data for chromotrope 2R, 30% w/w Pluronic® F127 in water (♦) and toluidine blue O, 24% w/w Pluronic® F127 in water(■).
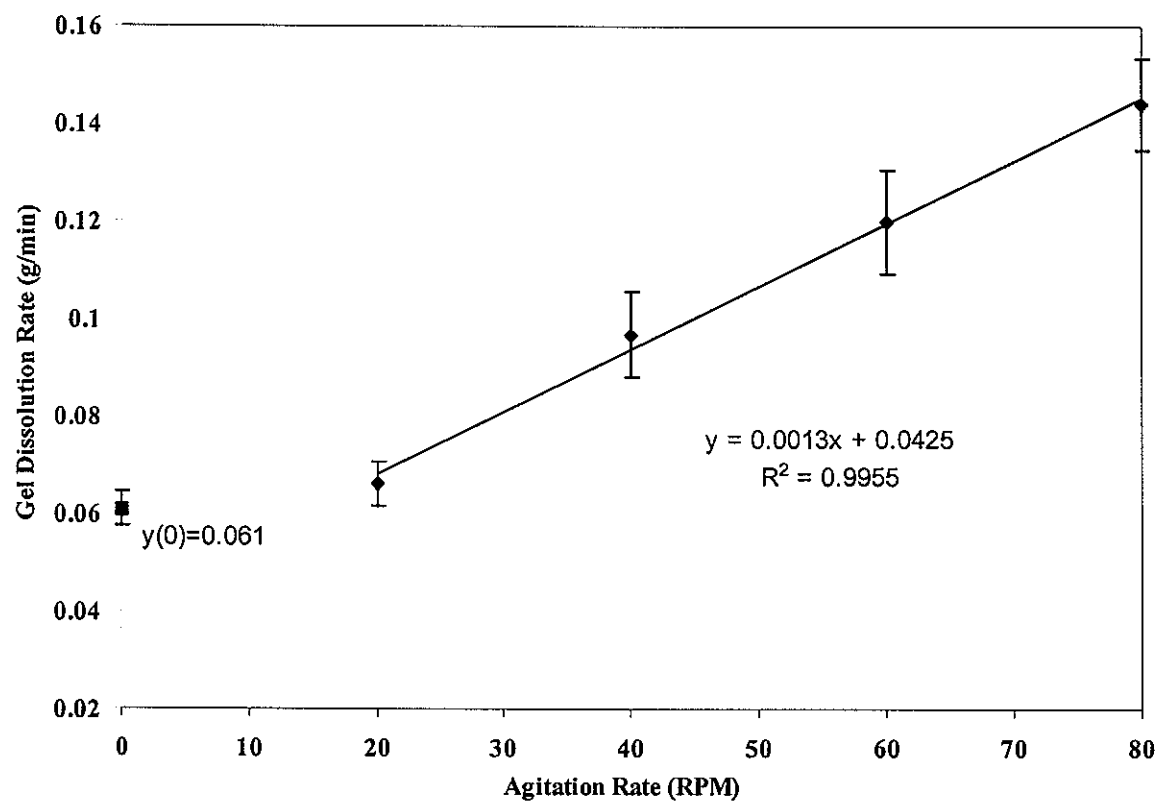
Figure 10 – Gel dissolution as a function of agitation rate. Data points represent the dissolution rate at the given agitation rates. (♦-Stirred System, ■-Inverted Static System)
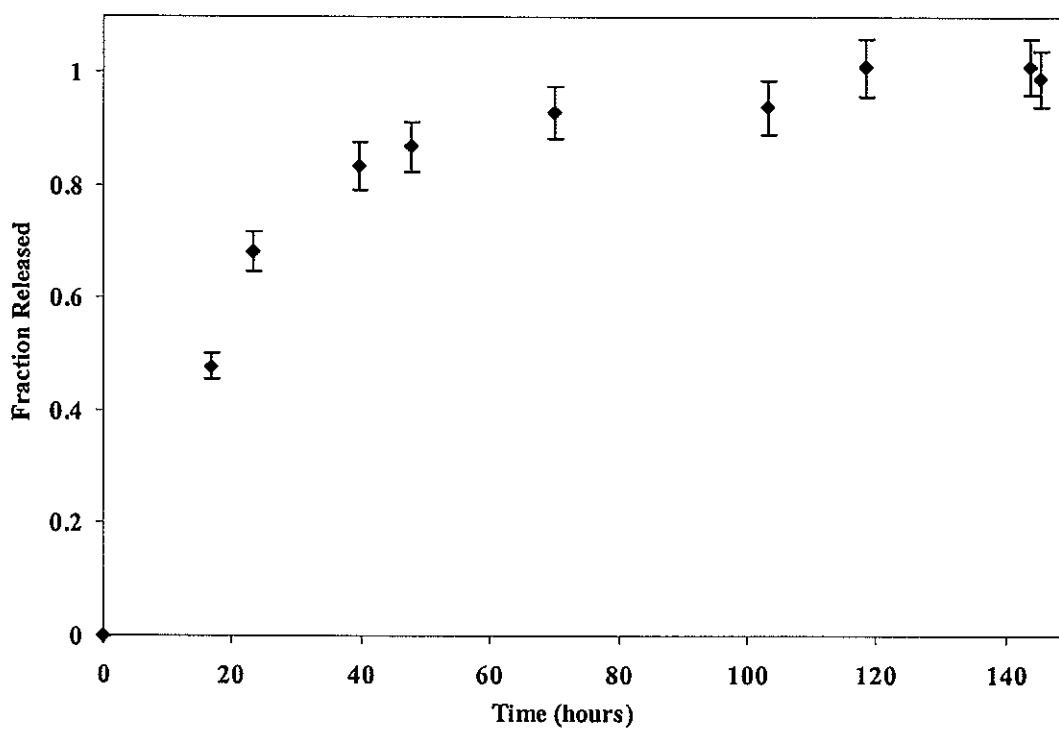
Figure 11 – Metronadiazole release from a system that is not adequately stirred and device is not inverted.

CHAPTER 3. The Effect of Salts on the Micellization Temperature of Aqueous Poly(ethylene oxide)-b-poly(propylene oxide)-b-poly(ethylene oxide) Solutions and the Dissolution Rate and Water Diffusion Coefficient in their Corresponding Gels

A paper published in the Journal of Pharmaceutical Sciences[1]

Brian C. Anderson[2], Suzan M. Cox[2], Amar V. Ambardekar[2] and Surya K. Mallapragada[2]

Abstract

Studies were performed to examine the effect of ionic salts on phase transitions, dissolution rates and diffusion coefficients of water in gels of poly(ethylene oxide)-*b*-poly(propylene oxide)-*b*-poly(ethylene oxide) with polymer concentrations ranging from 22 to 32% w/w and salt concentrations ranging from 0 to 1.5% w/w. Salts tested include Na_3PO_4, Na_2SO_4, Na_2HPO_4, NaH_2PO_4, $NaCH_3CO_2$, $NaCl$, and KI. Micellization transition temperatures were obtained using differential scanning calorimetry. The dissolution rates were obtained by measurement of the surface erosion rates and diffusion coefficients were obtained using a method to analyze the intrusion of water into the aqueous gels. It was found that salts had no effect on the dissolution rate of the polymer gels into deionized water. However, when the salt concentration in the aqueous dissolution media was adjusted to match the concentration in the gels, the dissolution rate of the polymer gel decreased with increasing salt concentration. The salts also had a profound effect on the critical

---

micellization temperature (CMT) and the diffusion coefficient of water within the gel. The diffusion coefficient and CMT decreased in the presence of salts. The magnitude of these effects was comparable to their placement on the Hofmeister, or lyotropic series for salts. The effects of polymer and salt concentrations on the CMT were quantified and a single correlation was proposed to predict the micellization temperatures for a wide range of salt and polymer concentrations.

Introduction

In the last decade, advances in drug delivery have led to the refinement of polymeric devices that deliver a drug with zero order kinetics over an extended period of time. These devices can be designed to release based either on swelling or on interfacial dissolution. The delivery devices of interest here are injectible thermoreversible aqueous gels of poly(ethylene oxide)-*b*-poly(propylene oxide)-*b*-poly(ethylene oxide) triblock copolymers. These polymers (trademarked Pluronic® by BASF; also known as Poloxamers) are surface active polymers that are mass produced for use in industry as cleaners and degreasers. The particular Pluronic® formulation studied here is Pluronic® F127, with a molecular weight of 12,600 g/mol composed of 70 w/w% ethylene oxide and 30 w/w% propylene oxide.

The main reason these polymers have been studied is their unique property of thermoreversible gelation at elevated temperatures. At low temperatures, just above 0°C, up to about 15°C for lower polymer concentrations, the polymer is completely soluble in water and has a relatively low viscosity. At higher temperatures, between 0°C and 18°C depending on polymer concentration, the individual polymer chains aggregate to form spherical micelles in solution consisting of a poly(propylene oxide) core surrounded by a poly(ethylene oxide)

layer [1-11]. At higher temperatures, from about 15°C to 35°C based on the polymer

concentration, the micelles entangle to form a homogeneous gel[12-14]. This allows an

aqueous solution of polymer and drug to be injected into the body, where it will form a stiff

gel without surgical implantation. This has been tested *in vitro* [15-19] and *in vivo* [20-22]

both for specific applications and general drug release behavior.

The effects of ionic salts on several phase transition points in aqueous solutions of

non-ionic surfactants have been investigated by others in various ways. Several researchers

have investigated the role that salts play in lowering or raising the cloud point[23-32],

gelation points[33], aggregation number[34-36], micellization points[37-39], drug delivery

properties[40], micelle characteristics[41-42] and hydrophobic parameters [43] of non-ionic

polymers. Many of these studies focused on the particular class of polymers of interest here,

Pluronic® co-polymers [28-36,38-40,42]. Although cloud points show the trends exhibited

by various salt/surfactant combinations, they do not give us any direct information on

physical characteristics that are of interest when classifying and creating drug delivery

devices. The phase transition that would be more of interest is the micellization temperature.

The effect of salts on the micellization temperature and properties of the micelles in aqueous

solutions of Pluronic® have been studied using light scattering [32,33,35] and fluorescence

quenching [36]. Micellization concentrations of Pluronic® and other surfactants have been

measured using surface tension measurements [38] or dye spectral methods[39]. Properties

of the micelles have been studied with small angle neutron scattering [42]. The problem with

these measuremental techniques are that they are primarily not used when the concentration

of the polymer in solution is sufficiently high so that the micellization occurs just before the

onset of thermoreversible gelation. Unfortunately, these are the concentrations of interest for

drug delivery devices. We have studied the effect of ionic salts on aqueous Pluronic®
solutions using differential scanning calorimetry in order to obtain the micellization
temperature at these higher polymer concentrations.

It has already been established that the micellization temperatures of Pluronic®
solutions are affected by the concentration of the polymer in the aqueous solution under
concentrated conditions [1-12]. Our goal was to merge the polymer concentration
dependence and the salt concentration dependence to have one equation that calculates the
micellization temperatures for combinations of these two effects.

Another property of Pluronic® gels that is affected by the presence of ionic salts is the
diffusion coefficient of water inside the gel state. We have investigated the role that salts
play in modifying this property. By understanding the effect of salts on the dissolution
process and diffusion coefficient of water, and critical micellization temperature, we can
modify the characteristics of the drug delivery device to take on properties like an earlier
onset of gel formation to better customize the device to different situations.

The effect of salts on polymer solutions, including biopolymers, has been known for
more than a century. In the late 1800s, Hofmeister studied the effect various salts had on the
precipitation of proteins[44]. He created an ordered list of ions with increasing effect on the
solubility of large molecules in aqueous solutions. This is known as the Hofmeister series, or
the lyotropic series. Ions have the ability to either make the water more structured by
additional bonding or to create a more disordered state in the aqueous solution. Which ions
decrease order and which are increase order and the magnitude of these effects varies from
solute to solute [45]. These Hofmeister series lists are readily available in literature for

important ions in protein purification [44-47]. We used these lists as a comparison to the relative effect salts have on the properties of Pluronic® solutions and gels.

Materials and Methods

Chemicals – Culture tested Pluronic® F127 was obtained from Sigma Corp. (St. Louis, MO) and used with no purification for all studies. The dye toluidine blue O used to color the Pluronic® solutions was obtained from Sigma Corp. Na_3PO_4, Na_2SO_4, Na_2HPO_4, NaH_2PO_4, $NaCH_3CO_2$, NaCl, and KI were obtained and used without purification from Fisher Scientific (Itasca, IL).

Methods – *Preparation of Gels* – Gels without salts were prepared by dissolving the appropriate amount of solid polymer into ultrapure water and maintaining a temperature of approximately 2°C for 24 to 48 hours until the solid had fully dissolved. The appropriate amounts were on a mass basis with concentrations ranging from 22 to 32% w/w. Gels with salts were prepared by dissolution of the salts into gels of the appropriate polymer concentration that were prepared as outlined above. Trace amounts of toluidine blue O were used in the dissolution measurements to make a visibly more distinct boundary between the gel and water.

Micellization Temperature Measurements – The micellization temperatures of the solutions (with and without salt) were obtained using a Perkin-Elmer (Shelton, CT) differential scanning calorimeter (DSC-7) with sub-ambient intercooler attachment. The aqueous samples were placed in aluminum sample pans and held at −10°C for 10 minutes to ensure that the samples were at a uniform temperature in an aqueous liquid state. The

samples were then scanned from –10°C to 25°C at 8 °C/min. The DSC output was analyzed

using Perkin-Elmer's Pyris™ software for Windows NT™. Curve onset temperatures were

evaluated and used as the micellization temperature. All measurements were performed in

triplicate.

Dissolution Rate Measurements – The dissolution rates of the polymer gels were

analyzed by measuring the velocities of the eroding interfaces as described in Anderson, et

al. [48]. Dyed aqueous solutions were poured into 13x100 mm culture tubes at 2°C. The

samples were kept at 2°C for 1 hour to liquefy any solution that had formed a gel on the sides

of the tubes. The samples were heated to 37°C to ensure gelation in the tubes. The height of

the gel in the tubes was marked and the gels were inverted and placed into a deionized water

bath at 37°C. At set times, the samples were measured with a digital micrometer with an

accuracy of 0.01 mm. A device was constructed to facilitate these measurements. By

collecting this data at different times, an estimate of the interfacial velocity could be

calculated. Samples were also placed in baths with a salt concentration equal to that in the

gels.

Diffusion Coefficient Measurements – A method to measure the diffusion coefficient

of water in the gel was used that was reported in our previous work [48]. The tip of a 25 ml

plastic syringe was removed, leaving a cylindrical tube with a plunger. Approximately 15 g

of gel were placed in the tube and allowed to reach 37°C. These samples were inverted and

suspended in a container of water that was also at 37°C. After set amounts of time (1, 2, and

3 hours), the samples were removed from the water and the gel was extruded by pushing the

syringe plunger. A gel cutting device was fabricated that cut the gel into 0.25 cm slices by

pressing down on the top of the cutter. The slices were then weighed, dried in an oven at

37°C overnight and then placed in a vacuum oven for at least 8 hours at 37°C to remove all water from the sample. The slices were then weighed without water to find the solids concentration. By this method, the amount of water in the sample as a function of distance could be calculated. This information was then fit to an equation that models Fickian diffusion into a semi-infinite slab in one dimension with a constant moving boundary. This model is given as eq. 1 with the boundary conditions eqs. 2 and 3. Here, D is the diffusion coefficient of water, v_I is the interfacial velocity of the gel, C_o is the initial water concentration and C_i is the interfacial concentration. C, the concentration of water, is the dependent variable. These equations were solved to yield eq. 4. By fitting the model to the data, the best-fit diffusion coefficient was obtained.

$$v_I \frac{\partial C}{\partial x} = \frac{\partial}{\partial x}\left(D \frac{\partial C}{\partial x} \right) \tag{1}$$

$$C(x = \infty) = C_o \tag{2}$$

$$C(x = 0) = \text{constant} = C^* \tag{3}$$

$$C(x) = (C_i - C_o)exp\left(\frac{-D}{v_I}x \right) \tag{4}$$

Results and Discussion

Micellization Temperature – The CMT of several Pluronic® solutions was tested both as a function of polymer concentration in the absence of salts and as a function of salt concentration for selected polymer concentrations. A representative temperature scan over the appropriate range is given as Fig. 1. The peak represents the endothermic phase transition from a fully solvated solution of unimers to a solution consisting of solvated

micelles with a poly(propylene oxide) microphase inner core. The onset of this peak, characterized by the intersection of the baseline heat flow and the line tangential to the upward curve of the micellization peak. This intersection was calculated using the Pyris software from Perkin Elmer. A plot of micellization temperature versus polymer concentration in the absence of salts is given as Fig. 2. The linear trend and values we obtained is similar to data in the literature [14]. However, this analysis was needed as a control sample for the experiments in which both the salt and polymer concentrations were varied. The effect of polymer concentration on CMT is represented by an empirical equation, eq. 5, where θ_p is the polymer concentration in weight percent and CMT_o is the micellization temperature.

$$CMT_o = 31.491 - .8946\theta_p \tag{5}$$

Micellization temperatures were measured as a function of salt concentration for several different salts from different parts of the Hofmeister series. Comparisons of these salts were made (Figs. 3, 4) for solutions containing 24% initial polymer concentration. In these figures, the intercept of the regression lines was held at a uniform value, the CMT of the solution without salt. There is a negative linear trend for CMT as salt concentration increased. The effect we saw was ($PO_4^{3-} > HPO_4^{2-} > SO_4^{2-} > H_2PO_4^- > CH_3COO^- > Cl^- > I^-$), whereas the Hofmeister series for these ions is ($PO_4^{3-} > SO_4^{2-} > HPO_4^{2-} > H_2PO_4^- > CH_3COO^- > Cl^- > I^-$). There is a slight deviation from the Hofmeister series at the higher end, but in general the magnitude of this trend is dictated by the placement of the ions on the series. This is because of the relative ability of the salts to increase or decrease the structure

of the water in the aqueous solution. For salts like Na_2SO_4 or Na_3PO_4 that have a strong influence on the structure of the water by greatly increasing the hydrogen bonding, the decrease in CMT is the greatest. By changing the energy of the solvent, the thermodynamic advantage of micellization is changed just as it is changed because of an increased polymer concentration. The difference between the two measurements that were interchanged, SO_4^{2-} and PO_4^{3-}, is not significant at a 95% confidence level.

The effect of salts on the CMT can be characterized by eq. 6. In this equation, θ_s is the salt concentration in weight percent, the constant CMT_o is the CMT for that polymer concentration and no salt (from eq. 5), and the constant β is given for various salts in Table 1.

$$CMT = CMT_o - \beta\theta_S \tag{6}$$

The effect of one salt, Na_2SO_4, on the CMT was tested for several polymer concentrations to see if the effect was different for different polymer concentrations. For selected polymer concentrations (22.6, 24, 27.4%) micellization temperatures were plotted as a function of sodium sulfate concentration (Fig. 5). The slope of the lines shown are an average of the three regression lines obtained from linear regressions on the data shown. The lines show that there no appreciable change from the average slope for each of the concentrations tested, meaning that the effect of salt concentration on CMT depression is independent of polymer concentration. Because of this, eqs. 5 and 6 can be combined to form eq. 7. In this equation, β is still obtained from Table 1 and θ_s and θ_p are the polymer and salt concentrations respectively. This equation holds for polymer concentrations from 20 to 32 wt% and for salt concentrations up to 1 wt%.

$$CMT = 31.491 - .8946\theta_P - \beta\theta_S \qquad\qquad (7)$$

Diffusion Coefficient – The diffusion coefficient of water in the gel, fit to water concentration profiles, was found to be affected by the addition of salts. A sample of this statistical fit is given as Figure 6. Although smooth correlations could not be obtained, general trends were evident. The effect of sodium sulfate on the diffusion coefficient was less pronounced at the higher polymer concentrations (Fig. 7). The error on the measurements presented in Figures 7 and 8 were found as the standard error for the diffusion coefficient parameter as reported by the nonlinear regression procedure in SAS from SAS Incorporated. The standard error ranged from 8% to 17% of the diffusion coefficient with an average error of 12% of the diffusion coefficient, or about 0.5 cm^2/sec. There appears to be a limiting value the diffusion coefficient can take which happens around the solubility limit of the polymer in water, about 30 wt% at 2°C. This makes intuitive sense because the diffusion coefficient is a resistance to diffusive transport, which is a function of the viscosity of the diffusion media, in this case the gel. Because the viscosity is a function of the polymer concentration [27], there is a viscosity limit that occurs at the solubility limit of the polymer in the aqueous solvent. In fact, the 30 wt% gel that was tested showed no detectable lowering of the diffusion coefficient in response to the addition of salt. On the other hand, the 24 and 27 wt% solution were influenced by the presence of the sodium sulfate because they are sufficiently below the solubility limit of the polymer.

Also, a comparison of sodium sulfate and sodium chloride revealed a similar trend as the micellization temperature data. The salt that is higher on the Hofmeister series, sodium sulfate, appeared to be slightly better at reducing the diffusion coefficient than sodium chloride, which is positioned much lower on the series (Fig. 8). This is thought to be for the same reason that NaCl is not as effective at depressing the micellization temperature. This salt does not have as much ability to increase the structure of the water in the polymer solution as does Na_2SO_4, so it does not have as much influence on the reduction of the diffusion coefficient. The effect of position on the Hofmeister series does not seem to be as strong as for the effect on micellization temperature.

Dissolution Rate – Gel dissolution rate (represented by interfacial velocity) was also studied as a function of both polymer concentration and salt concentration. We have already reported in previous work the interfacial velocity of Pluronic® gels. From that we found a correlation between the dissolution rate and the polymer concentration [48]. This was not the case for the addition of salts. There was no statistical difference between the interfacial velocities for the different salt concentrations for the same polymer concentration to a 90% confidence level, as found by using the general linear model procedure on SAS.

It was thought that the dissolution rate should be influenced by the presence of ionic salts if the other physical characteristics, such as diffusion coefficient of water in the gel and CMT, are affected. The other two characteristics evaluated are bulk properties where the salt concentration within the gel is important. Dissolution rate is a surface property where the concentration of salt at the aqueous/gel interface seems to be important. It is possible that the salt is diffusing out at on a much shorter time scale than the dissolution of the polymer. If this is the case, even if the bulk gel is affected by the presence of salts, the salt concentration

at the interface is close to zero and no measurable effect will be seen. In our previous work [47] we found that internal diffusion of small molecules in Pluronic® F127 gels occurs on a very long time scale and would not be sufficiently fast to replace the salts that have diffused from the water swollen interface.

In order to test this hypothesis, the experiments were repeated in baths that consisted of Na_2SO_4 in water, specifically at the same concentration as in the gel, instead of a deionized water bath. This removes the chemical potential driving force for diffusion and leaves the salts in the interfacial gel as it dissolves. What was found was that the dissolution rate in fact is affected by the presence of ionic salts under this experimental setup. The measurements are statistically different to a 90% confidence level and show a trend of decreasing the dissolution rate as the salt concentration increases (Fig. 9). One implication of this is that if there are salts present in the release medium, as would be the case in the human body, there can be an induced change in drug release properties of Pluronic® gels with the addition of salts to the gel makeup. This is in contrast to the drug release properties of Pluronic® gels when the receiving bath is absent of salt [40].

Just as with the CMT and diffusion coefficient measurements, polymer concentration seems to have much more of an influence on the properties of the polymer solution than salt concentrations over the range of solubility.

Conclusions

It was found that ionic salts have an effect on the onset temperature of micellization in an order that closely follows the well known Hofmeister Series (Na_3PO_4, Na_2SO_4, Na_2HPO_4, NaH_2PO_4, $NaCH_3CO_2$, $NaCl$, KI). The structure making ability of the salts

increases the order in the water and decreases the temperature necessary to trigger micellization. Even KI, a salt that actually breaks water's structure for many polymers, produces a very slight decrease in CMT. Stronger salts, like Na_3PO_4, Na_2SO_4, and Na_2HPO_4 have a much more powerful effect on micellization. An empirical correlation was obtained for the prediction of CMT as a function of salt concentration and polymer concentration for several salts.

The diffusion coefficient of water inside the hydrogel was also affected by the presence of salts, resulting in a general decrease in diffusion coefficient in the presence of salts. The decrease was less pronounced for higher initial polymer concentrations and for NaCl, which is quite low on the Hofmeister series. The dissolution rate of the non-crosslinked hydrogel was reduced by the presence of salts as long as the salt did not diffuse from the gel/bath surface. If the salt was not prevented from diffusing from the interface, no reduction in dissolution was seen with increasing salt concentration in the gel.

Acknowledgments

References

[1] Wanka, G.; Hoffmann, H.; Ulbricht, W. Phase Diagrams and Aggregation Behavior of Poly(oxyethylene)-Poly(oxypropylene)-Poly(oxyethylene) Triblock Copolymers in Aqueous Solutions. *Macromolecules*. 27, (1994) 4115-4159.

[2] Chu, Benjamin. Structure and Dynamics of Block Copolymer Colloids. *Langmuir*. 11, (1995) 414-421.

[3] Tanodekaew, Siriporn; Deng, Nan-Jie; Smith, Sibyl; Yang, Yung-Wei; Attwood, David; Booth, Colin. Micellation and Gelation of block-Copoly(oxyethylene/oxybutylene) in Aqueous Solutions. *J. Phys. Chem.* 97, (1993) 11847-11852.

[4] Alexandridis, Paschalis; Holzwarth, Josef F.; Hatton, T. Alan. Micellization of Poly(ethylene oxide)-Poly(propylene oxide)-Poly(ethylene oxide) Triblock Copolymers in Aqueous Solutions: Thermodynamics of Copolymer Association. *Macromolecules*. 27, (1994) 2414-2425.

[5] Beezer, A. E.; Loh, W.; Mitchell, J. C.; Rowall, P. G.; Smith, D. O.; Tute, M. S.; Armstrong, J. K.; Chowdhry, B. Z.; Leharne, S. A.; Eagland, D.; Crowther, N. J. An Investication of Dilute Aqueous Phase Behavior of Poly(oxyethylene)+Poly(oxypropylene)+Poly(oxyethylene) Block Copolymers. *Langmuir*. 10, (1994) 4001-4005.

[6] Mortensen, Kell; Brown, Wyn; Jorgensen, Erling. Phase Behavior of Poly(proplene oxide)- Poly(ethylene oxide)-Poly(propylene oxide) Triblock Coploymer Melt and Aqueous Solutions. *Macromolecules*. 27, (1994) 5654-5666.

[7] Zhou, Zukang; Chu, Benjamin. Phase Behavior and Associatin Properties of Poly(oxypropylene)-Poly(oxyethylene)-Poly(oxypropylene) Triblock Copolymer in Aqueous Solution. *Macromolecules*. 27, (1994) 2025-2033.

[8] Mortesen, K. Phase Behaviour of Poly(ethylene oxide)-Poly(propylene oxide)-Poly(ethylene oxide) Triblock-Copolymer Dissolved in Water. *Europhys. Lett.* 19(7), (1992) 599-604.

[9] Kabanov, Alexander V.; Nazarova, Irina R.; Astafieva, Irena V.; Batrakova, Elena V.; Alakhov, Valery Yu.; Yaroslavov, Alexander A.; Kabanov, Victor A. Micelle Formation and Solubilization of Florescent Probes in Poly(oxyethylene-b-oxypropylene-b-oxyethylene) Solutions. *Macromolecules*. 28, (1995) 2303-2314.

[10] Nagarajan, R.; Ganesh, K. Block Coploymer Self-Assembly in Selective Solvents: Spherical Micelles with Segregated Cores. *J. Chem. Phys.* 90(10), (1989) 5843- 5856

[11] Wanka, G.; Hoffmann, H.; Ulbricht, W. The Aggregation Behavior of Poly-(Oxyethylene)-Poly-(Oxypropylene)-Poly-(Oxyethylene)-Block-Copolymers in Aqueous Solution. *Colloid Poly. Sci.* 268, (1990) 101-117.

[12] Cabana, Alain; Ait-Kadi, Abdellatif; Juhasz, Julianna. Study of the Gelation Process of Polyethylene Oxide$_a$-Polypropylene Oxide$_b$-Polyethylene Oxide$_a$ Copolymer (Poloxamer 407) Aqueous Solutions. *J. Colloid. Int. Sci.* 190, (1997) 307-312.

[13] Vadnere, Madhu; Amidon, Gordon; Lindenbaum, Siegfried; Haslam, John L. Thermodynamic Studies on the Gel-Sol Transition of Some Pluronic Polyols. *Int. J. Pharm.* 22, (1984) 207-218.

[14] Wang, P; Johnston, T. P. Kinetics of Sol-to-Gel Transition for Poloxamer Polyols. *J. Appl. Polym. Sci.* 43, (1991) 283-292.

[15] Chi, Sang C.; Jun, H. W. Release Rates of Ketoprofen from Poloxamer Gels in a Membraneless Diffusion Cell. *J. Pharm. Sci.* 80(3), (1991) 280-283.

[16] Safwat, Salwa M. Drug Release From Pluronic Gels. *Bull. Pharm. Sci.* 17(1), (1994) 41-48.

[17] Yang, Lin; Talukdar, Suddha S.; Alexandridis, Paschalis. Controlled Drug Release from Poloxamer Formulations: Diffusion vs. Erosion Mechanism. *Polym. Prepr.* 40(1), (1999) 347-348.

[18] Gilbert, Julian C.; Hadgraft, Jonathan; Bye, Alan; Brookes, Leonard G. Drug Release From Pluronic F-127 Gels. *Int. J. Pharm.* 32, (1986) 233-228.

[19] Desai, Suketu D.; Blanchard, James. In Vitro Evaluation of Pluronic F127-Based Controlled-Release Ocular Delivery Systems for Pilocarpine. *Jounal of Pharmaceutical Sciences.* 87(2), (1998) 266-230.

[20] Johnston, Thomas P.; Miller, Susan C. Inulin Disposition Following Intramuscular Administration of an Inulin/Poloxamer Gel Matrix. *J. Parenter. Sci. Technol.* 43(6), (1989) 280-285.

[21] Bhardwaj, Renu; Blanchard, James. Controlled-Release Delivery System for the a-MSH Analog Melanotan-I Using Poloxamer 407. *Journal of Pharmaceutical Sciences.* 85(9), (1996) 915-919.

[22] Johnston, Thomas P.; Punjabi, Monika A.; Froelich, Christopher J. Sustained Delivery of Interleukin-2 from a Poloxamer 407 Gel Matrix Following Intraperitonal Injection in Mice. *Pharmaceutical Research.* 9(3), (1992) 425-433.

[23] Schott, Hans; Royce, Alan E. Effect of inorganic additives on solutions of nonionic surfactants. VI: Further cloud point relations. *J. Pharm. Sci* 73(6), (1984) 793.

[24] Schott, Hans; Royce, Alan E. Effect of inorganic additives on solutions of nonionic surfactants. VII: Cloud Point Shift Values of Individual Ions. *J. Pharm. Sci* 73(6), (1984) 793.

[25] Ananthapadmanabhan, K. P.; Goddard, E. D. Aqueous biphase formation in polyethylene oxide-inorganic salt systems. *Langmuir.* 3(1), (1987). 25.

[26] Thiyagarajan, P.; Chaiko, D. J.; Hjelm, R. P., Jr. A Neutron Scattering Study of Poly(ethylene glycol) in Electrolyte Solutions. *Macromolecules.* 28(23), (1995) 7730-6.

[27] Jorgensen, Erling B.; Hvidt, Soren; Brown, Wyn; Schillen, Karin. Effects of Salts on the Micellization and Gelation of a Triblock Copolymer Studied by Rheology and Light Scattering. *Macromolecules.* 30(8), (1997) 2355-2364.

[28] Pandit, Nivedita; Trygstad, Troy; Croy, Scott; Bohorquez, Maria; Koch, Cody. Effect of Salts on the Micellization, Clouding, and Solubilization Behavior of Pluronic F127 Solutions. *J. Colloid Interface Sci.* 222(2). (2000) 213-220.

[29] Malmsten, M.; Lindman, B. Self-assembly in aqueous block copolymer solutions. *Macromolecules.* 25, (1992) 5540-5445.

[30] Pandya, Ketan; Lad, Kishor; Bahadur, Pratap. Effect of additives on the clouding behavior of an ethylene oxide-propylene oxide block copolymer in aqueous solution. *J. Macromol. Sci., Pure Appl. Chem.* A30(1), (1993) 1-18.

[31] Bahadur, P.; Pandya, K.; Almgren, M.; Li, P.; Stilbs, P. Effect of inorganic salts on the micellar behavior of ethylene oxide-propylene oxide block copolymers in aqueous solution. *Colloid Polym. Sci.* 271(7), (1993) 657-67.

[32] Bahadur, Pratap; Li, Puyong; Almgren, Mats; Brown, Wyn. Effect of potassium fluoride on the micellar behavior of Pluronic F-68 in aqueous solution. *Langmuir.* 8(8), (1992) 1903-1907.

[33] Pandit, Nivedita K.; Kisaka, Justin. Loss of gelation ability of Pluronic F127 in the presence of some salts. *Int. J. Pharm.* 145(1-2), (1996) 129-136.

[34] Attwood, D.; Collett, J. H.; Tait, C. J. The micellar properties of the poly(oxyethylene)-poly(oxypropylene) copolymer Pluronic F127 in water and electrolyte solution. *Int. J. Pharm.* 26(1-2), (1985) 25-33.

[35] Almgren, Mats; Bahadur, Pratap; Alsins, Jan. Fluorescence quenching and excimer formation to probe the micellization of a poly(ethylene oxide)-poly(propylene oxide)-poly(ethylene oxide) block copolymer, as modulated by potassium fluoride in aqueous solution. *Langmuir.* 7(3), (1991) 446-450.

[36] Binana-Limbele, W.; Van Os, N. M.; Rupert, L. A. M.; Zana, R. Aggregation behavior and micellar dynamics in aqueous solutions of the nonionic surfactant pentaoxyethyleneglycol monooctyl ether: effect of sodium halides. *J. Colloid Interface Sci.* 144(2), (1991) 458-67.

[37] Schott, Hans; Han, Suk Kyu. Effect of inorganic additives on solutions of nonionic surfactants. III: CMC's and surface properties. *J. Pharm. Sci.* 65(7), (1976) 975.

[38] Desai, Mihir; Jain, Nirmesh J.; Sharma, Rakesh; Bahadur, Pratap. Temperature and salt-induced micellization of some block copolymers in aqueous solution. *J. Surfactants Deterg.* 3(2), (2000) 193-199.

[39] Jain, N. J.; Gandhi, H.; Patel, K. C.; Bahadur, P. Properties of block copolymers in aqueous salt solutions. *Tenside, Surfactants, Deterg.* 36(3), (2000) 168-170,172

[40] Pandit, Nivedita K.; Wang, Diana. Salt effects on the diffusion and release rate of propranolol from poloxamer 407 gels. *Int. J. Pharm.* 167(1-2), (1997) 183-189.

[41] Turro, Nicholas J.; Kuo, Ping Lin. Pyrene excimer formations in micelles of nonionic detergents and of water-soluble polymers. *J. Phys. Chem.* 2(4), (1986) 438-442.

[42] Jain, Nirmesh J.; Aswal, V. K.; Goyal, P. S.; Bahadur, P. Micellar structure of an ethylene oxide-propylene oxide block copolymer: a small-angle neutron scattering study. *J. Phys. Chem. B.* 102(43), (1998) 8452-8458.

[43] Cserhati, T.; Forgacs, E.; Oros, Gy.; Kumar, K.; Khan, H. U. Effect of salt on the hydrophobicity parameters of nonionic surfactants. *Chem. Environ. Res.* 8(1,2), (1999) 137-150.

[44] Ducruix, A.; Giege, R. Chrystallization of Nucleic Acids and Proteins: A Practical Approach. IRL Press, New York, (1992) 211-212.

[45] Luck, W. A. P. Water in biological systems. *Top. Curr. Chem.* 64, (1976) 113-180.

[46] Bailey, James E; Ollis, David F. *Biochemical Engineering Fundamentals, second ed.* McGraw-Hill Inc, New York, (1986) 747.

[47] Belter, Paul A.; Cussler, E. L.; Hu, Wei-Shou. Bioseparations: *Downstream Processing for Biotechnology.* John Wiley and Sons, New York, (1988) 225-256.

[48] Anderson, Brian C; Pandit, Nividita K.; Mallapragada, Surya K. Understanding Drug Delivery from Poly(ethylene oxide)-b-poly(propylene oxide)-b-poly(ethylene oxide) Gels. *Journal of Controlled Release* 70(1), (2001) 157-167.

Table 1 – Constants for Equations 6 and 7

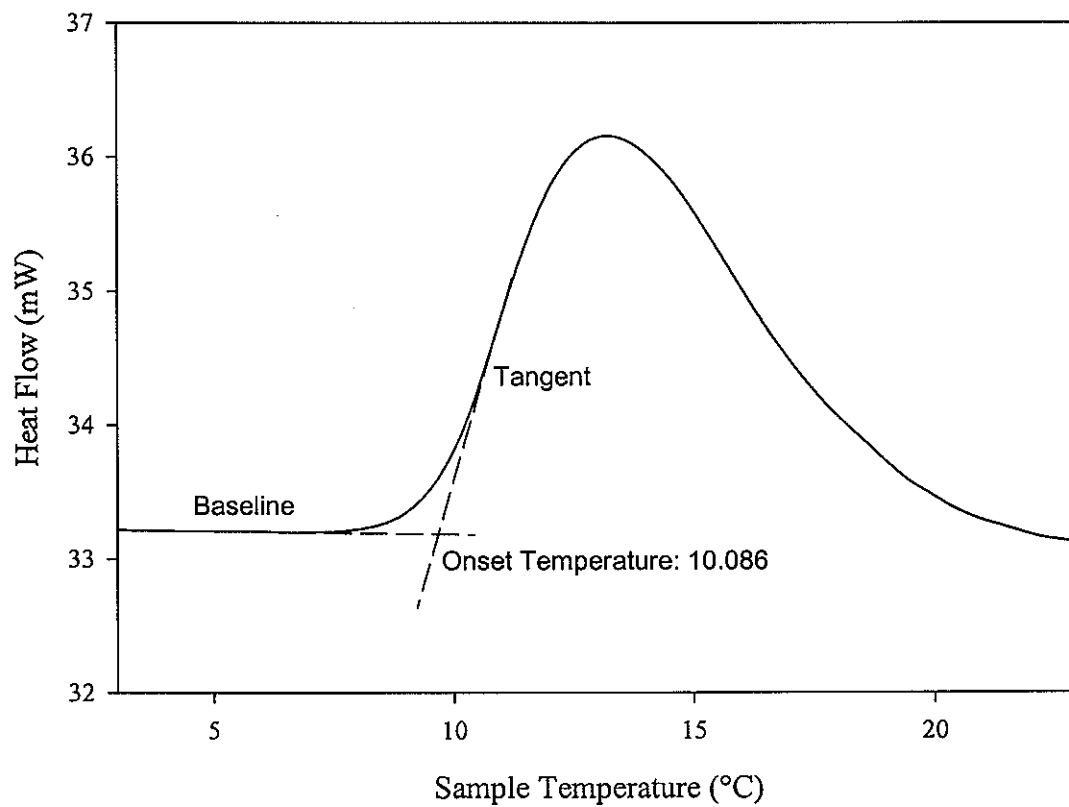| Salt	β (°C/wt%)
KI	0.1359
NaCl	3.0188
$NaCH_3CO_2$	3.1987
NaH_2PO_4	3.258
Na_2SO_4	3.7135
Na_2HPO_4	4.3871
Na_3PO_4	7.1575

Figure 1 – Sample Temperature Scan. The data is from 24 wt% polymer and 0.5% Sodium Sulfate. Dashed lines represent the tangent line to the endothermic curve and the baseline.
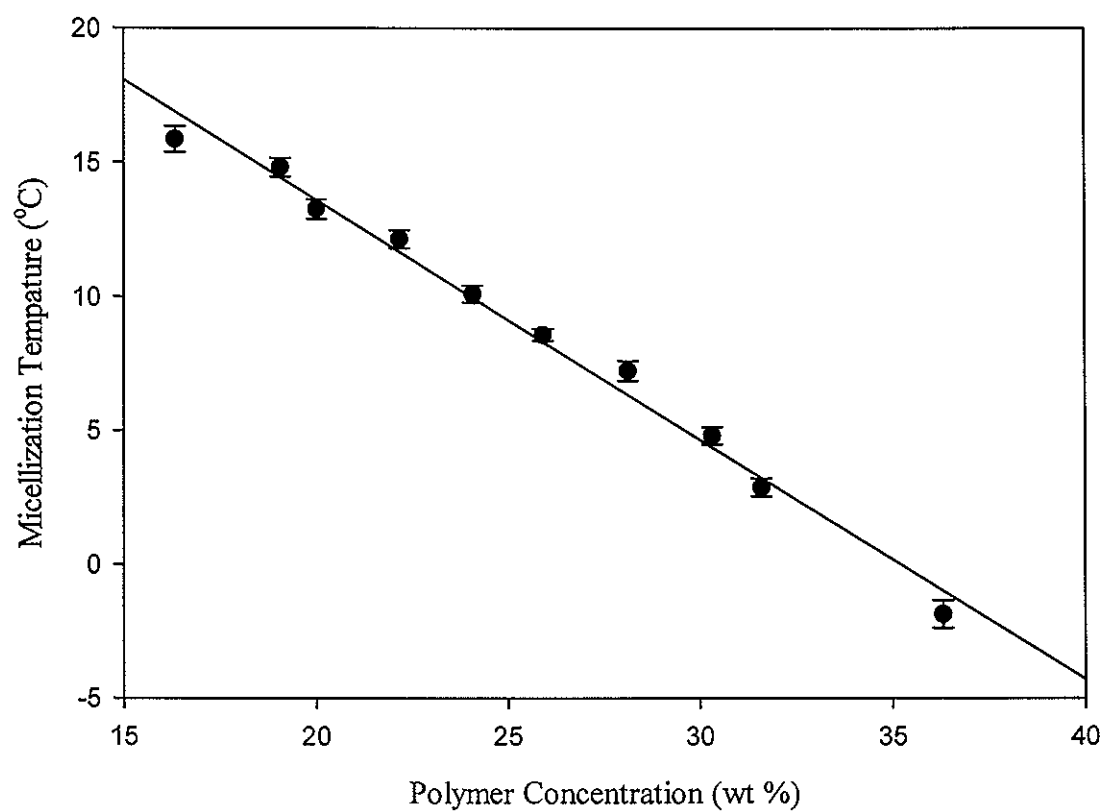
Figure 2 – Critical Micellization Temperature as a Function of Polymer Concentration. Error bars represent standard errors.
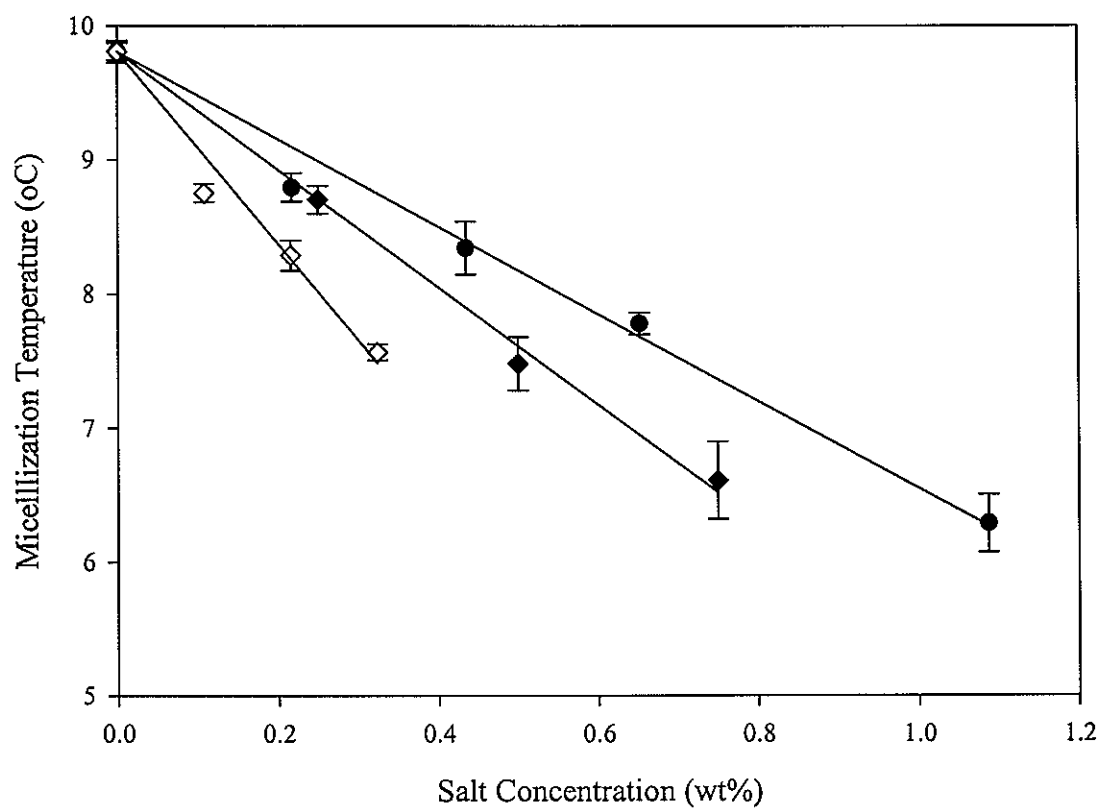
Figure 3 – Critical Micellization Temperature as a Function of Salt Concentration. All gels were 24 wt% polymer. Salts: ● - NaH_2PO_4, ◆ - Na_2HPO_4, ◊ - Na_3PO_4. Error bars represent standard errors.
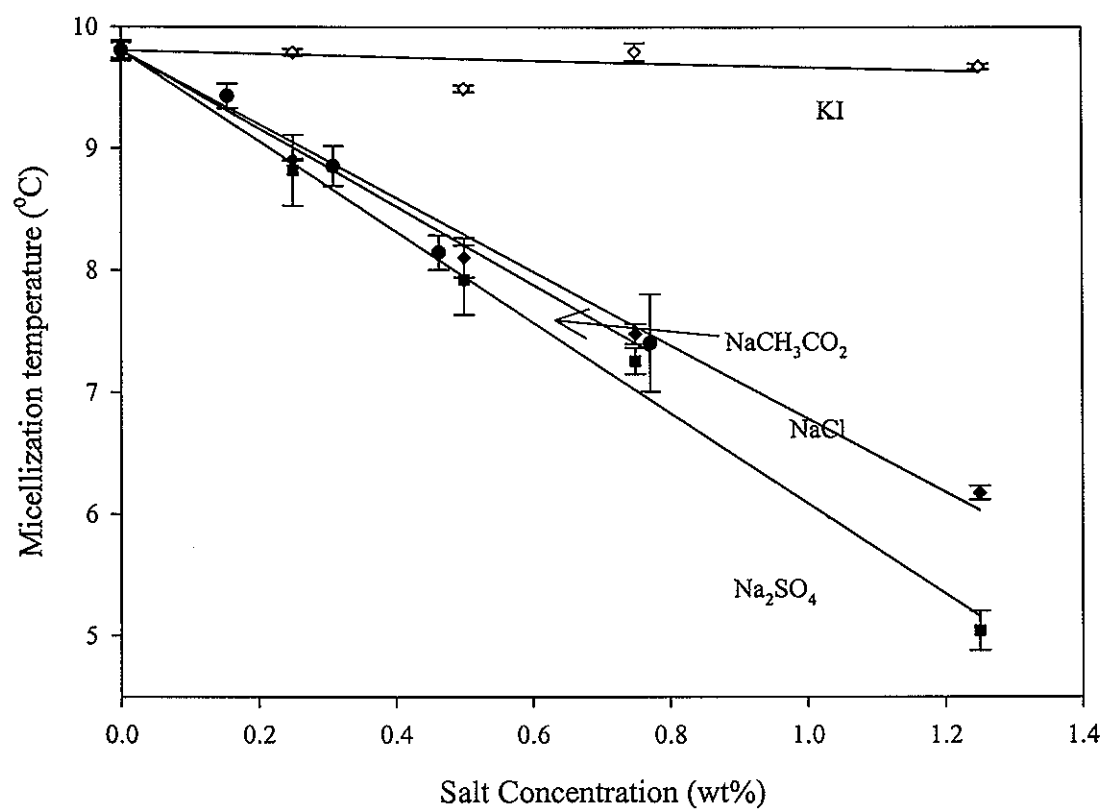
Figure 4 - Critical Micellization Temperature as a Function of Salt Concentration. All gels were 24 wt% polymer. Salts: $\lozenge$ - KI, $\blacklozenge$ - NaCl, $\bullet$ - NaCH$_3$CO$_2$, $\blacksquare$ - Na$_2$SO$_4$. Error bars represent standard errors.
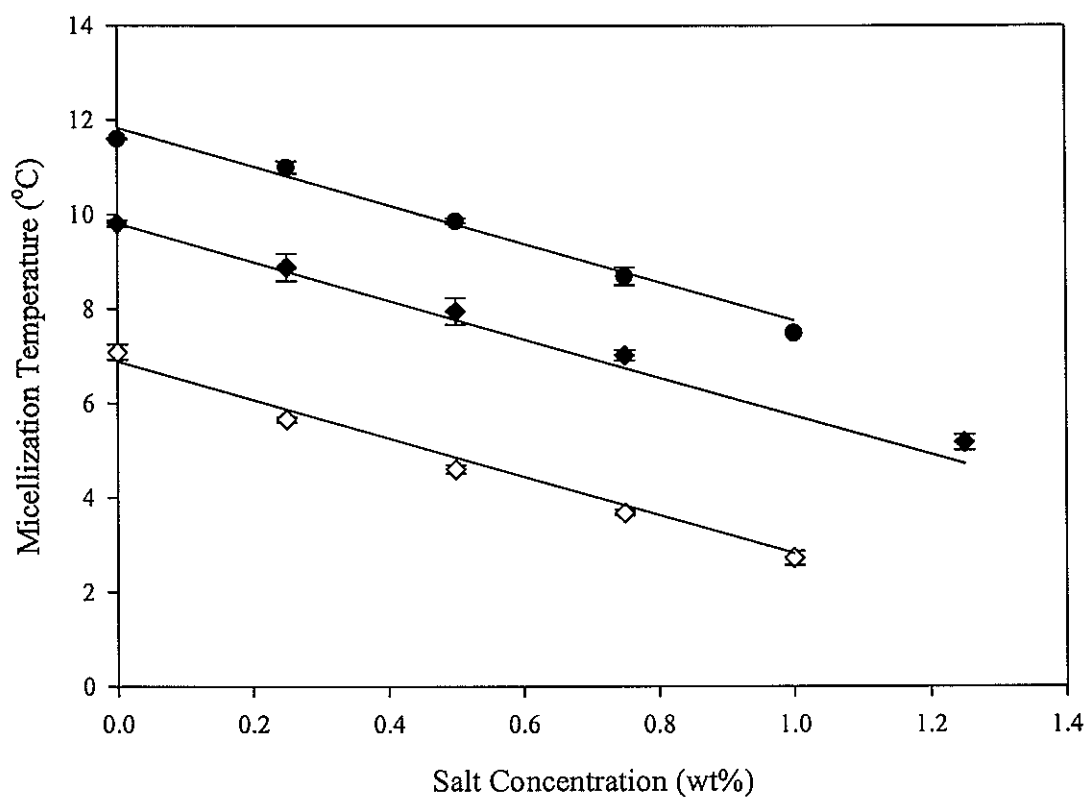
Figure 5 - Critical Micellization Temperature as a Function of Salt Concentration. Salt: Na_2SO_4. Polymer Concentrations: ● - 22.6 w/w%, ◆ - 24 w/w%, ◊ - 27.4 w/w%. Error bars represent standard errors.
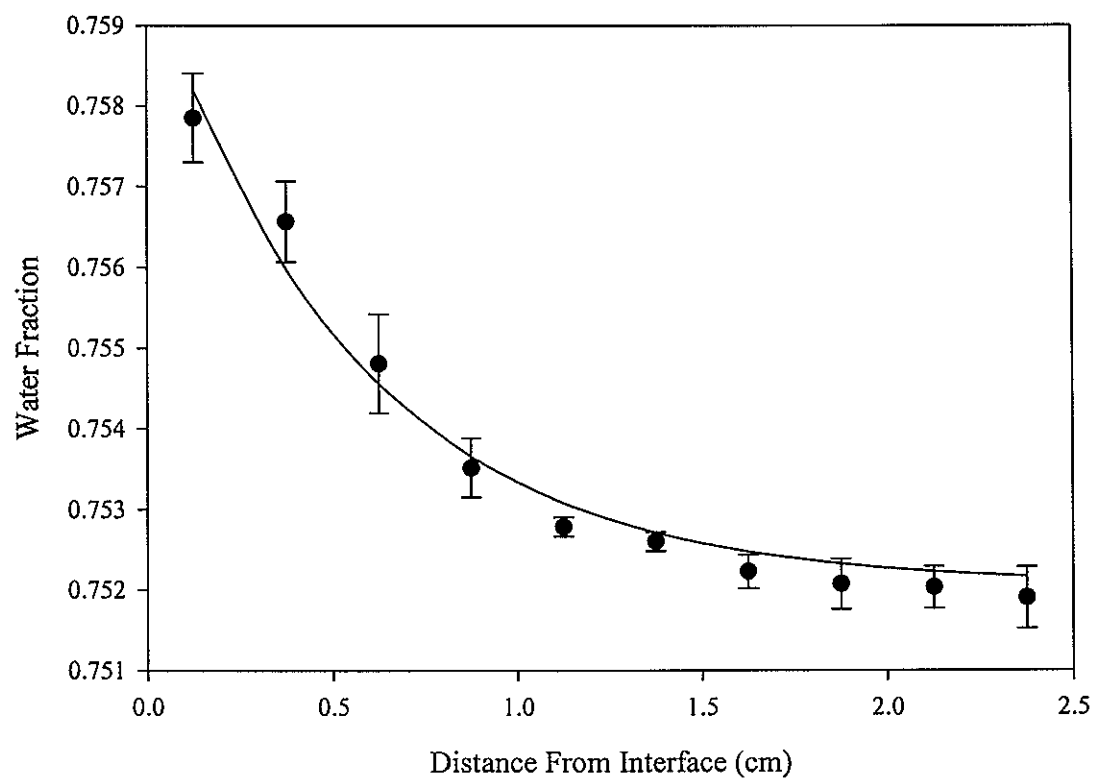
Figure 6 – Sample Data an Fit for Diffusion Coefficient Measurement. Sample is from 24 w/w% polymer and 0.5 w/w% NaCl. Error bars represent standard errors.
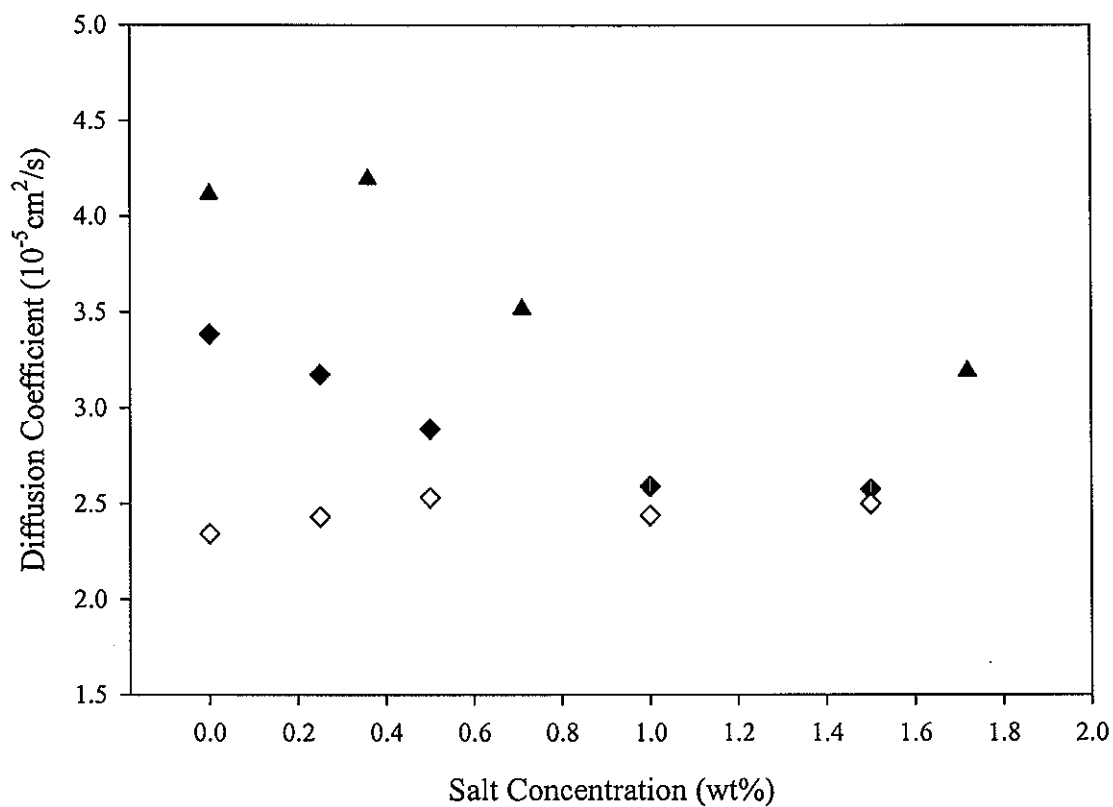
Figure 7 – Diffusion Coefficient as a Function of Salt Concentration. Salt : Na_2SO_4 Polymer Concentrations: ▲ - 24 w/w%, ● - 27 w/w%, ◊ - 30 w/w%. Error bars represent standard errors on the nonlinear fit parameter.
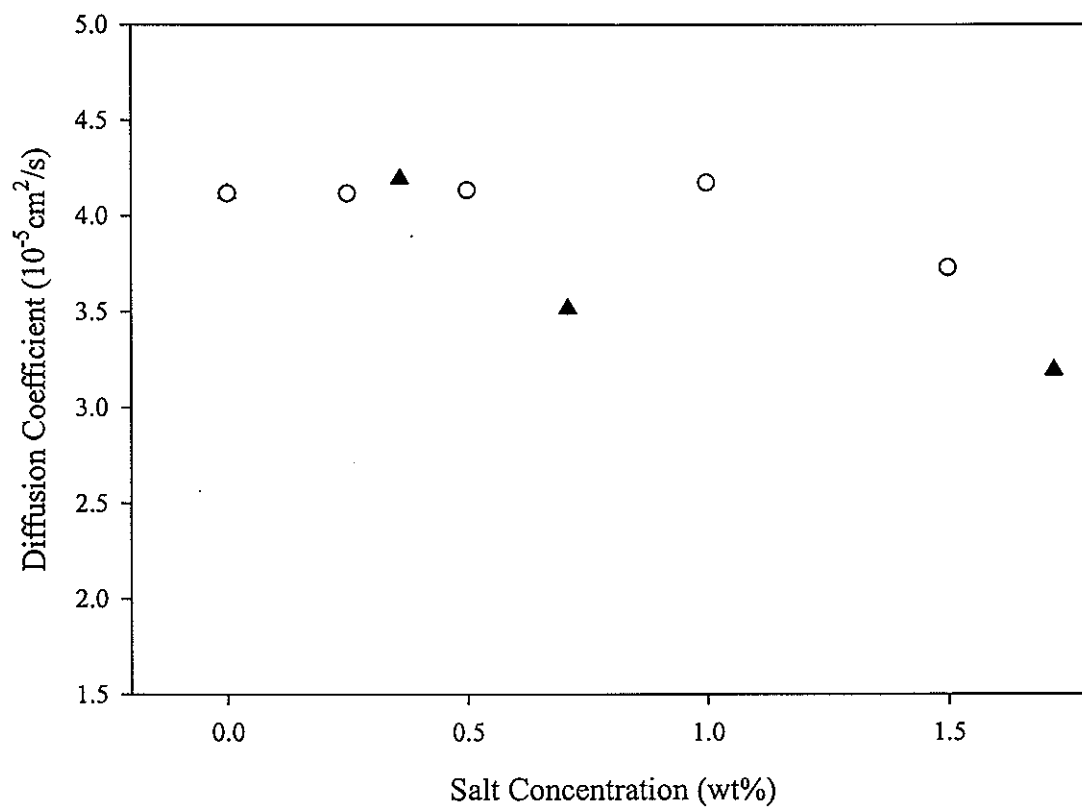
Figure 8 – Diffusion Coefficient as a Function of Salt Concentration. Salt : o- NaCl, ▲ - Na_2SO_4. Polymer Concentration: 24 w/w%.
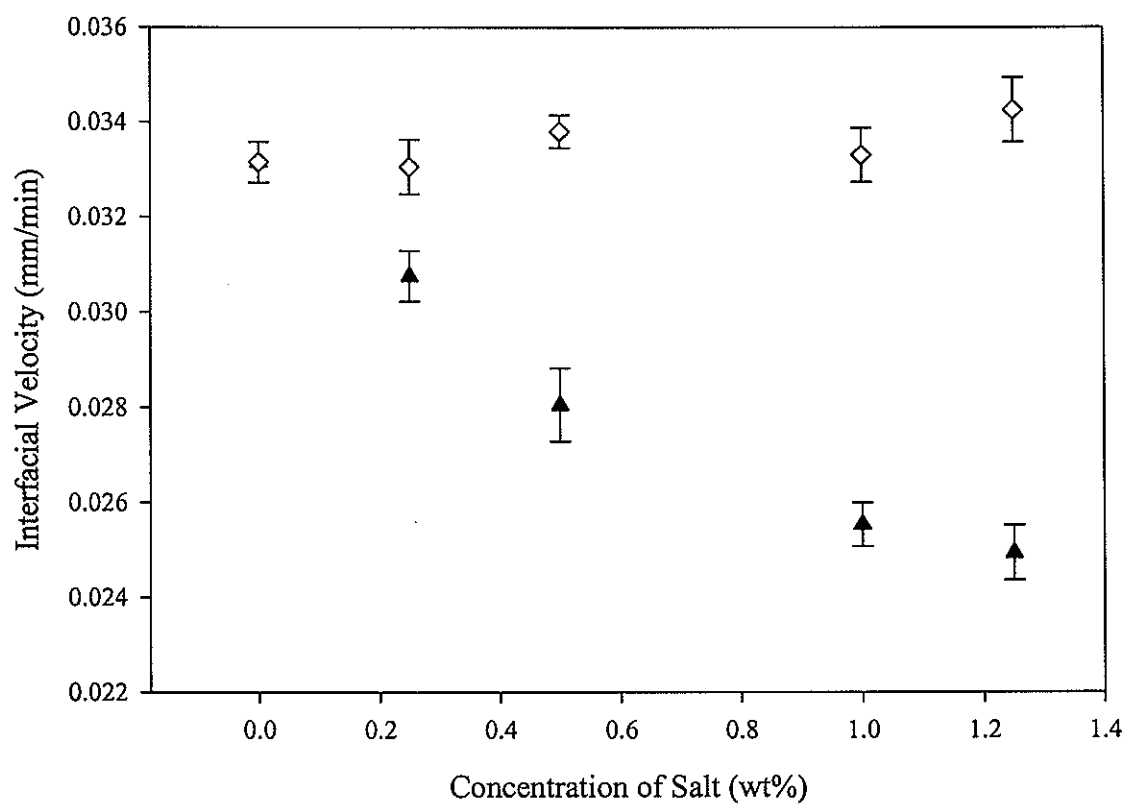
Figure 9 – Sample Data from Dissolution Rate Experiments. ▲- Bath and gel at same salt concentration, ♦- Deionized water bath. Error bars represent standard errors.

CHAPTER 4. Synthesis and Characterization of Water Soluble Block Copolymers for pH-Sensitive Delivery

A paper published in the Material Research Society Symposium Series Volume on 'Biomaterials for Drug Delivery and Tissue Engineering'[1]

Brian C. Anderson[2,3], Paul D. Bloom[3,4], Valerie V. Sheares[3,4], and Surya K. Mallapragada[2,3]

Abstract

A novel, water-soluble AB-block copolymer of diethylaminoethyl methacrylate (DEAEM) and poly(ethylene glycol) (PEG) was synthesized by anionic polymerization. Poly(ethylene glycol) methyl ether (PEGME) was converted into the corresponding potassium salt by reacting with potassium metal. The PEG salt was used as a macroinitiator for the polymerization of DEAEM to yield a PEG-*b*-PDEAEM block copolymer. Carbon dioxide was used to terminate DEAEM polymerization with a carboxylic acid group. This polymer, loaded with dye, was tested for pH sensitivity by release studies into solutions of various pH.

Introduction

One beneficial characteristic that polymeric materials have added to the field of drug delivery is their ability to be responsive to their environment. By modifying the chemical

---

composition of either the backbone or pendant groups, polymers can respond to a wide range

of stimuli. One of the stimuli that has been exploited for drug delivery purposes is pH

dependence.

This dependence can be expressed with polymers containing either anionic or cationic

character. Polymers with cationic functionality will tend to swell in low pH aqueous

solutions, whereas polymers with anionic functionality tend to swell in high pH solutions.

Crosslinked cationic polymer membranes of diethylaminoethyl methacrylate

(DEAEM) and dimethylaminoethyl methacrylate (DMAEM) have been synthesized for drug

delivery applications [1-5]. With the attachment of glucose oxidase, these polymers were

rendered glucose sensitive and have been studied for insulin release. The main disadvantage

of these materials was that they were not water-soluble and, if implanted, would remain in

the body long after the useful life of the delivery device.

Other research efforts have focused on graft and block copolymers comprised of

domains with anionic functionality and separate water soluble portions, such as poly(ethylene

glycol) (PEG) [6-8]. The use of these polymers was primarily for the release of drugs in the

intestines, where a rise in pH would indicate that the device had passed through the stomach

and is no longer in the harsh acidic conditions. Once in the intestines, where the pH is

higher, the delivery polymer is water-soluble and the polymer-bound drug is released.

The goal of this research is to develop a water-soluble block copolymer, containing

cationic functionality, that could be used for insulin delivery. A block copolymer approach is

chosen over other options such as grafting, due to the control over the size and properties

available with anionic polymerization of acrylates. The monomer chosen is DEAEM with a

PEG macroinitiator as the water-soluble portion. Initiation by a potassium salt is used in a similar fashion to other alcohol salts as demonstrated in the literature [9]. The polymerization of DEAEM is terminated with carbon dioxide, resulting in carboxylic acid end groups, to introduce the ability to further chemically modify this polymer.

Experimental Details

Poly(ethylene glycol) methyl ether (PEGME) with an $<M_n>$ of 2000 was obtained from Aldrich Chemical (Milwaukee, WI) and used without purification. The PEGME was dissolved in anhydrous tetrahydrofuran (THF) and transferred via syringe into a flask containing potassium metal in THF under argon. This mixture was then allowed to stir overnight until the potassium had fully dissolved to produce the PEGME potassium salt (Figure 1 **(1)**).

An appropriate amount of diethylaminioethyl methacrylate (Figure 1 **(2)**), DEAEM, (Sigma Chemical Company, St. Louis, MO), in this case 1.5 grams DEAEM per gram PEGME, was stirred over calcium hydride for 12 hours and distilled before use. The DEAEM was then added to the PEGME salt in THF at $0^{\circ}C$. The temperature was raised to room temperature for 30

minutes followed by 6 hours at $50^{\circ}C$. The reaction was terminated by bubbling carbon dioxide (Figure 1 **(4)**) through the flask for one hour. The polymer (Figure 1**(5)**) was precipitated in n-hexane at $-78\ ^{\circ}C$. The precipitate was collected and washed with cold n-hexane and dried at atmospheric pressure for 6 hours followed by 12 h at 10 mm Hg.

Molecular weights were determined relative to polystyrene standards with a Waters gel permeation chromatograph (GPC) system consisting of a Waters 510 pump, Waters 717 autosampler, and an Optilab differential refractive index detector (Wyatt Corporation, Santa Barbara, CA). The system was equipped with four PLgel columns (Polymer Laboratories, Amherst, MA) at 40 °C with THF as the mobile phase at a flow rate of 1.0 mL/min. Nuclear magnetic resonance spectra were acquired on a Varian VXR-300. Finally, the infrared spectrum of the polymer was acquired to determine the presence of carboxylic acid (BioRad, Hercules, CA).

Dissolution and dye delivery rate measurements were carried out to evaluate the pH sensitivity of the polymer. The polymer was heated to 70°C, above the 42.2°C melting temperature of the PEGME block, and a small amount, approximately 20 mg/g, of the dye Toluidine Blue O (MW=305.8 g/mol, UV/VIS absorbance max = 626nm, Sigma Chemical Company, St. Louis, MO) was added and mixed thoroughly with the polymer. The polymer and dye were then allowed to cool and solidify. Small amounts of the polymer, approximately 250mg, were then rolled into small pellets with an approximate radius of 4mm. The pellets were then placed in a USP approved dissolution testing apparatus (SR6, Hanson Research, Chatsworth, CA) maintained at 37°C under 60 RPM agitation and three different pH values; 2.6, 7.0, and 10.8. Samples were drawn at different times from the receiving water in the dissolution test chambers and measured using visible spectrophotometry (Shimadzu 1601 UV/VIS, Columbia, MD). Solid mass remaining after 200 minutes was determined by separating the solids with vacuum filtration and drying under vacuum overnight.

Discussion

NMR confirmed the presence of both the PDEAEM and PEGME blocks of the copolymer as well as the absence of residual monomer (Figure 2). As determined by Lascelles *et al.*, the peaks at 2.55 and 2.7 ppm represent the protons **a** and **b** in Figures 2 and 3 [9]. The peak at 4.0 ppm represents the protons labeled **c** in Figure 3. The small peaks around 2.0 ppm represent the protons on the DEAEM backbone. The large peak at 3.6 ppm represents the PEG backbone. The absence of peaks between 5 and 6 ppm verifies the absence of monomer protons. The average molecular weight of the polymer was calculated by GPC and ^{1}H NMR. First, using NMR the number of DEAEM units were calculated relative to the known number of units in the PEGME starting material. The peaks at 3.7 for the PEO and 2.6/2.7 ppm for the PDEAEM were used for this analysis. The result is that there are 14 DEAEM repeat units, or 2600 g/mol, for every molecule of PEGME initiator. The $<M_n>$ of 4600 g/mol calculated by NMR was in good agreement with the targeted $<M_n>$ of 5000 g/mol. GPC relative to polystyrene standards was also used for molecular weight determination. This method yielded a $<M_n>$ of 3550 g/mol and a polydispersity of 1.45. Samples were also prepared with a $<M_n>$ of approximately 2500 g/mol.

cm^{-1} is indicative of carboxylic acid groups in a dilute solution (Figure4) [10]. The importance of this endcapping group is that the PEG-*b*-PDEAEM-COOH polymer can easily be attached to many different polymers including amine terminated poly(ethylene oxide) or poly(propylene oxide). The flexibility of this modular multiblock technique will be exploited as this pH sensitive polymer is optimized for drug delivery applications.

Dye release studies showed that the release from pellets of the block copolymer is pH sensitive. The release rates of the dye (Figure 5) revealed that the dissolution rate is significantly stunted at higher pH and that the polymer dissolves only under lower pH conditions. It was also visibly seen that at lower pH (5.4) the polymer pellet dissolved and the ball shrank in size until the entire device had dissolved. On the other hand, at high pH (9.31), the polymer eroded as the polymer slowly fell apart into insoluble pieces. Under conditions that would not aid in this erosion, for example less vigorous agitation or no agitation, as is the case for subcutaneously injected polymer, the release rate difference is expected to be even more pronounced.

IR spectrophotometry verified the presence of carboxylic acid endcaps. The sharp peak at 3436 cm^{-1} is indicative of carboxylic acid groups in a dilute solution (Figure4) [10]. The importance of this endcapping group is that the PEG-b-PDEAEM-COOH polymer can easily be attached to many different polymers including amine terminated poly(ethylene oxide) or poly(propylene oxide). The flexibility of this modular multiblock technique will be exploited as this pH sensitive polymer is optimized for drug delivery applications.

Dye release studies showed that the release from pellets of the block copolymer is pH sensitive. The release rates of the dye (Figure 5) revealed that the dissolution rate is significantly stunted at higher pH and that the polymer dissolves only under lower pH conditions. It was also visibly seen that at lower pH (5.4) the polymer pellet dissolved and the ball shrank in size until the entire device had dissolved. On the other hand, at high pH (9.31), the polymer eroded as the polymer slowly fell apart into insoluble pieces. Under conditions that would not aid in this erosion, for example less vigorous agitation or no

agitation, as is the case for subcutaneously injected polymer, the release rate difference is expected to be even more pronounced.

Conclusions

A water-soluble polymer containing tertiary amine functionality was synthesized by novel anionic polymerization of DEAEM with a poly(ethylene glycol) methyl ether potassium salt initiator. The material was fully water soluble at low pH levels and only partially water soluble at higher pH levels. The release of dye from pellets of the polymer indicated that the release rate of small molecules was greatly reduced at higher pH levels. ^{1}H NMR suggested that the potassium salt of poly(ethylene glycol) methyl ether initiated the anionic polymerization of DEAEM . GPC indicated that the molecular weight distribution was not monodisperse. The high polydispersity of the PEGME-*b*-PDEAEM may have resulted from slow initiation of DEAEM by the PEGME macroinitiator and/or from poor correlation of PEGME-*b*-DEAEM to polystyrene standards. IR results indicated that the polymer was carboxylic acid terminated, leaving open the possibility for further functionalization of the polymer end group. Future studies will determine the optimum sizes of the blocks for drug delivery as well as investigate the addition of amine terminated polymers to the carboxylic acid endcaps to produce triblock and multiblock copolymers.

Acknowledgements

thank Robin Kumar and Amar Ambardekar for their hard work on the exploratory stages of this research.

References

1. G. Albin, T. A. Horbett, and B. D. Ratner, J. Controlled Rel. 2, 153 (1985).

2. J. Kost, T. A. Horbett, B. D. Ratner, and M. Singh, J. Biomed. Mater. Res. 19, 1117 (1985).

3. K. Ishihara, M. Kobayashi, N. Ishmaru, and I. Shinohara, Polymer J. 16 (8), 625 (1984).

4. D. Hariharan and N. A. Peppas, Polymer. 37 (1), 149 (1996).

5. L. M. Schwarte and N. A. Peppas, Polymer. 39 (24), 6057 (1998).

6. A. S. Hoffman, G. Chen, X. Wu, Z. Ding, B. Kabra, K. Randeri, M. Schiller, E. Ron, N. A. Peppas, C. Brazel, Polym. Prepr. 38 (1), 524 (1997).

7. L. Bromberg, Ind. Eng. Chem. Res. 37, 4267 (1998).

8. L. Bromberg, J. Phys. Chem. 102, 1956 (1998).

9. S. F. Lascelles, F. Malet, R. Mayada, N. C. Billingham, and S. P. Armes, Macromol. 32, 2462 (1999).

10. E. Pretsch, T. Clerc, J. Seibl, W. Simon, Tables of Spectral Data for Structure Determination of Organic Compounds, edited by W. Fresenius, J. F. K. Huber, E. Pungor, G. A. Rechnitz, W. Simon, Th. S. West (Springer-Verlag, New York, 1989) p. I165.
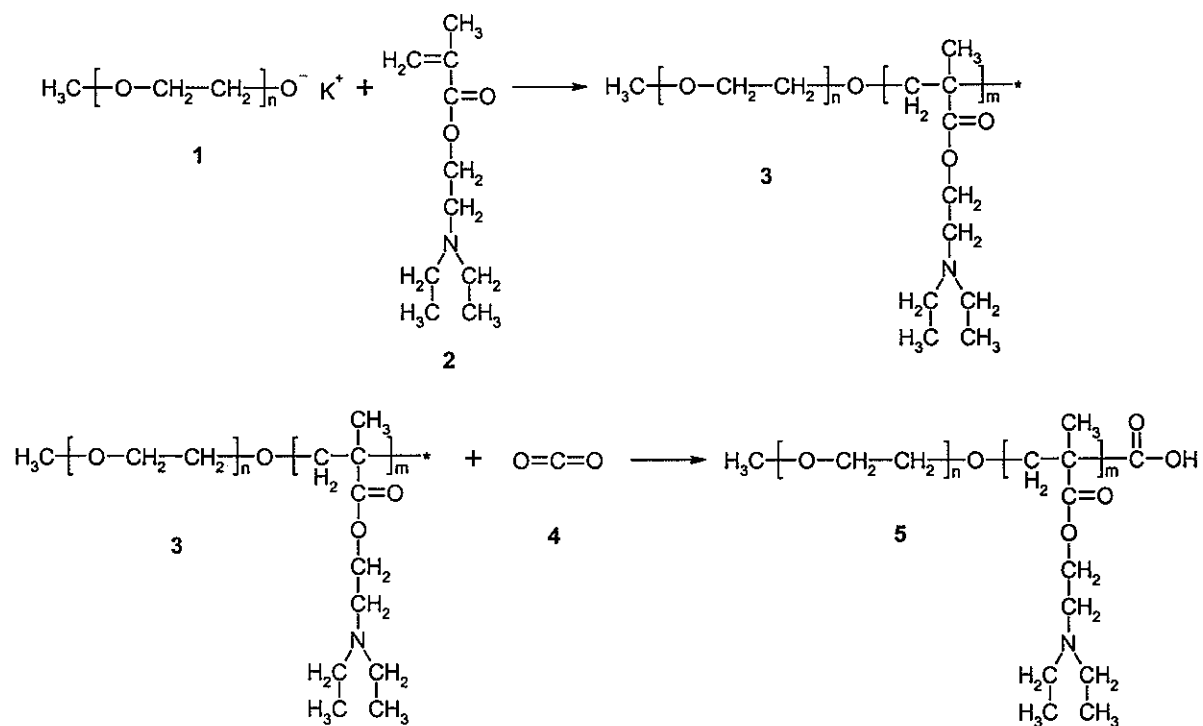
Figure 1 - PEG-b-PDEAEM synthesis route
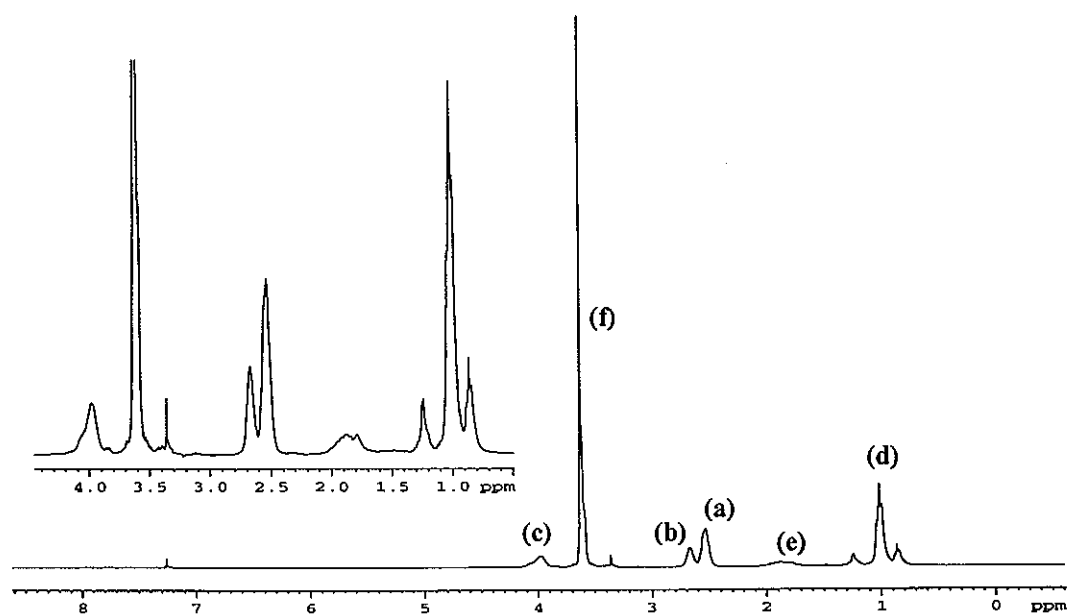
Figure 2 – NMR of PEGME-b-PDEAEM

Figure 3 – Assignment of the PEGME-b-PDEAEM ^{1}H NMR spectrum
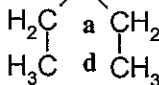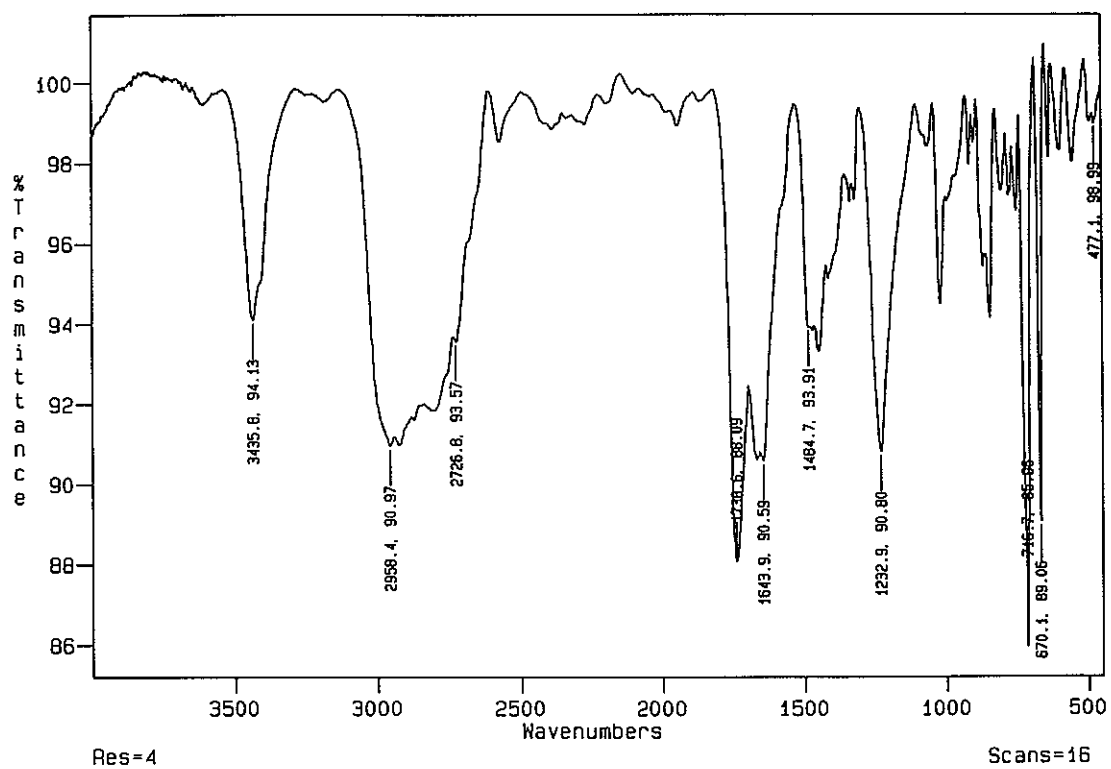
Figure 4 - IR of COOH terminated DEAEM
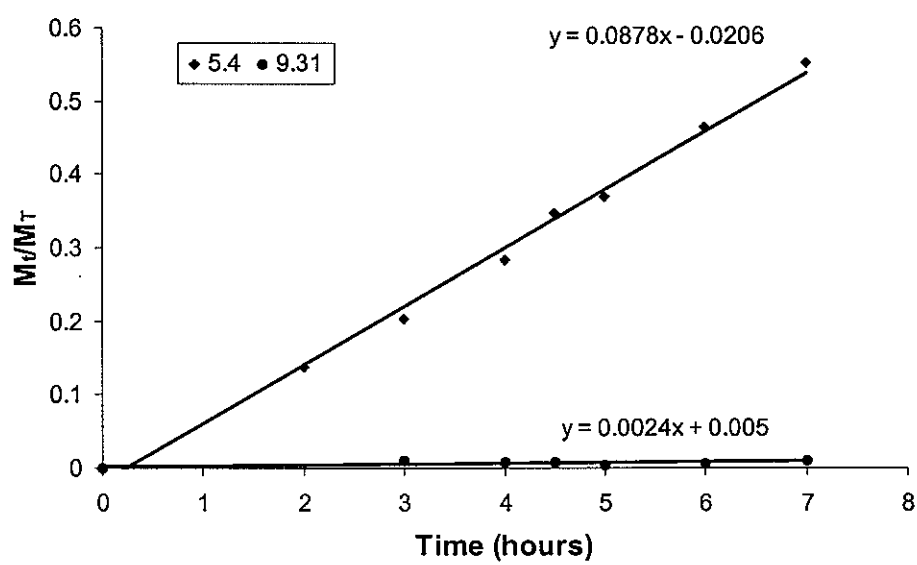
Figure 5 - Release of toluidine blue O from PEG-b-PDEAEM. ♦- pH=5.4, ●-pH=9.31

CHAPTER 5. Al-Cu-Fe Quasicrystal/Ultra-High Molecular Weight Polyethylene Composites as Biomaterials for Acetabular Cup Prosthetics

Brian C. Anderson[2,3], Paul D. Bloom[4,3], K.G. Baikerikar [4,3]
Valerie V. Sheares[4,3], Surya K. Mallapragada[2,3]

Abstract

Polymer composites of Al-Cu-Fe quasicrystals and ultra-high molecular weight polyethylene (UHMWPE) were investigated for use in acetabular cup prosthetics. The wear properties of the Al-Cu-Fe/UHMWPE samples and a 440 steel ball counterface were measured. The mechanical strength of the Al-Cu-Fe/UHMWPE composites was compared to UHMWPE and alumina/UHMWPE. The biocompatibility of the composite material was tested using a direct contact cytotoxicity assay. Al-Cu-Fe/UHMWPE demonstrated lower volume loss after wear and higher mechanical strength than UHMWPE. This composite material also showed no increase in counterface wear or cytotoxicity relative to UHMWPE. These combined results demonstrate that Al-Cu-Fe/UHMWPE composites are promising candidate materials for acetabular cup prosthetics.

Introduction

Hip arthroplasty is an important medical procedure in which the socket joints in the pelvic bone and/or the femoral head are replaced with prosthetic devices. The femoral head is usually replaced by a metal, attached by a stem inserted into the femur. The acetabulum in the pelvic bone is replaced by a prosthetic cup, typically made of a polymeric biomaterial. Recent work in the area of biomaterials for total hip arthroplasty has involved investigations of ceramic, metal, and polymeric materials for both the femoral head and acetabulum prostheses [1-4].

The current technology for the acetabular prosthetic cup is dominated by usage of ultra-high molecular weight polyethylene (UHMWPE). This polymer, usually in the molecular weight range of $\overline{M}_n$ =3x10^6 to 6x10^6, is both strong and bioinert. However, after prolonged shear stress from a metallic surface, for example a titanium femoral head prosthesis, the surface can wear and leave debris in the body. These particulates have been studied and have been found to cause osteolysis and subsequent device loosening and failure [5-7]. It has been reported that osteolysis does not usually occur in patients with low acetabular cup wear rates [8].

Quasicrystals, first discovered in 1984 [9], are complex metal alloys that possess physical properties such as low thermal conductivity, low coefficients of friction, high hardness, etc. The name quasicrystal stems from the unusual rotational symmetries and aperiodic lattice spacings found in these materials. Crystalline materials, that have periodically repeating unit cells that completely fill space must have two, three, four or six fold rotational symmetries. All other rotational symmetries are forbidden. Quasicrystals exhibit symmetries that are forbidden by classical crystallography, such as the six fivefold

axes found in icosahedral quasicrystals. In addition to the required rotational symmetries, diffraction patterns from crystalline materials have periodically spaced spots that can be used to determine lattice parameters. In contrast, diffraction patterns from quasicrystals contain aperiodic spacings.[10] The relationship between quasicrystalline structures and their novel physical properties is a current topic in quasicrystal research. Since their discovery, several hundred alloys are now known to exhibit quasicrystalline phases. The physical attributes of quasicrystals, coupled with their availability in fine powder form and potential low cost, have made them ideal materials for evaluation as reinforcing fillers in polymeric materials [11,12].

Quasicrystal filled polymers have displayed novel wear properties in addition to typical improvements in other mechanical properties associated with rigid, low aspect ratio fillers. Both thermoplastics and thermosets, such as poly(p-phenylene sulfide) bisphenol A polyarylene ether ketone, and Dow epoxy resins cured with diethylenetriamine have been investigated. Composites containing Al-Cu-Fe were determined to have enhanced wear resistance over unfilled plastics. In addition, the presence of the quasicrystalline powders in a polymer matrix caused almost no abrasion to counterface materials during wear testing [13,14]. Therefore, compared to its constituent metals and other abrasive, rigid fillers such as SiC and alumina, which are known to enhance the wear resistance of polymer composites [15], Al-Cu-Fe quasicrystals are attractive, new fillers for high-wear plastics.

The high wear resistance and low abrasive nature of these polymer composites has lead us to investigate the use of UHMWPE filled with quasicrystalline Al-Cu-Fe as a material for hip arthroplasty femoral components. These Al-Cu-Fe/UHMWPE composites have not been fabricated in the past. The possibility of lower wear rates on both the femoral head and acetabular cup is a valuable alternative to either the less wear resistant UHMWPE

or more abrasive polymer composites. This is the first study that investigates the suitability of Al-Cu-Fe/polymer composites for biomaterial applications.

As with any potential biomaterial, a central issue is the biocompatibility of this material. UHMWPE is commonly used as a negative control for direct contact cytotoxicity tests, and any substitute for this material in acetabular prosthetics would have to maintain this low level of cytotoxicity. To test the quasicrystal/polyethylene samples for cytotoxicity, a direct contact assay was performed, as described by an ASTM standard [16] to determine whether or not the material warrants further biocompatibility testing. It has been found that *in vitro* cytotoxicity tests are even more sensitive than *in vivo* studies [17]. The direct contact test was preferred over agar diffusion or elution tests because the only difference between the negative control material (UHMWPE) and the sample material (Al-Cu-Fe/UHMWPE) is the addition of Al-Cu-Fe quasicrystalline powder at 30 volume percent.

The mechanical strength and wear resistance of alumina/UHMWPE were also tested as a comparison to the Al-Cu-Fe/UHMWPE. Alumina filled polymer composites have been studied for increasing the mechanical strength of polymers for industrial [18,19] and orthopaedic [20] applications. In the mechanical testing, alumina/UHMWPE serves as a comparison of Al-Cu-Fe/UHMWPE with other particulate-filled polyethylene composites. The alumina/UHMWPE also serves as an appropriate comparison for the wear properties of the Al-Cu-Fe/UHMWPE due to the presence of the thin aluminum oxide layer known to form on the surface of Al-Cu-Fe quasicrystals in air. It has been speculated that the thin aluminum oxide layer contributes to the unique wear properties of the quasicrystals [21,22].

Materials and Methods

Sample Preparation

UHMWPE was purchased from Aldrich and used as received. Quasicrystalline Al-Cu-Fe icosahedral phase powders, with the composition $Al_{65}Cu_{23}Fe_{12}$, were prepared at Ames National Laboratory, Ames, IA 50011 [23]. These powders were prepared by gas atomization with an approximate 60 % icosahedral (quasicrystal, i-Al-Cu-Fe) and 40 % β-cubic (β-Al-Cu-Fe) phase composition. Mixtures of polyethylene (70 volume percent) and Al-Cu-Fe quasicrystal powders (30 volume percent, size fraction of 45-53 μm) were weighed, added together and shaken vigorously in a sealed container for 10 min. to provide optimum mixing. The resulting Al-Cu-Fe /polymer powder mixture was placed in a die mold that had a diameter of 2.54 cm and a final volume of 1.58 cm^3 when fully compressed. The mold was equipped with a thermocouple to monitor temperature during the compression molding process. The filled mold was heated in a variable temperature hydraulic press under a pressure of 7 MPa to 180 °C. The resulting composite surfaces were polished with 320-grade sandpaper followed by washing with deionized water. Alumina/UHMWPE samples were prepared in a similar fashion to the Al-Cu-Fe/UHMWPE samples, using 45-53 μm alumina powder. UHMWPE samples were prepared as above with no addition of metal filler. *cis*-Polyisoprene samples, the positive control for cytotoxicity tests, were prepared by coating the polymer onto stainless steel disks and removing all the solvent under vacuum overnight.

Wear Testing

The wear testing of polymer and polymer composite disks were performed on a Falex friction and wear test machine model # ISC450PC. A schematic of this machine is shown in Fig. 1. A polymer sample was placed on the rotating plate with a stationary pin as the counterface subjected to an induced load. The stationary pin materials were 440 stainless steel balls with a diameter of 0.635 cm. The wear test conditions used in each case were a: linear speed of 0.10 ms^{-1}, 10 N load, radius of 8.0 mm and 200,000 cycles (revolutions). The total linear distance was approximately 10 km. All tests were performed at room temperature under dry sliding conditions. Wear tests for unfilled UHMWPE and the Al-Cu-Fe/UHMWPE samples were performed in triplicate and the results are reported as the average and standard deviation of the measurements. The aluminum oxide/UHMWPE sample was tested one time in order to establish the abrasive nature of other fillers known to prevent polymer wear [15]. Volume loss from the composite samples was determined from profilometery measurements of the wear tracks. Pin wear was determined from the mass lost from the stationary 440 stainless steel pin after testing. Wear tracks were characterized by scanning electron microscopy (Hitachi) equipped with a secondary electron detector (Hitachi) and energy dispersive spectrometer (Oxford) for X-ray analysis. Following the wear experiments, polymer samples were coated with a thin conductive layer of gold for analysis by scanning electron microscopy.

Mechanical Testing

Mechanical testing was performed using three-point bending tests on a dynamic mechanical analyzer (Perkin Elmer DMA7e). Samples of UHMWPE, alumina/UHMWPE,

and Al-Cu-Fe/UHMWPE were cut into bars approximately 1.5 mm in height and 3 mm in width. They were subjected to 55 mN of static force and 50 mN of oscillatory dynamic force (1Hz frequency). The samples were examined over a temperature range of 30-100 °C at a scan rate of 5 °C/min. The storage modulus (E', Pa) and tan δ (E''/E' or ratio of loss modulus (E'') to storage modulus) were used to compare the mechanical strength of the materials.

Cytotoxicity Evaluation

Cytotoxicity tests of Al-Cu-Fe/ UHMWPE samples were performed by a direct contact assay outlined by the American Standards for Tests and Measures [16]. NIH/3T3 mouse fibroblasts were used as the cell line for these experiments. Cells were cultured using low-glucose Dulbecco's modified eagle medium (DMEM, Sigma) with 10% fetal bovine serum (FBS, Sigma), 10 µg/ml insulin (Sigma), 10 units/ml penicillin/streptomycin (Sigma), and 100 µg/ml L-ascorbic acid (Sigma) in a humidified incubator with 5% CO_2 at 37°C. Once the cells were cultured to confluency, they were transferred by trypsinization [0.25% trypsin (Sigma) in Hank's balanced salt solution (HBSS, Sigma)] into 6-well plates at a cell density of approximately 300 cells/mm^2. The cells were allowed to adhere to the plates and grow for 24 hours to near confluency.

Samples of UHMWPE, Al-Cu-Fe/ UHMWPE, and stainless steel disks with a coating of *cis*-polyisoprene were sterilized by swabbing with 70 % ethanol and allowing them to dry in aseptic conditions under ultraviolet light for longer than 6 hours. The media was removed from the well plates containing the cells and the samples were placed into the wells, leaving

one well empty for comparison. Media was added to the wells and the plates with samples were placed in an incubator for another 24 hours.

After 24 h, the media was removed and replaced with Karnovsky's fixative (2.5% gluteraldehyde, 2.0% paraformaldehyde, 0.1M sodium cacodylate). The fixative was allowed to stand for 24 h before replacing with crystal violet dye (CVD) in a 20% ethanol solution. After 24 h, the CVD solution was replaced with 70 % ethanol for 2 h. The ethanol was removed and the samples were allowed to air dry. The samples were then inspected for any cytotoxic response at the polymer interface using light microscopy. UHMWPE served as the negative control and *cis*-polyisoprene served as the positive control.

Results and Discussion

Wear Testing

Results from pin-on-disk wear testing showed that Al-Cu-Fe filled UHMWPE disks had enhanced wear resistance to volume loss, as compared to unfilled UHMWPE and alumina filled UHMWPE, rotating against a stationary 440 stainless steel pin (Fig. 2). The volume loss from Al-Cu-Fe/UHMWPE was shown to be statistically less than the UHMWPE ($p<0.001$). The Al-Cu-Fe/UHMWPE samples showed approximately a 35% decrease in volume loss compared to the UHMWPE samples. The wear tracks were further characterized by SEM (Fig. 3). The SEM micrographs show the behavior of the substrate after the induced wear. The UHMWPE samples (Fig. 3A) showed a smooth wear track surface approximately 900 μm in width. The Al-Cu-Fe/UHMWPE samples (Fig. 3B) showed similar wear to the UHMWPE with a slightly narrower wear track, approximately 850 μm. This is indicative of less indentation of the spherical counterface pin into the

sample and low abrasion of the counterface. The small, light-colored, circular areas on the wear track in Fig. 3B are the Al-Cu-Fe quasicrystals exposed at the wear interface.

The alumina sample (Fig. 3C) showed a much wider wear track than the UHMWPE and Al-Cu-Fe/UHMWPE samples, approximately 1500μm. This is due to the abrasion of the 440 stainless steel counterface by the exposed aluminum oxide particles in the composite at the wear interface. In addition, irregular, light-colored patterns are observed in the wear track on the aluminum oxide/UHMWPE composite (Fig. 3C) X-ray elemental mapping (Fig. 4) of these areas indicate the lighter areas are rich in iron, chromium and their metal oxides. This result confirms that the counterface stainless steel pin was abraded by the aluminum oxide particles and the debris was imbedded in the polymer composite.

The volume loss of the unfilled UHMWPE was due to both deformation and removal of the polymer during wear. The improved wear resistance of the Al-Cu-Fe/UHMWPE composites has been attributed to the high hardness, high Young modulus, and low coefficient of friction of the Al-Cu-Fe quasicrystalline filler and the increased strength of the polymer composite in comparison to unfilled UHMWPE. Low coefficients of friction for quasicrystalline alloys were first reported by Dubois et al [24]. Other materials, such as hard Cr-steel, have high hardness and a Young modulus that is approximately double that of i-Al-Cu-Fe but display higher coefficients of friction. The low coefficients of friction for quasicrystals were determined to arise from reduced electronic interactions whereas higher electronic interactions in materials such as Cr-steel contribute to sticking effects [24]. As specified in the experimental section, the Al-Cu-Fe material used in these experiments was a mixture of icosahedral (i-Al-Cu-Fe, 60 %) and β-cubic (β-Al-Cu-Fe, 40%) phases. Coefficients of friction for i-Al-Cu-Fe and β-Al-Cu-Fe were found to be very similar [25,26].

However, the presence of β-Al-Cu-Fe in bulk i-Al-Cu-Fe samples caused rapid deterioration in wear resistance [25]. In contrast, when used as a filler in epoxy composites, the mixed phase i,β-Al-Cu-Fe powder imparted comparable wear resistance to single phase i-Al-Cu-Fe powders [27].

The wear of the counterface 440 stainless steel ball by the UHMWPE composites has been summarized in Fig. 5. Abrasion of the 440 pin from contact with the Al-Cu-Fe/UHMWPE composite was low and statistically the same as the unfilled UHMWPE to a 0.05 level. SEM micrographs of the 440 stainless steel pins used for wear testing are shown in Fig. 6. By contrast, the aluminum oxide filled UHMWPE sample was very abrasive. Aluminum oxide is known for its high hardness, abrasive nature, and aspherical particle morphology. During these tests, noticeable amounts of the counterface 440 stainless steel pin material were worn away by the aluminum oxide filled composite. Steel from the pin was embedded in the alumina/UHMWPE composite and observed by SEM/EDS (Fig. 4). While aluminum oxide filled polymers typically offer excellent wear resistance [18-20], the high wear of the alumina/UHMWPE composite was attributed to the steel rich wear interface that developed on the aluminum oxide composite during wear. The wear resistance of steel filled polymer composites has been shown to be very poor [14].

Mechanical Testing

Results from the mechanical testing revealed that the Al-Cu-Fe/UHMWPE shows better mechanical properties than neat UHMWPE or the alumina/UHMWPE composite. The storage modulus of the Al-Cu-Fe/UHMWPE was higher than the UHMWPE for the entire temperature range of 30-90°C (Fig. 7). The materials were tested at higher temperatures

because these measurements give an indication of long term polymer behavior due to time-temperature superposition principles. The higher storage modulus indicates that a composite material has a higher "stiffness" than the pure material. This is almost always the case with filled polymer composites containing a particulate that has a much higher modulus than that of the polymer used as the composite matrix. If there is good bonding between the filler and the polymer matrix the modulus will increase due to a strengthening of the polymer-filler heterogeneous interface. The alumina/UHMWPE also showed a higher modulus than the unfilled material. However, the strength quickly decayed with temperature, which was as much with the Al-Cu-Fe/UHMWPE. At 37°C, the storage modulus of the Al-Cu-Fe/UHMWPE was 1.26×10^9 Pa, whereas the UHMWPE was only 1.00×10^9 Pa.

The tan δ data showed a trend similar to the storage modulus. The Al-Cu-Fe/UHMWPE displayed a higher tan δ, meaning that the storage modulus remained higher than the UHMWPE relative to their loss moduli. Alumina/UHMWPE displayed a lower tan δ value for the entire temperature range indicating an increased energy disipation via viscous deformation.

Cytotoxicity Evaluation

The results of the cytotoxicity evaluations indicated that the Al-Cu-Fe/UHMWPE composites displayed no cytotoxic behavior. Images of the cell/polymer interface for the Al-Cu-Fe/UHMWPE, positive control (*cis*-polyisoprene), and negative control (UHMWPE) are shown in Fig. 8. The positive control (Fig. 8B) elicited a cytotoxic response, as expected. The cell density near the *cis*-polyisoprene interface is extremely low and the few cells that are present appear to have detached from the surface of the well plate. There is also

considerable cellular debris present, likely due to cell lysis. At a distance greater than 2 mm from the polymer interface, the cell layer is thick and the cells are confluent. The negative control (Fig. 8A) elicited no cytotoxic response. The cell density is constant from the bulk to the interface. The Al-Cu-Fe/UHMWPE sample (Fig. 8C) displayed similar cytotoxic characteristics as the negative control. The cell density is constant up to the sample interface with all the cells fully adhered to the well plate.

Conclusions

It was concluded that Al-Cu-Fe/UHMWPE composites are potential candidate materials for prosthetic acetebular cups used in total hip replacement procedures. The wear on Al-Cu-Fe/UHMWPE composites, as tested by pin-on-disk tribology, was statistically lower than neat UHMWPE. The wear on the counterface material in these tests, a 440 stainless steel ball, was statistically the same for both the Al-Cu-Fe/UHMWPE and the UHMWPE. The wear on both the substrate and the counterface for the alumina/UHMWPE sample was much higher than either the UHMWPE or Al-Cu-Fe/UHMWPE samples. Dynamic mechanical analysis determined that the mechanical strength, represented by the storage modulus and tan δ, was improved by the addition of the Al-Cu-Fe quasicrystals to UHMWPE. The storage modulus increased by over 25 % at 37°C and tan δ was lower over the entire temperature range for the Al-Cu-Fe/UHMWPE relative to the UHMWPE. Direct contact cytotoxicity tests revealed that the Al-Cu-Fe/UHMWPE composites elicited the same cytotoxic response as pure UHMWPE that is routinely used for acetabular cup prosthetics.

References

1. Wang A, Lin R, Polineni VK, Essner A, Stark C, Dumbleton JH. Carbon fiber reinforced polyether ether ketone composite as a bearing surface for total hip replacement. Tribology International 1998;31:661-667.

2. Bonfield W. Composites for bone replacement. J Biomed Eng 1998;10:522-526.

3. Roberts JC, Ling FF, Jones WR Jr. Fabrication and wear test of a continuous fiber/particulate composite total surface hip replacement. ASLE Transactions 1983;26:367-375.

4. Goldsmith AAJ, Dowson D, Isaac GH, Lancaster JG. A comparative joint simulator study of the wear of metal-on-metal and alternative material combinations in hip replacement. Proc Instn Mech Engrs 2000;214:39-47.

5. Amstutz HC, Campbell P, Kossovsky N, Clarke IC. Mechanism and clinical significance of wear debris-induced osteolysis. Clin Orthop 1992;276:7-18.

6. Howie DW, Haynes DR, Rogers SD, McGee MA, Pearcey MJ, The response to particulate debris. Orthop Clinics North America 1993;24:571-581.

7. Maloney WJ, Peters P, Engh CA, Chandler H. Severe osteolysis of the pelvis in association with acetabular replacement without cement. J Bone Joint Surg 1993;75A:1627-1635.

8. Dowd JE, Sychterz CJ, Young AM, Engh CA. Characterization of long-term femoral-head-penetration rates. Association with and prediction of osteolysis. J Bone Joint Surg Am 2000 Aug;82-A(8):1102-7.

9. Shechtman D, Blech I, Gratias D, Cahn JW, Metallic phase with long-range orientational order and no translational symmetry. Phys Rev Lett 1984;53:1951-1953.

10. Bloom PD, Sheares VV. Quasicrystal-Polymer Composite Materials and Methods. PCT Int Appl 2000, WO 0056538, US Patent (filed 5/99).

11. Bloom PD, Otaigbe JU, Sheares VV. High-performance quasicrystal-reinforced polymer composites. Proceedings of the American Chemical Society Division of Polymeric Materials: Science and Engineering 1999;80:406-407.

12. Bloom PD, Baikerikar KG, Otaigbe JU, Sheares VV. Development of novel polymer/quasicrystal composite materials. J Mat Sci & Eng A 2000;294-296:156-159.

13. Bloom PD, Baikerikar KG, Anderegg JW, Sheares VV. Development of Al-Cu-Fe quasicrystal-poly(p-phenylene sulfide) composites. Mat Res Soc Symp 2001;643: K16.3.1-K16.3.12

14. Durand JM, Vardavoulias M, Jeandin M. Role of reinforcing ceramic particles in the wear behavior of polymer-based model composites. Wear 1995;181-183:833-839.

15. Standard practice for direct contact cell culture evaluation of materials for medical devices – Designation F813-83. In: The 2000 Annual Book of ASTM Standards, Philadelphia, 2000, 240-243.

16. Ulreich JB, Chavapilin M. In vitro toxicity testing: a quantitative microassay. In: Brown SA, editor. Cell-culture Test Metods, ASTM, Philadelphia, 1983, 102-113.

17. Brotzman RW, Aikens J, Batllo F, Kullberg M, Kritchevsky G. Nanomaterials and wear resistant polymers. Ceram Ind 2000;150:39-43.

18. Kumar K, Kumar K. Sliding wear studies in epoxy containing alumina powders. High Temperature Materials and Processes 1998;17;271-274.

19. Rieu J, Goeuriot P. Ceramic Composites for Biomedical Applications. Clinical Materials 1993;12:211-217.

20. Wehner BI, Koster U. Microstructural evolution of alumina layers on an Al-Cu-Fe quasicrystal during high-temperature oxidation. Oxidation of Metals 2000;54:445-456.

21. Gil-Gavatz M, Rouxel D, Pigeat P, Weber B, Dubois J –M. Surface oxidation of the $Al_{62}Cu_{25.5}Fe_{12.5}$ icosahedral quasicrystal. Philosophical Magazine A 2000;80;2083-2097.

22. Shield JE, Goldman AI, Anderson IE, Ellis TW, McCallum RW, Sordelet DJ. Method of making quasicrystal alloy powder, protective coatings and articles U.S. Patent No. 5,433,978, 1995.

23. Dubois JM, Kang SS., von Stebut JJ. Quasicrystalline Low-Friction Coatings. Mat Sci Lett 1991;10:537-541. (journal of materials science letters)

24. Brunet P, Zhang LM, Sordelet DJ, Besser M, Dubois JM. Comparative study of microstructural and tribological properties of sintered, bulk icosahedral samples. J Mat Sci & Eng A 2000; 294-296:74-78.

25. Zhang LM, Dong C, Brunet P, Dubois JM. Influence of valence electron concentration over friction coefficient of B2-based approximants. J Mat Sci & Eng A 2000;294-296:810-812.

26. Manuscript in preparation.

27. Goldman AI, Anderegg JW, Besser MF, Chang S-L, Delaney DW, Jenks CJ, Kramer MJ, Lograsso TA, Lynch DW, McCallum RW, Shield JE, Sordelet DJ, Thiel PA Quasicrystallin Materials. American Scientist, 1996, Volume 84, 230-241.
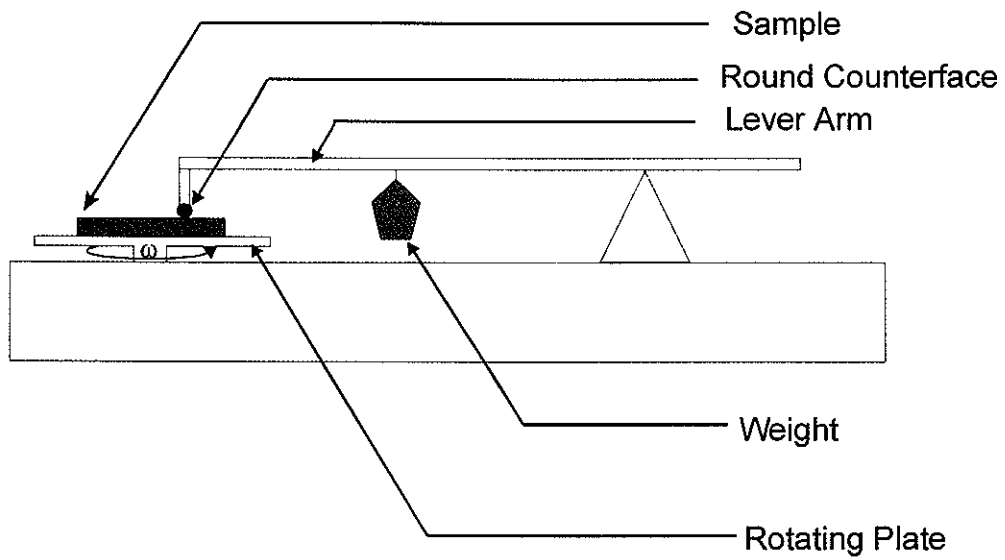
Fig. 1. Schematic of pin-on-disk wear testing apparatus.
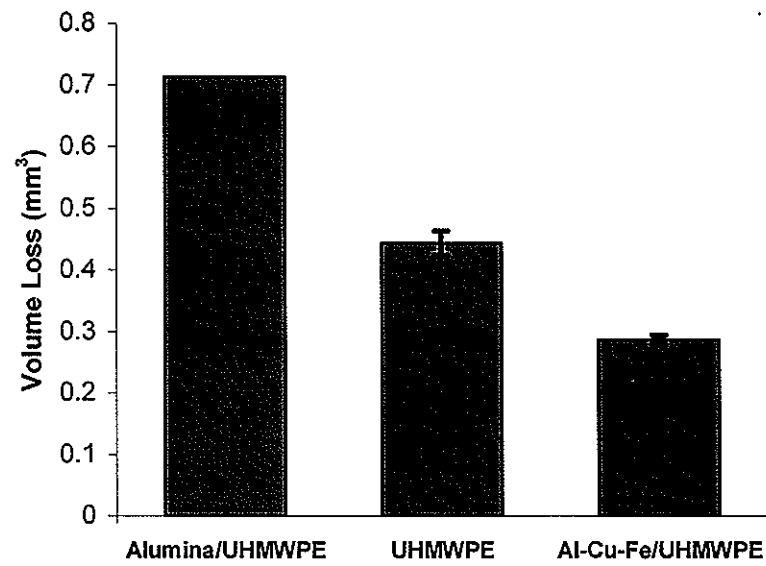
Fig. 2. Volume loss from UHMWPE, Al-Cu-Fe/UHMWPE, and Al_2O_3/UHMWPE samples after wear testing. Error bars represent standard deviations of the measurements.
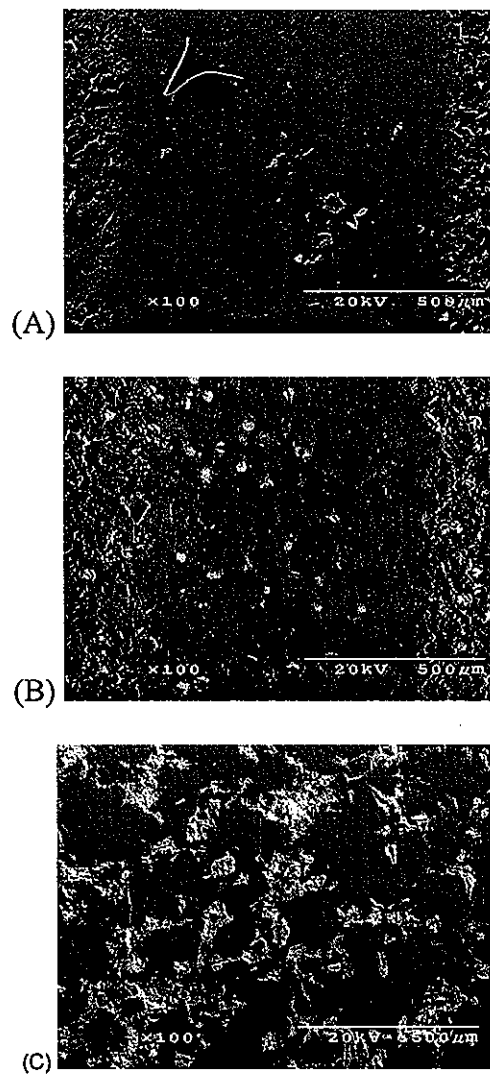
Fig. 3. Wear tracks analysis of (A) UHMWPE (B) Al-Cu-Fe/UHMWPE and (C) alumina/UHMWPE samples by SEM.
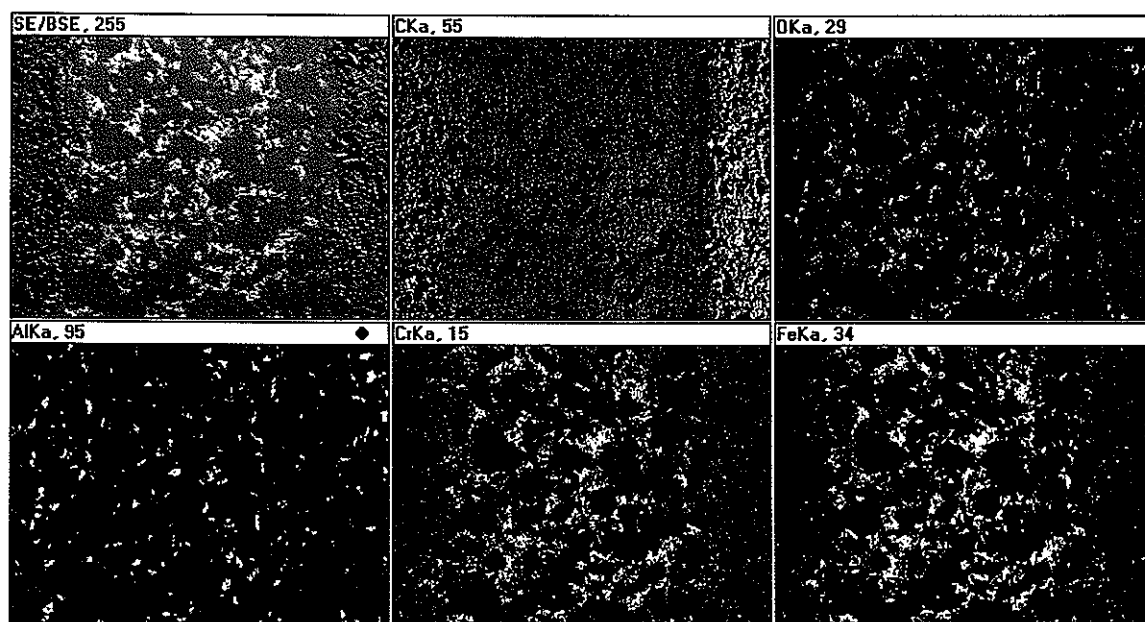
Fig. 4. SEM/EDS X-ray elemental mapping of the aluminum oxide/UHMWPE composite. Left to right: Secondary Electron Image, Carbon, Oxygen; Row two: Aluminum, Copper, Iron.
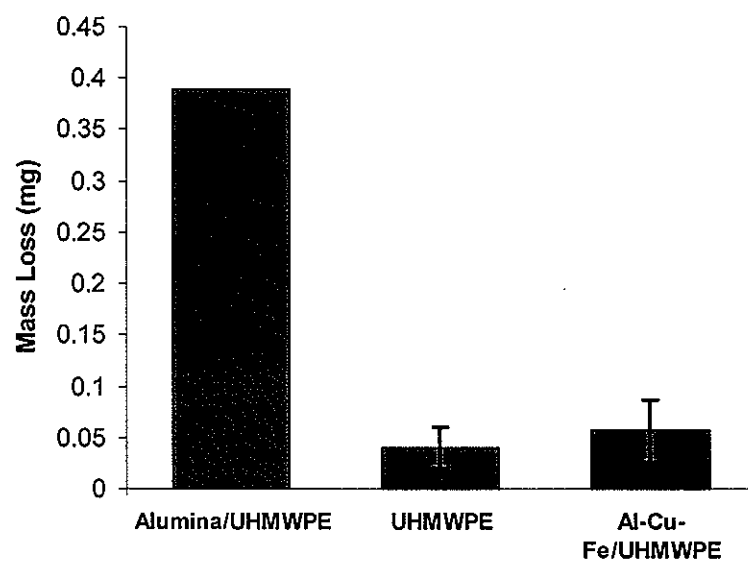
Fig. 5. Mass loss from 440 stainless steel pin after wear testing on UHMWPE, Al-Cu-Fe/UHMWPE, and Al_2O_3/UHMWPE surfaces. Error bars represent standard deviations of the measurements.
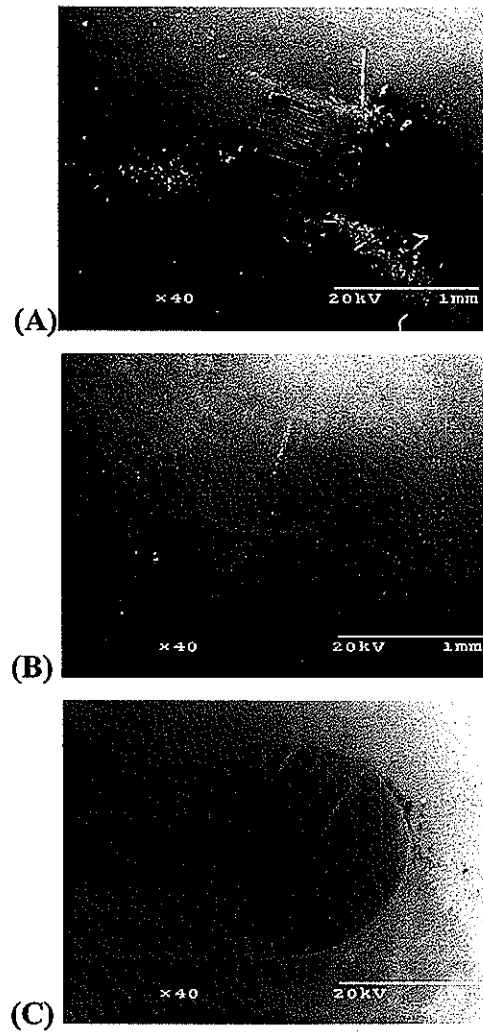
Fig. 6. Analysis of 440 stainless steel pin from wear testing in contact with (A) UHMWPE (B) Al-Cu-Fe/UHMWPE and (C) alumina/UHMWPE samples by SEM.
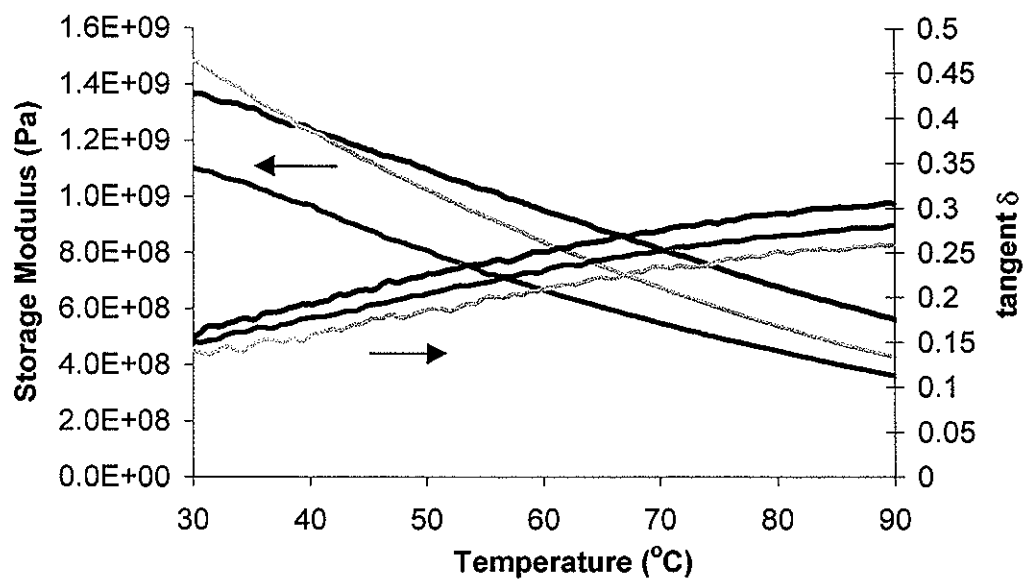
Fig. 7. Dynamic mechanical analysis of polymer samples.▬ UHMWPE,▬Al-Cu-Fe/UHMWPE, ▭▭▭
alumina/UHMWPE.
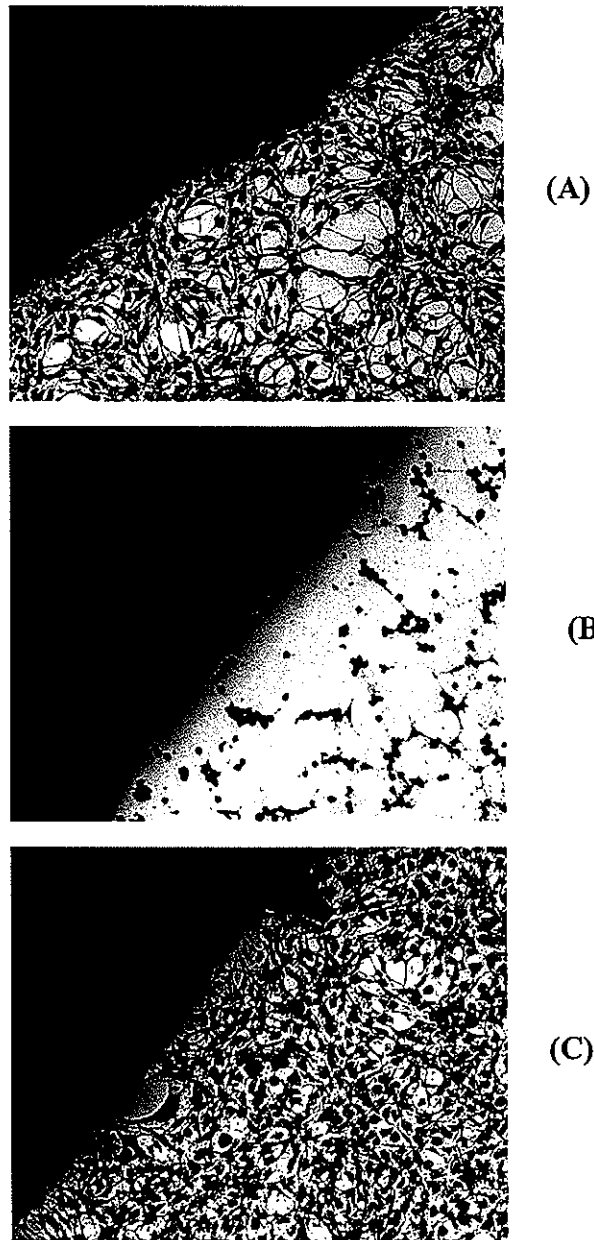
Fig. 8. 3T3 fibroblasts after direct contact cytotoxicity testing (100 times). (A) Negative control, UHMWPE, (B) Positive control, *cis*-polyisoprene, (C) Al-Cu-Fe/UHMWPE sample.

CHAPTER 6. Synthesis and Characterization of Injectable, Water-Soluble Copolymers of Tertiary Amine Methacrylates and Poly(Ethylene Glycol) Containing Methacrylates

Brian C. Anderson[2,3] , Surya K. Mallapragada[2,3*]

Abstract

Several homopolymers and copolymers of 2-(diethylamino)ethyl methacrylate (DEAEM) and poly(ethylene glycol) methyl ether methacrylate (PEGMEM) were synthesized using anionic polymerization initiated by potassium t-butoxide. The polymers were characterized by average molecular weight, polydispersity and monomeric unit composition. A very narrow molecular weight distribution was achieved with a well controlled composition. The glass transition temperatures and compositions of the copolymers followed a Gordon-Taylor relationship. The water solubility and biocompatibility of the copolymers was compared to their parent homopolymers to determine if the addition of a poly(ethylene glycol) group was sufficient to solubilize the polymers in aqueous buffer solutions and to increase the biocompatibility of the polymers. These water-soluble, injectable cationic copolymers have potential applications in gene delivery as well as other biomaterial applications.

Introduction

Synthetic polyelectrolytes are valuable tools in a variety of bioapplications ranging from drug delivery and protein separations to gene therapy. Beyond bioapplications, there are several industrial applications for specialty polyelectrolytes [1]. The ability to carry an ionic charge, yet incorporate a wide range of complementary thermal, solubility, processing, and other properties has made polymers with cationic and anionic character an active research topic.

Polymers like polyethyleneimine have been used for years as vehicles to induce flocculation of proteins [2] and other biomacromolecules [3]. The electrostatic interaction between the biomolecule and the selected polyelectrolyte provides the means to selectively precipitate charged molecules out of an aqueous solution, for example a fermentation broth[3].

In addition to the electrostatic interactions between charged pendent groups and biomolecules, cationic polymers also exhibit swelling due to electrostatic interactions between neighboring polymer molecules. This leads to pH-dependent swelling as the polymer molecules are repelled from each other upon protonation or deprotonation. Many polyelectrolytes, however, are not sufficiently biocompatible or soluble over a wide enough range of pH conditions to be useful in more applications where the polymer would be in contact with human cells and body fluids [4,5,6]. One common approach to increase the biocompatibility of these, and many other, polymers is to add small amounts of poly(ethylene glycol) [7]. Crosslinked polymer membranes made of a methacrylate containing a tertiary amine, either diethyl- or dimethyl- amino ethyl methacrylate, and a poly(ethylene glycol)

derivative [8] or another methacrylate [9] have been studied for pH-sensitive drug release devices.

The newest use for polycation polymers is the delivery of genetic material to mammalian cells for gene therapy applications. There have been studies outlining the use of tertiary amine methacrylate homopolymers for gene delivery and the effect the type of methacrylate has on the transfection efficiency [10]. It was found that a homopolymer of 2-(diethylamino)ethyl methacrylate (DEAEM) might be a useful delivery material for plasmid DNA, but could not form polymer/DNA complexes like many other cationic methacrylates [10]. It was hypothesized that this was because of the low water solubility of the polymer.

Other studies have investigated free radical initiated copolymers of 2-(dimethylamino)ethyl methacrylate (DMAEM) with poly(ethylene glycol) methyl ether methacrylate (PEGMEM), N-vinyl-pyrrolidone (NVP), and methyl methacrylate (MMA) [11,12]. It was found that copolymers of DMAEM with NVP or PEGMEM were less toxic than the DMAEM homopolymer and still maintained a high transfection ability.

Two more controlled approaches to synthesizing appropriate random and block copolymers of methacrylates for gene delivery are group transfer polymerization and anionic polymerization. Group transfer polymerization has been used to synthesize block copolymers of DMAEM and low molecular weight PEGMEM as well as random copolymers of DMAEM and higher molecular weight PEGMEM [13].

Our approach is to use anionic polymerization of a lower molecular weight PEGMEM and DEAEM to synthesize a copolymer that is water soluble, but has the diethylamino moiety on the pendent groups of the methacrylate. The synthesis route uses an oxyanion initiator, as first proposed by Nagasaki for DEAEM homopolymers [14]. This

procedure has been elaborated on since then for both PDEAEM [15] and PDMAEM [16-17] as well as for block copolymers [16,18,19].

Because of the desire to obtain materials that are biocompatible, cationic and water-soluble, several tests were used to verify that these goals were achieved. Cytotoxicity tests were used to determine the biocompatibility of the synthesized polymers and dynamic solubility tests were used to test the solubility and dissolution rate of the homopolymers and copolymers. Cloud point experiments were performed to verify the absence of a pH-induced precipitation by the copolymers.

Materials and Methods

Materials – The monomers N,N-diethylaminoethyl methacrylate (DEAEM) and poly(ethylene glycol) methyl ether methacrylate (PEGMEM, $\overline{M}_n$=300) were purchased from Sigma (St. Louis, MO). Both were stirred over calcium hydride for at least 24 hours prior use. The dried monomer was then distilled under vacuum immediately prior to use. Distilled monomer was stored for up to 12 hours under argon pressure at 4°C in a plastic desiccator, at which point unused monomer was discarded. Tetrahydrofuran (THF) was dried over sodium metal in the presence of benzophenone until a purple color was present. The dry THF was then distilled under argon and used immediately. Potassium t-butoxide (KtBu) was purchased from Sigma and was used under a dry, inert atmosphere with no purification.

Polymerization – A stock solution of 0.817M KtBu initiator in dry THF was prepared immediately prior to polymerization. An appropriate amount of monomer (DEAEM, PEGMEM or a combination of the two) was transferred via air-tight syringe into a flame

dried 100 ml round bottom flask with magnetic stir bar. All flasks used were flame dried for at least 2 minutes and cooled under flowing argon. Rubber septa sealed the flasks with copper ties to allow pressurization with argon. The monomer was then diluted to approximately 20% by mass with THF. 2.0 ml of the stock KtBu solution was injected into the solution using an air-tight syringe. The solution was stirred at 400 RPM at room temperature for 20 minutes followed by 20 minutes at 50°C. The polymerization was terminated by injection of methanol into the reaction vessel. The resultant polymer was precipitated in −78°C n-hexane and dried for at least 48 hours under vacuum at 50°C.

NMR characterization – ^{1}H NMR was collected on a Varian VXR300 300 MHz spectrometer. The solvent used was chloroform, $CDCl_3$, for all samples.

Gel Permeation Chromatography – GPC was used to obtain the average molecular weight of the polymer as well as the polydispersity index. THF was used as the mobile phase with a sample volume of 300 µl per sample injection. Four PLgel columns (Polymer Laboratories, Amherst, MA) heated to 40°C achieved the appropriate separation. An Optilab inline refractomenter (Wyatt Corp, Santa Barbara, CA) was used as the detector for retention times of the synthesized polymers relative to poly(methyl methacrylate) standards.

Multi-Angle Laser Light Scattering – In order to obtain a more accurate assessment of the molecular weight and molecular weight distribution, inline light scattering data was obtained. A DAWN multi angle light scattering detector (Wyatt Corp., Santa Barbara, CA) was used to detect the scattered light at 90° from the incident beam. A dn/dc value of 0.049 mL/g was

used for all copolymers and homopolymers. This value was determined by assuming 100%

mass recovery with a known injection concentration and was consistent for the homopolymer

and the various copolymers.

Differential Scanning Calorimetry – Sub-ambient differential scanning calorimetry detection

of the glass transition temperature was performed on a Pyris1 DSC (Perkin Elmer, Shelton,

CT). Samples were cooled to -100°C and held at this temperature for 15 minutes before

beginning a temperature scan from -100°C to 40°C at a rate of 3°C/min under a nitrogen

purge. The T_g was determined using an inflection point method.

Solubility Testing – Solubility of the various homopolymers and copolymers was determined

at three different pH levels; pH 6.5, pH 7.4, and pH 8.5. A small sample of the polymer,

approximately 30-40 mg, was placed on a clean glass slide that had been dried at 160°C

overnight. The sample was submerged in a phosphate or ammonium buffer at one of the pH

levels and allowed to rotate radially for either 0.25, 0.5, 1 or 24 hours. At this point, the

sample slide was removed from the buffer, rinsed quickly with deionized water to remove

any residual buffer and placed face up in a vacuum oven for at least 24 hours. After the

samples were dried, they were weighed to determine the mass of original polymer remaining.

Cloud Point Determination – Cloud points were determined by dissolving a small amount of

the polymer, approximately 35 mg, into approximately 10 ml of a well stirred pH 6.5 buffer

solution and adding 0.1 M NaOH until the solution became turbid. The tests were performed

at room temperature and carried out in triplicate for samples that exhibited a pH induced cloud point.

Biocompatibility Testing – The cytotoxicity of the materials was determined using an elution-type test. Approximately 30 mg of the polymers to be tested were dissolved in 100 ml of low-glucose Dulbecco's modified eagle medium (DMEM, Sigma) with 10% fetal bovine serum (FBS, Sigma), 10 µg/ml insulin (Sigma), 10 units/ml penicillin/streptomycin (Sigma), and 100 µg/ml L-ascorbic acid (Sigma). This solution was diluted to achieve the desired polymer concentration for all tests. NIH/3T3 mouse fibroblasts were grown on a 25mm^2 tissue culture treated polystyrene flask until they had achieved a cell density of approximately 150 cells/mm^2. The DMEM was removed from the flasks and replaced with one of the following: DMEM, DMEM with phenol, DMEM with the polymer to be tested. The phenol served as a positive control and the pure DMEM served as a negative control for these tests. The concentrations of phenol and polymer tested were 3 mg/L, 0.3 mg/L and 0.03 mg/L. This concentration range was chosen because of the potential gene therapy applications of the polymer.

After 24 hours of incubation in a humidified incubator with 5% CO_2 at 37°C the samples were removed and the media was replaced with Karnovsky's fixative (2.5% gluteraldehyde, 2.0% paraformaldehyde, 0.1M sodium cacodylate) for 12 hours. The fixative was then washed off the samples and was replaced with crystal violet dye (CVD) in a 20% ethanol solution. After 6 hours, the CVD was removed and the cells were dehydrated with ethanol and the cell layer was inspected for a cytotoxic response. Cell density, morphology and adherence were compared for the positive control, negative control and test samples.

Results and Discussion

NMR characterization – In addition to detecting residual monomer in the homopolymers and random copolymers, NMR was also used to determine the ratio of diethylaminoethyl methacrylate and poly(ethylene glycol) methyl ether methacrylate for the copolymers. Both DEAEM and PEGMEM have a ^{1}H NMR peak at approximately 4.3 ppm (Figure 1). The peak integral from the peak near 4.3 ppm is a combination of the first -CH$_2$- groups (α position) next to the methacrylate in both the monomers. However, PEGMEM contains the characteristic poly(ethylene glycol) peak at 3.6 ppm (Figure 1). The peak at 3.6 ppm for the PPEGMEM homopolymer was then given a normalized integral of 1.000 and the peak around 4.3 ppm was then integrated with respect to this peak. This ratio of the 3.6 ppm peak to the 4.3 ppm peak in the homopolymer was considered to be the ratio of the peaks from pure PEGMEM monomer in the absence of DEAEM monomer. The same procedure was then carried out for the copolymers.

The peak area associated with the PEGMEM monomer was then subtracted from the combined peak area to find the area associated with the DEAEM monomer. Because both monomers have two protons associated with this peak, the ratio of the deconvoluted peak areas is the ratio of the monomers in the copolymer. The tabulated data for the target ratio and the ratio obtained from this characterization method are given in Table 1. The ratios reported in Table 1 are the ratios of PEGMEM:DEAEM in all cases.

Because the deshielding of the protons on the α-position carbon relative to the ester in the two monomers is not exactly the same, there is a slight shift in the location of this peak using NMR. This is visualized in Figure 2, where the copolymer and homopolymer NMR spectra are stacked to track the formation of the slightly bimodal peak in the copolymers and

the shifted peaks of the homopolymers as well as the presence of the 3.6 ppm poly(ethylene glycol) peak in the PEGMEM containing polymers.

Gel Permeation Chromatography – Gel permeation chromatography results relative to poly(methyl methacrylate) standards were drastically lower than what was expected based on initiator concentration (Table 1). The polydispersity index (PDI), however, was on the order that is expected for anionic polymerization. In the absence of premature termination or slow initiation, both of which would cause a much broader molecular weight distribution, there is little explanation of a $\overline{M}_n$ much lower than the expected $\overline{M}_n$. Due to the high mass fraction of the polymer contained in the pendent groups of the PDEAEM and PEGMEM/DEAEM copolymers, a relative calibration to linear polystyrene or poly(methyl methacrylate) could yield measured molecular weights much lower than their actual values. In order to verify the relative calibration measurements light scattering was used to obtain an absolute molecular weight measurement.

Multi-Angle Laser Light Scattering – The values for $\overline{M}_n$ resulting from laser light scattering were much higher than the values obtained from relative RI measurements. The $\overline{M}_n$ values were also slightly higher than the target values, which could be due to the fact that the initiator was not titrated prior to each polymerization. If some of the potassium t-butoxide became inactive then the amount of active initiator would be lower, resulting in higher molecular weight values. If an exact $\overline{M}_n$ was desired, such a practice could be performed

immediately prior to the polymerization. The polydispersities obtained from light scattering were slightly lower than from relative RI measurements.

Differential Scanning Calorimetry – Differential scanning calorimetry was used to characterize the glass transition temperatures (T_g) of the PPEGMEM and PDEAEM homopolymers and the copolymers. Because of the low T_g for these polymers, a liquid nitrogen cooled DSC was used. The Tg ranged from –49.1°C for the PPEGMEM homopolymer to –19.8°C for the PDEAEM homopolymer. The T_g of these and the copolymers as a function of molar monomer ratio and mass monomer ratio are given in Table 2. Using the Gordon-Taylor equation for glass transition temperatures of random copolymers (Equation 1, 20), a predicted value for the T_g was calculated (Table 2). A value 0.15 was used for k, which was treated as a fitting factor. In Equation 1, x_2 is the mass fraction of the PEGMEM in the copolymer. It should be noted that the Gordon-Taylor equation uses the T_g of the homopolymers as endpoints of the model, so the accuracy can be no better than the accuracy of the homopolymer measurement. There is good agreement between the modeled T_g and the measured T_g.

$$Tg = \frac{x_1 Tg_1 + kx_2 Tg_2}{x_1 + kx_2} \qquad (1)$$

Solubility Testing – One of the characteristics of PDEAEM we had hoped to modify with the synthesis of a PPEGMEM/PDEAEM copolymer is the poor water solubility of PDEAEM under non-acidic conditions. This property can be a benefit in some pH-sensitive drug and gene delivery applications, but in cases where the polymer needs to have cationic character

and be fairly water-soluble at body pH (around 7.4) PDEAEM fails [10]. The copolymers of

PDEAEM and PPEGMEM were then tested for water solubility under several pH conditions

to assess the increased water solubility with the addition of the PEGMEM moiety.

Samples of the synthesized polymers were tested over several time scales ranging

from immediately soluble (15 minutes) to near-infinite solubility (24 hours). The results for

the long term test are given in Figure 3. It appears that the addition of as little as 30 mol%

PEGMEM monomer in the copolymer results in full solubility under all of the conditions

tested. The PDEAEM homopolymer, on the other hand, displayed no solubility under

slightly basic conditions and only partial solubility under acidic conditions after 24 hours. A

closer comparison of the PDEAEM homopolymer and 30% PEGMEM/ 70% DEAEM

copolymer under all pH conditions and for several times is given in Figure 4. This

comparison further illustrates the water-soluble character of the copolymers relative to the

PDEAEM homopolymer. The mass fraction of 30:70 PEGMEM:DEAEM copolymer

remaining after 15 minutes was nearly zero, whereas after 24 hours 100% of the PDEAEM

homopolymer remained for the basic conditions. Even at relatively neutral (pH 7.4)

conditions, the PDEAEM had 80% remaining after one hour and nearly 40% remaining after

24 hours. This compares to the copolymer that dissolved completely in under 15 minutes at

this pH. This small amount of copolymer that appears at 24 hours is simply an artifact of the

measurement accuracy of the tests. No copolymer was visible to the eye at any time at or

after 15 minutes.

Cloud Point Determination – All of the copolymer compositions as well as the

homopolymers were tested for pH-induced cloud point (CP) at room temperature. The

homopolymer PDEAEM exhibited a CP at pH 7.7. None of the copolymers exhibited a cloud point for a pH as high as 12. This is further indication that the PDEAEM homopolymer is not soluble in many aqueous solutions, but any of the copolymer formulations tested are soluble under a wide range of pH conditions. It should be noted that these tests were only carried out at one concentration and were simply used to verify that the PEGMEM:DEAEM copolymers would not precipitate out of solution under high pH conditions, as the parent homopolymer does. Due to the dynamic range of pH in the human body, a polymer that could precipitate and accumulate under certain conditions would not be acceptable for many biomedical applications.

Cytotoxicity Testing – The results of the polymer samples tested were compared to results of the same tests using a known cytotoxic material, phenol, and a negative control. The phenol elicited the expected positive cytotoxic results (Figure 5a). The cell bodies are small and the cells do not appear to be confluent. This can be compared to the positive control (Figure 5b) where the cell bodies are large and cover the entire surface. The PDEAEM homopolymer (Figure 5c) elicited a response similar to the phenol, indicating the material is, in fact, cytotoxic. The 30:70 PEGMEM:DEAEM copolymer (Figure 5d) appeared to have the same effect on the density of the cell layer as the negative control. Although the test is subjective, it seems apparent that the copolymer is much less cytotoxic than the parent DEAEM homopolymer. This contrast was seen at all the concentrations tested; 3 mg/L, 0.3 mg/L, and 0.03 mg/L.

Conclusions

Copolymers of DEAEM and low molecular weight PEGMEM ($\overline{M_n}$~300) can be synthesized using anionic polymerization initiated by potassium alcoholates like potassium t-butoxide. The molecular weights tended to be higher than expected as determined by inline laser light scattering. This was assumed to be because of initiator deactivation during short periods of storage. The polydispersity as determined by light scattering was below 1.25 for all polymers and below 1.15 for many examples.

It was determined that a relative calibration molecular weight measurement was not appropriate for these polymers using a PMMA standard. This is probably due to the non-linearity of the polymer as a result of the rather bulky pendant groups. Light scattering is a more appropriate measurement technique for this application because it does not rely on a relative standard. Glass transition temperatures were in line with what is expected by the Gordon-Taylor expression for glass transition temperatures for random copolymers.

Cloud point and water solubility tests verified that the addition of as little as 30 % (molar basis) of the poly(ethylene glycol) moiety leads to solubility of the polymer in aqueous solutions over a wide range of pH levels. Cytotoxicity tests have shown that a homopolymer of DEAEM elicits a cytotoxic response by 3T3 fibroblasts, whereas the DEAEM/PEGMEM copolymer did not elicit a cytotoxic response in concentrations as high as 3 mg/L. Copolymers of DEAEM and PEGMEM are therefore potential injectable water-soluble carriers of plasmid DNA for gene therapy. Further tests will determine if the copolymers have the ability to complex with plasmid DNA and transfect cells; however the addition of the PEGMEM moiety has eliminated some of the limitations of the parent DEAEM homopolymer by improving biocompatibility and solubility in water.

Acknowledgments

References

1. Mortimer DA. Synthetic polyelectrolytes – a review. Polymer International 1991;25:29-41.

2. Chen W, Walker S, Berg, JC. The mechanism of floc formation in protein precipitation by polyelectrolytes. Chemical Engineering Science 1992; 47:1039-1045.

3. Milburn P, Bonnerjea J, Hoare M, Dunnill P. Selective flocculation of nucleic acids, lipids, and colloidal particles from a yeast cell homogenate by polyethyleneimine, and its scale up. Enzyme and Microb. Technol. 1990; 12: 527-532.

4. Fischer D, Zange T, Kissel T. Comparative in vitro cytotoxicity studies of polycations for gene therapy. Proc. Int. Symp. Control. Rel. Bioact. Mat. 1997; 24: 647-648.

5. Fischer D, Li YX, von Harpe A, Beiber T, Elasser HP, Kissel T. Poly(ethyleneimine-co-2-hydroxyethyl ethylenimine) polymers: relation between polymer structure, biocompatibility and transfection efficiency. Proc. Int. Symp. Control. Rel. Bioact. Mat. 1999; 26: 104-105.

6. Asayama S, Maruyama A, Cho CS, Akaike T. Design of comb-type polyamine copolymers for a novel pH-sensitive DNA carrier. Bioconjugate Chemistry 1997; 8: 833-838.

7. Ogris M, Brunner S, Shuller S, Kircheis R, Wagner E. PEGylated DNA/transferring-PEI complexes: reduced interaction with blood components, extended circulation in blood and potential for systemic gene delivery. Gene Therapy 1999; 6: 595-605.

8. Schwarte LM, Podual K, Peppas NA. Cationic hydrogels for controlled release of proteins and other macromolecules. ACS Symp. Ser. 1998; 709:56-66.

9. Ishihara K, Kobayashi M, Ishimaru N, Shinohara I. Glucose induced permeation control of insulin through a complex membrane consisting immobilized glucose oxidase and a poly(amine). Polymer Jounal 1984; 16: 625-631.

10. van de Wetering P, Moret EE, Schuurmans-Nieuwenbroek NME, van Steenbergen MJ, Hennink WE. Structure-activity relationships of water-soluble cationic methacrylate/methacrylamide polymers for nonviral gene delivery. Bioconjugate Chemistry 1999; 10: 589-597.

11. van de Wetering P, Cherng JY, Talsma H, Crommelin DJA, Hennik WE. 2-(dimethylamino)ethyl methacrylate based (co)polymers as gene transfer agents. Journal of Controlled Release 1998; 53: 145-153.

12. van de Wetering P, Schuurmans-Nieuwenbroek NME, van Steenbergen MJ, Crommelin DJA, Hennink WE. Copolymers of 2-(dimethylamino)ethyl methacrylate with ethoxytriethylene glycol methacrylate or N-vinyl-pyrrolidone as gene transfer agents. Journal of Controlled Release 2000; 64: 193-203.

13. Rungsardthong U, Deshpande M, Bailey L, Vamvakaki M, Armes SP, Garnett MC, Stolnik S. Copolymers of amine methacrylate with poly(ethylene glycol) as vectors for gene therepy. Journal of Controlled Release 2001; 73: 359-380.

14. Nagasaki Y, Sato Y, Kato M. A novel synthesis of semitelechelic functional poly(methacrylate)s through an alcoholate-initiated polymerization. Synthesis of poly[2-(N,N-diethylaminoethyl) methacrylate] macromonomer. Macromol. Rapid Commun.1997; 18: 827-835.

15. de Paz Bánez MV, Robinson KL, Butun V, Armes SP. Use of oxyanion-initiated polymerization for the synthesis of amine methacrylate-based homopolymers and block copolymers. Polymer 2001; 42: 29-37.

16. Lascelles SF, Malet F, Mayada R, Billingham NC, Armes SP. Latex syntheses using novel tertiary amine methacrylate-based macromonomers prepared by oxyanionic polymerization. Macromolecules 1999; 32: 2462-2471.

17. Shen Y, Zeng F, Zhu S, Pelton R. Novel cationic macromonomers by living anionic polymerization of (dimethylamino)ethyl methacrylate. Macromolecules 2001; 34: 144-150.

18. Anderson BC, Bloom PD, Sheares VV, Mallapragada SK. Synthesis and characterization of water soluble block copolymers for pH-sensitive delivery. Mat. Res. Soc. Symp. Proc. 2001; 662: NN1.8.1-NN1.8.6.

19. Vamvakaki M, Billingham NC, Armes SP. Synthesis of controlled structure water-soluble diblock copolymers via oxyanionic polymerization. Macromolecules 1999; 32, 2088-2090.

20. Schneider HA. Conformational Entropy Contributions to the Glass Temperature of Blends of Miscible Polymers. J. Res. Natl. Inst. Stand. Technol. 1997; 102, 229-248.

Table 1 – Monomer ratios (PEGMEM:DEAEM) and molecular weights of the synthesized polymers

ID	Target ratio	Ratio(NMR)	Target $\overline{M_n}$	$\overline{M_n}$(GPC)	$\overline{M_n}$(LS)	PDI (GPC)	PDI (LS)
A	100:0	100:0	10,000	8123	22600	1.19	1.15
B	50:50	43.1:56.9	10,000	7694	31200	1.18	1.25
C	30:70	28.6:71.4	10,000	6624	22100	1.18	1.13
D	0:100	0:100	10,000	6208	28300	1.18	1.24
E	100:0	100:0	20,000	7879	19600	1.22	1.21
F	70:30	74.9:25.1	20,000	8772	28700	1..22	1.13
G	50:50	49.1:50.9	20,000	8834	25100	1.20	1.15
H	30:70	31.5:68.5	20,000	8930	47200	1.20	1.14
I	0:100	0:100	20,000	7985	18200	1.21	1.20
J	100:0	100:0	20,000	8150	18400	1.21	1.20
K	70:30	62.6:37.4	20,000	9315	29600	1.18	1.15
L	50:50	53.3:46.7	20,000	9232	27800	1.24	1.17
M	30:70	33.4:66.6	20,000	9312	34600	1.27	1.13
N	0:100	0:100	20,000	8749	44500	1.32	1.12

Table 2 – Glass transition temperatures of DEAEM/PEGMEM copolymers and homopolymers

ID	Ratio(molar)	Ratio (mass)	Tg (^{o}C)	Tg (Gordon-Taylor)
E	100:0	100:0	-49.1	-49.1
F	74.9:25.1	64.8:35.2	-47.4	-46.9
G	49.1:50.9	37.3:62.7	-44.7	-43.2
H	31.5:68.5	22.1:77.9	-37.4	-38.9
I	0:100	0:100	-19.8	-19.8
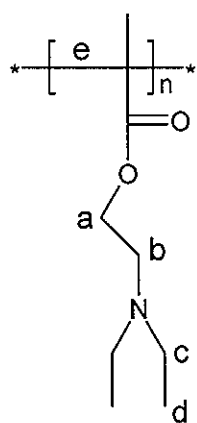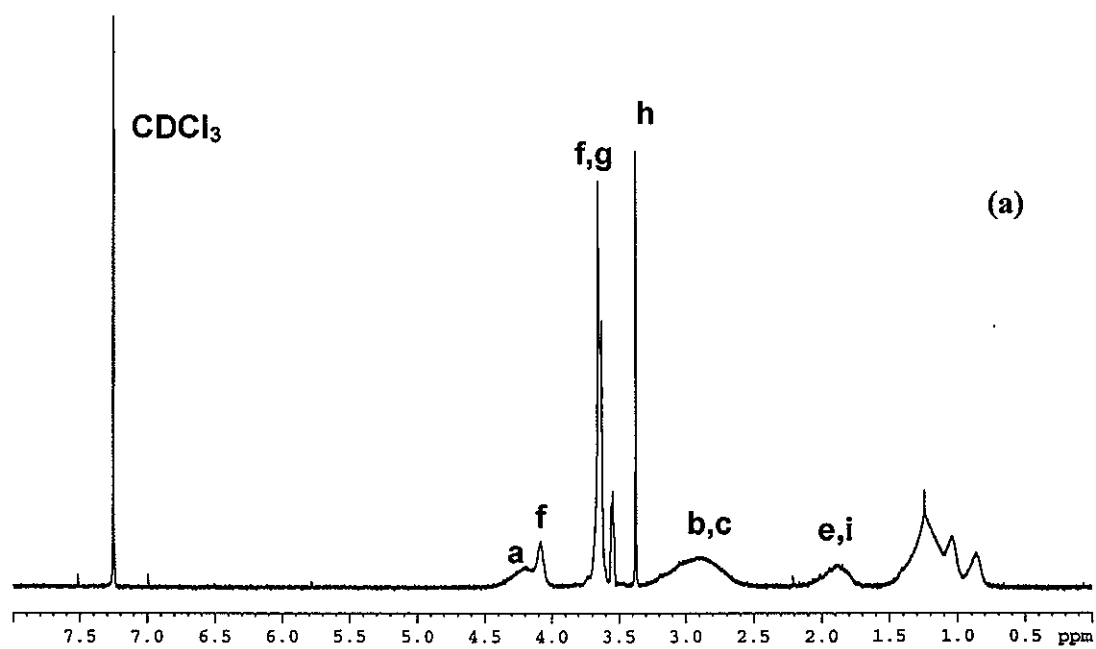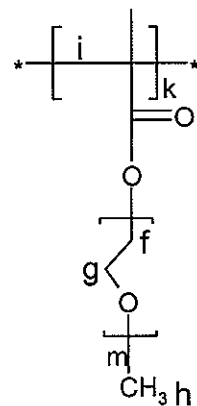
Figure 1. Analysis of copolymer with PEGMEM:DEAEM ratio of 30:70 (a) ^{1}H NMR spectra. (b) Structure of DEAEM unit. (c) Structure of PEGMEM unit.
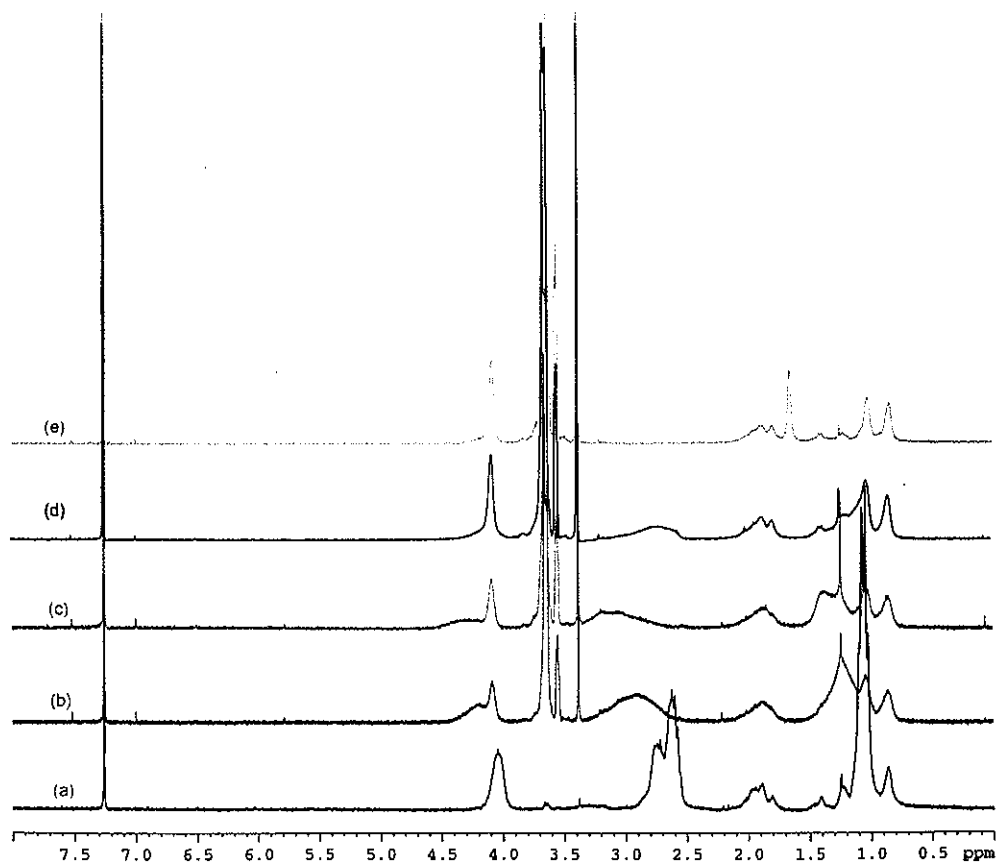
Figure 2. Stacked NMR spectra of (a) PDEAEM homopolymer, (b) copolymer with PEGMEM:DEAEM ratio of 30:70, (c) copolymer with PEGMEM:DEAEM ratio of 50:50, (d) copolymer with PEGMEM:DEAEM ratio of 70:30, (e) PPEGMEM homopolymer.
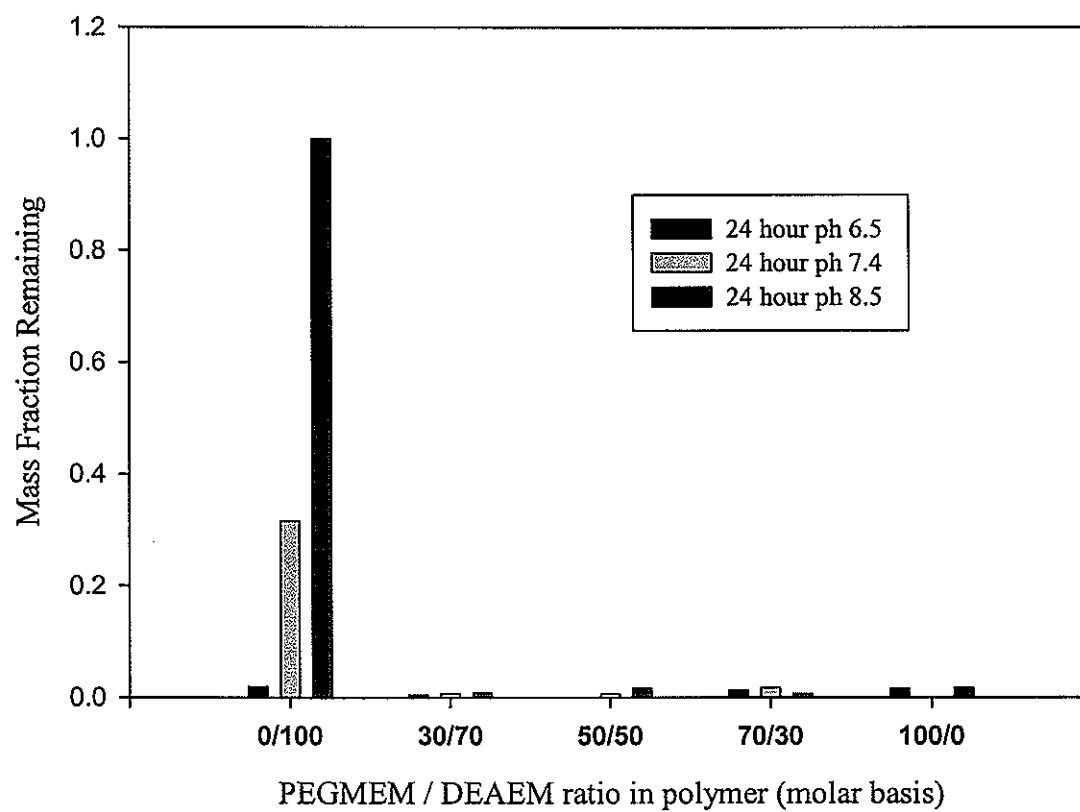
Figure 3. Solubility of homopolymers and copolymers after 24 hours under three different pH conditions.
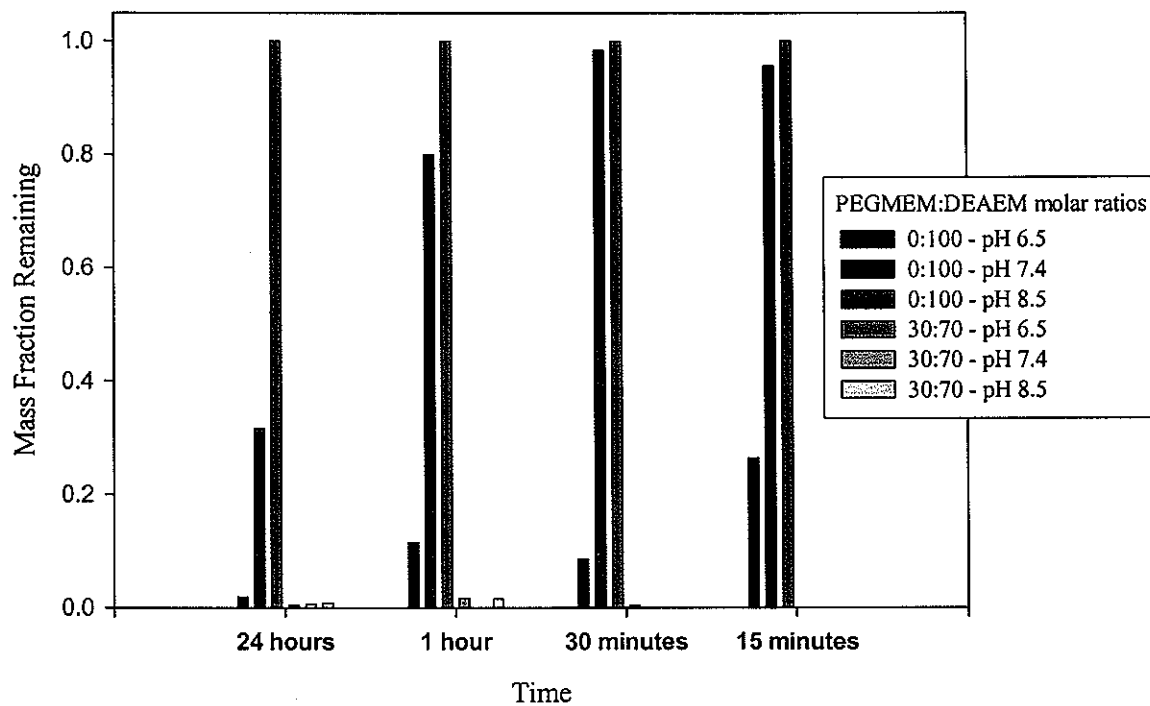
Figure 4. Solubility of PDEAEM homopolymer and PEGMEM:DEAEM 30:70 copolymer for different pH conditions and several times.
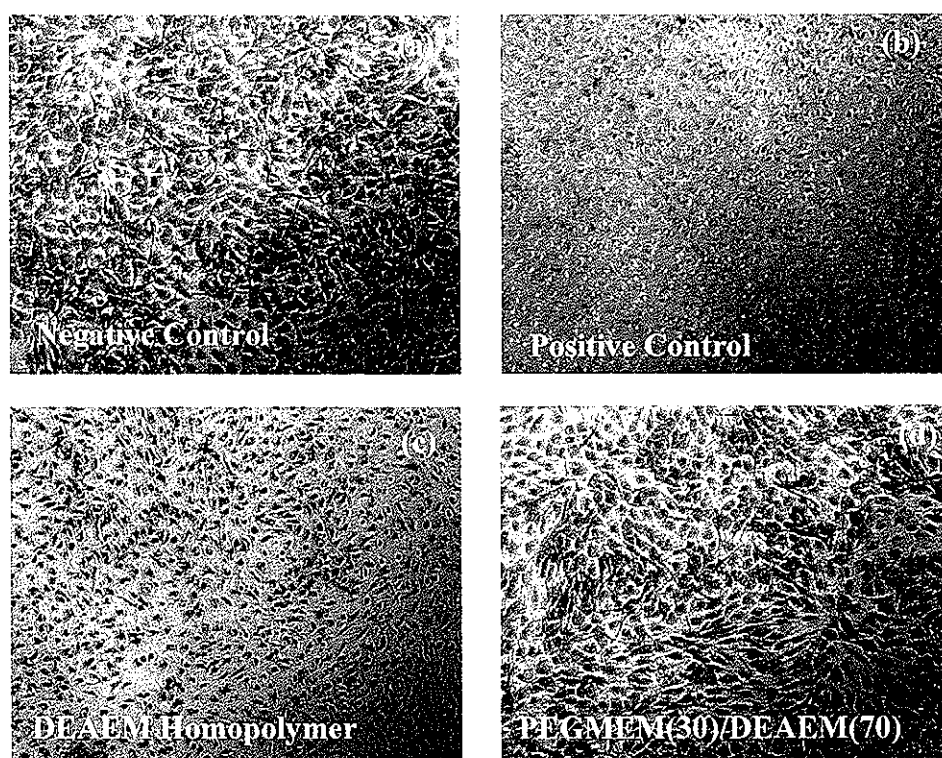
Figure 5. Cytotoxity of (a) negative control, growth media, (b) positive control, phenol, (c) PDEAEM homopolymer, (d) 30:70 PEGMEM:DEAEM copolymer. Polymer and phenol concentrations are all 0.3 mg/L.

CHAPTER 7. Synthesis and Characterization of Diblock and Gel Forming Pentablock Copolymers of Tertiary Amine Methacrylates, Poly(Ethylene Glycol) and Poly(Propylene Glycol)

Brian C. Anderson[1,2] , Suzan M. Cox[1,2], Paul D. Bloom[2,3], Valerie V. Sheares[2,3]

Surya K. Mallapragada[1,2*]

Abstract

Novel pH-sensitive gel forming pentablock copolymers based on commercially available Pluronic® (poly(ethylene oxide)-*b*-poly(propylene oxide)-*b*-poly(ethylene oxide), PEO-*b*-PPO-*b*-PEO) triblock copolymers and cationic diblock copolymers based on poly(ethylene glycol) methyl ether, PEGME, were synthesized by oxyanionic polymerization. Polymerization of the cationic moiety, poly(diethylamino ethyl methacrylate), PDEAEM, was initiated by a difunctional potassium alcoholate of the triblock Pluronic® copolymer F127 (PEO$_{106}$-PPO$_{69}$-PEO$_{106}$) or PEGME. The difunctionality of the initiation using the triblock macroinitiator, indicating formation of a pentablock copolymer rather than a tetrablock copolymer, was verified by functionalized termination of the living polymer chains. Critical micellization temperatures, CMT, of the synthesized polymers were obtained from differential scanning calorimetry (DSC) for the pentablock materials. The pentablock copolymers retained the thermoreversible gel forming properties of Pluronic® F127, as well as similar CMT values. The polydispersity of both the diblock and pentablock

---

[1] Department of Chemical Engineering, Iowa State University, Ames, IA, 50011
[2] Ames Laboratory, United States Department of Energy, Ames, IA, 50011
[3] Department of Chemistry, Iowa State University, Ames, IA, 50011

copolymers was similar to the macroinitiators, indicating a very low polydispersity associated with the addition of the cationic PDEAEM blocks. Both of the materials show pH-sensitive release behavior, whereas the native polymers do not.

Introduction

Interest in the development of novel environmentally sensitive biomaterials for drug delivery applications has grown in the past several years. Crosslinked hydrogels have been developed that incorporate characteristics such as pH and/or temperature sensitivity for stimuli-sensitive release[1,2].

It has been established that the incorporation of monomeric units containing tertiary amines introduces pH-dependent swelling in crosslinked polymeric membranes[3-5]. Many of the studies involving crosslinked copolymer membranes of tertiary amines and other materials focus on the use of these materials for glucose-sensitive drug delivery[4,5]. With the incorporation of the enzyme glucose oxidase, materials that swell under low pH conditions will swell under conditions of high glucose concentration[6]. However, there have been very few studies that attempt to exploit these pH-dependent functionalities in non-crosslinked systems.

The triblock copolymer Pluronic® (poly(ethylene oxide)-*b*-poly(propylene oxide)-*b*-poly(ethylene oxide)) has distinct amphiphilic properties that have been utilized in applications ranging from degreasing agents to de-foaming additives used in fermentation. Under the appropriate concentration and thermal conditions, aqueous solutions of this polymer form micellar systems consisting of dehydrated poly(propylene oxide) cores surrounded by solvated poly(ethylene oxide) coronas[6-8]. The segregated lipophilic

nanophase can increase the total aqueous solution solubility of small organic molecules like naphthalene[9] and ibuprofen[10], molecules that are relatively insoluble in non-micellar aqueous solutions.

At sufficient polymer concentrations, these materials undergo a sol-gel transition at temperatures slightly higher than the critical micellization temperature (CMT)[11]. This non-crosslinked gel is soluble in an aqueous medium as water penetrates the gel, lowering the total concentration of polymer at the gel interface below a concentration sufficient to maintain the gel state at that temperature. This thermoreversible gelation property has been investigated for use as a controlled release delivery device both *in-vitro*[12-14] and *in-vivo*[15,16]. Aqueous polymer/drug solutions can be injected intramuscularly[15] or inraperitoneally[16] to produce non-crosslinked matrix delivery devices that do not require surgical insertion or removal. Drug release is controlled by the dissolution of the polymer gel as water penetrates the device at the polymer/tissue interface[14].

However, typical *in vitro* dissolution times for such a device are on the order of 5-6 hours[12,14]. Although *in vivo* release times are slightly longer, on the order of 10-20 hours[15-16], devices based on Pluronic® polymers may not be extremely useful for controlled drug or bioactive molecule delivery. Because of the availability of orally administered controlled released tablets, injectable devices must release their dosage over a time period much longer than that available with Pluronic® based devices in order to compete with the available technology.

The incorporation of stimuli-sensitive functionality, for example pH-sensitivity, into a Pluronic® based delivery device could, however, provide modulated delivery over a time period similar to or longer than current controlled release devices. Typical orally

administered devices provide a constant, non-modulated release. In the past, research on self-monitoring modulated delivery included implanted electronic microsensors and micropumps[17,18], however current research has focused on devices that do not have to be implanted. An injectable system would be superior to implantable technologies from an administration standpoint. Non-invasive delivery, for example stimuli-sensitive transdermal patches, often lack the ability to be environmentally responsive, due to their lack of direct contact with most body fluids. Our work has focused on the synthesis of novel materials that can be used as self-regulating injectable and water soluble delivery devices to rectify these shortcomings.

Recently, homopolymers and random copolymers of N,N-diethylaminoethyl methacrylate (DEAEM) and poly(ethylene glycol) methyl ether methacrylate (PEGMEM) have been synthesized using a oxyanion initiated anionic route[19]. Ni et al. have reported the synthesis of triblock materials based on a poly(propylene glycol) (PPG) based macroinitiator using a similar synthesis route[20]. There is no verification, however, that the materials synthesized are truly triblock or are in fact diblock materials.

Our approach involves utilizing a difunctional potassium alcoholate initiator based on the Pluronic® triblock copolymer formulation F127, as well as monomethyl ether terminated poly ethylene oxide (PEGME), to produce pentablock and diblock copolymers of DEAEM, PEG, and PPG to be used for pH-sensitive drug delivery. The pentablock materials retain the thermodynamic phase transitions present in the triblock base polymer while providing a stimuli-sensitive release profile suitable for self regulated drug release. The diblock materials do not form gels like their pentablock counterparts, however they do supply environment-sensitive release of small molecules in dehydrated tablet form. We have used

benzyl endcaps to quantify the average functionality of the synthesized pentablock materials to verify the presence of pentablock rather than tetrablock materials.

Experimental Section

Materials

N,N-(diethyl amino)ethyl methacrylate (DEAEM, Sigma-Aldrich, St. Louis, MO) was dried over calcium hydride and purified by distillation under reduced pressure. Tetrahydrofuran (THF, Sigma-Aldrich Co., St. Louis MO) was dried by passing through solvent purification columns of alumina and Q5 copper/silica/alumina catalyst (columns, Solv-Tek, Berryville, VA; Q5, Engelhard Corp, Iselin, NJ). Poly(ethylene oxide)-*b*-poly(propylene oxide)-*b*-poly(ethylene oxide) (Pluronic® F127, $\overline{M}_n$=12,600, 70% w/w PEG, Sigma-Aldrich Co St. Loius, MO) and poly(ethylene glycol) methyl ether (PEGME $\overline{M}_n$ ~5000, Polysciences Inc., Warrington, PA) were dried by heating under vacuum. Sodium phosphates were obtained from Fisher Scientific. Nile blue chloride (NBCl, visible absorbance maximum at 636 nm, MW=375.0) was obtained from Sigma-Aldrich. All other materials were purchased from Sigma-Aldrich Co. and used as received.

Techniques

Polymerization- All flasks and magnetic stir bars used were either flame dried and cooled under an inert atmosphere or heated overnight at 180°C and cooled under an inert atmosphere. Flasks were sealed with metal-tied rubber septa to allow for argon pressurization. Potassium hydride, stored under mineral oil, was washed with THF in an

inert atmosphere in a round bottom flask. Enough dry THF was added to completely submerse the solid potassium hydride.

F127 (1) or PEGME (2) was dissolved in THF in a round bottom flask. It was necessary to heat the THF and F127/PEGME to slightly above room temperature in order to dissolve the polymer. The solvated polymer was transferred via canulla into a flask containing potassium hydride (3) to form either the monofunctional alcoholate (4) or the difunctional alcoholate (5) (Scheme 1).

An appropriate amount of DEAEM (6) was added via air-free syringe or canulla to the solution of either (4) or (5) while stirring at 400 rpm at room temperature for 20 min, followed by 50°C for 20 minutes (Scheme 2). The living polymers (7) and (8) were terminated with an injection of methanol (9) or benzyl bromide (10) (Scheme 3). The resulting polymers (11), (12), or (13) were precipitated in -78°C *n*-hexane and dried under vacuum for at least 24 hours. The polymer was then characterized and its pH sensitivity was tested using the following techniques.

NMR characterization – ^{1}H NMR data was collected on Varian VXR400 (400 MHz) and Varian VXR300 (300MHz) spectrometers. Chloroform-d was used as the solvent for most samples. For samples in which phenyl protons were used as a functionality marker, acetone-d_6 was used to avoid peak overlap.

Gel Permeation Chromatography – GPC was used to obtain the polydispersity index of the polymer. THF was used as the mobile phase with a sample injection volume of 100 µl. The system was equipped with three PLgel columns (Polymer Laboratories, Amherst,

MA) heated to 40°C. An Optilab inline refractive index detector (Wyatt Corp, Santa Barbara, CA) was used as the detector for retention times of the synthesized polymers relative to poly(methyl methacrylate) and polystyrene standards.

Differential Scanning Calorimetry – Differential scanning calorimetry measurement of the critical micellization temperature was performed on a DSC7 (Perkin Elmer, Shelton, CT). Samples were cooled to -10°C and held at this temperature for 15 minutes before beginning a temperature scan from -10°C to 35°C at a rate of 5°C/min under a nitrogen purge. The critical micellization temperature was determined as the onset of the deviation of the endothermic micellization transition peak from the baseline.

Buffer preparation – Sodium phosphate buffers were prepared by adding the appropriate amount of anhydrous monobasic sodium phosphate (NaH_2PO_4) and anhydrous dibasic sodium phosphate (Na_2HPO_4) to deionized water. The total ionic strength of the solutions was 0.5 M. These buffers were used to test the pH sensitivity of the polymers that were synthesized.

Molecule Release Rates – The dye nile blue chloride (NBCl) was used as a model drug for all release studies. Its moderate water solubility, and molecular weight of 375.0 g/mol make it a suitable model drug for many small molecules that do not partition exclusively into lipophilic or aqueous phases. The absorbance maxima of NBCl in the visible spectra at 636 nm makes release rates easy to measure without interference from the dissolved polymer.

Dissolution of polymer samples was tested using one of two methods. For the pentablock materials, a 10:1 polymer to dye solution was prepared in ethanol. The ethanol was evaporated leaving a homogeneous polymer/dye solid. Cold aqueous solutions were prepared from this material as reported in other studies[14,21]. The samples were then placed in appropriate containers, typically glass dishes with a radius of 14 mm and height of 10 mm, and were placed in a 37°C oven where they formed non-crosslinked hydrogels. These samples were tested in a stirred dissolution tank at 37°C and allowed to dissolve over a period of time. Samples were removed from the dissolution tanks at various intervals and tested for dye concentration using visible wavelength spectrophotometry. The agitation rate used for the tests was 60 RPM with a 10:1 F127:NBCl solution as a control.

For the diblock materials, tablets were prepared from a similar homogeneous polymer/dye solid by compression molding at 7000 PSI for 5 minutes. The tablets were placed in a dissolution testing apparatus and tested for NBCl concentration in a similar manner to the gel-forming polymers. For both types of materials various pH values were investigated and measurements were preformed in triplicate. Poly(ethylene glycol) with $\overline{M_n}$ values of 5000 g/mol and 8000 g/mol were used as non-ionic controls and were used as received from Sigma-Aldrich (St. Louis, MO).

Cytotoxicity Testing – The cytotoxicity of the materials was determined using an elution-type test reported in our previous work[22]. Briefly, approximately 30mg of the polymers to be tested were dissolved in 100 ml of low-glucose Dulbecco's modified eagle medium (DMEM, Sigma) with 10% fetal bovine serum (FBS, Sigma), 10 μg/ml insulin

(Sigma), 10 units/ml penicillin/streptomycin (Sigma), and 100 μg/ml L-ascorbic acid

(Sigma). This solution was diluted to achieve the desired polymer concentration for all tests.

NIH/3T3 mouse fibroblasts were grown in polystyrene flasks until reaching

confluence at 150 cells/mm^2. The growth media was removed from the flasks and replaced

with one of the following: DMEM (negative control), DMEM with phenol (positive control),

DMEM with the pentablock material. The concentrations of the pentablock material and

phenol were 3 mg/L, 0.3 mg/L and 0.03 mg/L.

After 24 hours of incubation in a humidified incubator with 5% CO_2 at 37°C the

samples were removed and the media was replaced with Karnovsky's fixative (2.5%

gluteraldehyde, 2.0% paraformaldehyde, 0.1M sodium cacodylate) for 12 hours. The

samples were then stained with a 20% crystal violet dye (CVD) solution in ethanol for 6

hours followed by dehydration with ethanol. The cell layer was then inspected for a

cytotoxic response by noting changes in cell density, morphology and adherence relative to

the positive and negative control samples.

Results and Discussion

Molecular Weight – All the samples prepared showed PDI values similar to the

macroinitiators used, indicating very little added polydispersity due to the PDEAEM blocks

(Table 1). The relative amount of PDEAEM is reported as percent mass of the methacrylate

blocks relative to the total weight of the copolymer. The apparent slight decrease in PDI

from the macroinitiator (samples H and I) to the block copolymers, especially for the

pentablock copolymer, is assumed to be due to a higher reactivity of the lower molecular

weight initiators relative to the higher molecular weight initiators. This is more evident in

the case of the pentablock, due to the bimodal nature of the Pluronic® copolymer macroiniator[23]. For Pluronic® F127, the lower molecular weight mode is on the order of $\overline{M}_p$=6000 g/mol, whereas the upper mode has an $\overline{M}_p$ of approximately 14,000 g/mol. The distance between the modes appears to get smaller as DEAEM is added to the polymers, resulting a slightly lower PDI. As appears to be the case in other studies with PDEAEM, GPC is not always an accurate measure of $\overline{M}_n$ or $\overline{M}_w$ most likely because of binding of the DEAEM moiety with the column packing and the high molecular weight of the DEAEM pendent groups. Often NMR values are used for $\overline{M}_n$ and the PDI is approximated from GPC[24]. A sample NMR of a pentablock material with peak assignments is given as Figure 1 and a sample NMR of a diblock material is given as Figure 2. The $\overline{M}_n$ values for the DEAEM blocks for both materials can cover a wide range, however our release studies focused on a specific range of molecular weight. Simple dissolution and gelation tests indicated the pentablock material A (Table 1) and the diblock material F appeared to be in a molecular weight range and DEAEM/initiator ratio that produced interesting pH-sensitive behavior while maintaining the properties of PEG and F127 that were desirable. Because of this, these two materials were used for the bulk of the release studies. However, materials with customized DEAEM block lengths and mass fractions can easily be prepared by the addition of slightly more or less of the cationic moiety.

Differential Scanning Calorimety – DSC was used to evaluate two thermodynamic properties of the pentablock materials. First, the onset of the micellization temperature, T_m, was determined as reported in the literature for triblock materials[21]. Second, the endothermic

enthalpy (ΔH) of the micellization phase transition was measured by integrating the micellization peak. Values for ΔH, T_m and ΔS are given for 28% w/w aqueous samples over a wide range of PDEAEM block lengths in Table 2. Samples at lower polymer concentrations are also reported for the 36.2% DEAEM pentablock copolymer and the Pluronic® triblock copolymer.

The trend seen in the data presented in Table 2 indicates that the addition of the PDEAEM blocks slightly depresses T_m and reduces the magnitude of the endothermic ΔH. The magnitude of this depression is not great for the smaller PDEAEM block lengths, namely 10% and less, however the magnitude increases for the larger PDEAEM block lengths. Although the trend is clear, a Tukey multiple comparison test ($\alpha=0.05$) indicated that only the extreme samples, 0% - 36.2% and 0% - 20%, are statistically significant for ΔH and ΔS. For T_m, all samples were statistically the same at a 0.05 level due to the large variance in measured values. However, the values for samples H* and A* are a good example of the T_m and ΔH depression. The difference between these samples, as seen in a t-test for different means, are statistically significant to a $p<0.01$ level for both T_m and ΔH.

The reason for the ΔH depression is an apparent reduction in the entropic driving force for micellization. The PPO core of the micelles are the influential factor for micellization[8]. It is assumed that the PDEAEM portions of the pentablock material partition into the hydrophobic micelle core due to the fact PDEAEM is quite hydrophobic itself and would at least partially be solvated by the PPO nanophase. This would lead to a reduction in entropic advantage to micellization, and thus the observed change in enthalpy and entropy of micellization. In addition, limited hydrogen bonding with the methacrylate at temperatures

below the CMT may partially disrupt the hydrophobic effect, the entropic driving force for micellization[25]. The depression in T_m with increasing PDEAEM block length is most likely due to an increase in the amount of hydrophobic characteristic of the polymer. The more monomeric units of hydrophobic species, the lower the micellization temperature.

Pentablock Functionality – For pentablock materials terminated with benzyl bromide, the phenyl peaks were integrated relative to the known PEG Pluronic® peaks at ~3.7 ppm to determine the average number of benzyl termini per molecule. The terminal signals integrated against the PEG peak divided by the number of equivalent PEG protons in the initiator showed a ration of 10:1, or two benzyl groups, per Pluronic® initiator molecule. This indicates that according to our procedure, we are able to prepare materials that are fully pentablock in nature. Whether the block lengths are identical cannot be verified, however this benzyl termination procedure allows some insight into the material's molecular structure.

Release Studies – The tablet dissolution studies of the diblock materials revealed a dramatic pH dependence on the release rate of dye from the polymer tablets. The specific material reported here has a $\overline{M_n}$ of 8120 g/mol, or 38.4% PDEAEM. At the higher pH values, specifically 7.4 and 8.2, the release rate is markedly slower than the lower pH values (Figure 3). The release rate at a pH value of 5.7 (0.290 fraction/hour) is over an order of magnitude faster than at the pH value of 8.2 (0.021 fraction/hour). The tablets submerged in the lower pH buffers dissolved at the polymer/buffer interface and released the contained dye. At the higher pH values, the tablets merely broke apart into small fragments that did not dissolve. The entrapped dye released very slowly, probably from dye dissolving at the

fragment interfaces. In the high pH buffers, the PDEAEM portion of the diblock material remains insoluble, as we have reported previously[23]. At the low pH values, however, the materials become charged by protonation of the tertiary amine methacrylate. The increased water solubility of the charged amine and electrostatic repulsion of the protonated pendent groups allow the tablets to dissolve at low pH values.

As a comparison to the diblock materials, two controls, PEG $\overline{M_n}$ =5000 and PEG $\overline{M_n}$ =8000, were used. The PEG$_{5000}$ was used because it is the starting material for the polymerization and the PEG$_{8000}$ was used because it mimics a material of similar molecular weight to the specific diblock material tested without the PDEAEM block. A lack-of-fit test was used the determine that the PEG$_{5000}$ and PEG$_{8000}$ release rates are statistically the same for all pH values and the release rate is the same for both materials. A regression fit data for all pH values and both materials versus regression fits assuming the release rates are different at different pH values yielded a p-value of 0.89 from an F-statistic value of 0.47. On the other hand, a similar test for the diblock material yielded a p-value of < 0.0001 from an F-statistic value of 135.5, indicating that there is a significant difference between the pH values. The regression for the pH-independent PEG release data gave an estimate of 0.91 fraction/hour, a much faster release rate than the pH-sensitive diblock material of a similar molecular weight.

The release of dye from 28% w/w gels of the pentablock materials also displayed pH sensitivity for similar reasons. Once the material sets into a non-crosslinked gel, the release of molecules is dependent on the pH of the buffer (Figure 4). As water penetrates the gel, as described in previous work[14] for Pluronic® systems, protons are carried into the interfacial area of the gel. It has been shown that when crosslinked membranes containing PDEAEM

become protonated, they swell due to electrostatic interactions of the charged cations[5]. The same is true in the non-crosslinked case, however swelling leads to dissolution of the gel and thus release of the entrapped molecules.

At the higher pH values, the gel is relatively insoluble. In lower pH buffers, the gel is soluble with a rate of dye release more than five times the rate at higher pH values. Again the non-ionic base material proved to be pH-insensitive in its release profile, and had a release rate similar to the pentablock copoylmer at low pH values. The release from Pluronic® F127 gels occurred at a rate of 0.57 mg/cm^2/hour for a loading of 30 mg/cm^3. A lack-of-fit test for this data indicated a p-value of 0.54 from an F-statistic value of 0.898.

Cytotoxocity testing - Elution tests were performed on one sample of the pentablock material in order to assess the cytotoxic properties of the block copolymers. The results of the tests were compared to a negative control and a positive control. The negative control (Figure 5a), pure growth media, was taken as the result expected for a non-cytotoxic material. The positive control (Figure 5b), phenol laced media, was taken as the result expected for a cytotoxic material. The pentablock material (Figure 5c), at the same concentration as the phenol positive control, led to results similar to the negative control. The fibroblast cells used in the tests showed good adhesion to the polystyrene cell culture substrate and the cells remained confluent after the 24 hour test period, neither of which is true for the positive control.

Conclusions

Novel pentablock and diblock materials were synthesized that possess a variety of properties applicable to environment-sensitive drug or biomolecule release. The pentablock materials synthesized maintain the properties of thermoreversible gelation as well as thermally induced micellization in aqueous solutions, two properties the macroinitiator possesses that have been studied for their application to injectable drug delivery systems. In addition to these thermodynamic properties, the materials also exhibit pH-dependent release profiles for entrapped molecules by virtue of the added cationic moiety.

The diblock materials show a dramatic increase in the release rate of small molecules when tested in tablet as the pH of the tablet dissolution medium decreases. There is an order of magnitude change in the release rate of nile blue chloride between a pH 6.2 phosphate buffer solution and a pH 8.2 phosphate buffer solution. This increase in release rate over a rather small range of pH values that are only slightly more acidic or alkaline than physiological pH has the potential to be useful for pH-sensitive drug release.

The pentablock materials have a direct biomedical application, as the material mimics the pH-sensitive release behavior of extensively studied crosslinked polycation systems while adding the benefits of device injectability. Initial cytotoxicitiy tests have shown that these materials are not cytotoxic.
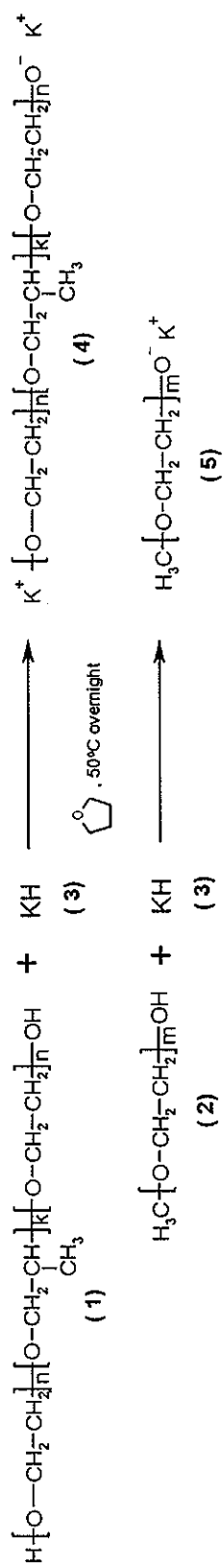
References

1. Lowman, A. M.; Morishita, M.; Kajita, M.; Nagai, T.; Peppas, N. A. *Journal of Pharmaceutical Sciences* **1999**, 88, 933.
2. Brazel, Christopher S.; Peppas, Nicholas A. *Macromolecules* **1995**, 28, 8016.
3. Siegel, R. A; Falamarzian, M.; Firestone, B. A.; Moxley, B. C. *J. Controlled Release* **1988**, 8, 179.
4. Schwarte, L. M.; Podual, K.; Peppas, N. A. *ACS Symposium Series* **1998**, 709, 56.
5. Albin, G.;Horbett, T. A.; Ratner, B. D. *J. Controlled Release* **1985**, 2, 153.
6. Wanka, G.; Hoffmann, H.; Ulbricht, W. *Macromolecules* **1994**, 27, 414594149.
7. Alexandridis, P.; Holzwarth, J. F. *Macromolecules* **1994**, 27, 2414.
8. Wu, G.; Chu, B.; Schneider, D. K. *J. Phys. Chem.* **1995**, 99, 5094.
9. Hurter, P. N.; Scheutjens, J. M. H. M.; Hatton, T. A.. *Macromolecules* **1993**, 26, 5592.
10. Lee, J.-W.; Park, E.-S.; Chi, S.-C. *Yakche Hakhoechi* **1997**, 27, 279.
11. Wanka, G.; Hoffmann, H.; Ulbricht, W. *Colloid Polym. Sci.* **1990**, 268, 101.
12. Chi, S. C.; Jun, H. W. *J. Pharm. Sci.* **1991**, 80, 280.
13. Gilbert, J. C.; Hadgraft, J.; Bye, A.; Brookes, L. G. *Int. J. Pharm.* **1986**, 32, 233.
14. Anderson, B. C.; Pandit, N. K.; Mallapragada, S. K. *Journal of Controlled Release* **2001** 70 157.
15. Johnston, T. P.; Miller, S. C. *J. Parenter. Sci. Technol.* **1989** 43 280.
16. Bhardwaj, R.; Blanchard, J. *Journal of Pharmaceutical Sciences* **1996** 85 915.
17. Horvath, V; Zingg, W.; Sefton, M. V. *ASAIO Trans.* **1990**, 36, 78.
18. Ishikawa, M.; Schmidtke, D. W.; Raskin, P.; Quinn, C. A. Journal of Dabetes and its Complications **1998**, 12, 295.
19. Nagasaki, Y.; Sato, Y.; Kato, M. *Macromol. Rapid Commun.* **1997**, 18, 827.
20. Ni, P.-H.; Pan, Q.-S.; Zha, L.-S.; Wang, C.-C.; Elaissari, A.; Fu, S.-K. *Journal of Polymer Science, Part A: Polymer Chemistry* **2002**, 40, 624.
21. Anderson, B. C.; Cox, S.; Ambardaekar, A. V.; Mallapragada, S. K. *Journal of Pharmaceutical Sciences* **2002**, 91, 180.
22. Anderson, B. C.; Mallapragada, S. K. *Biomaterials*, In Press.
23. Gallet, G.; Carroccio, S.; Rizzarelli, P.; Karlsson, S. *Polymer* **2002**, 43, 1081.
24. de Paz Banez, M. V.; Robinson, K. L.; Vamvakaki, M.; Lascelles, S. F.; Armes, S. P. *Polymer* **2000**, 41, 8501.
26. Tanford, Charles. The Hydrophobic Effect: Formation of Micelles and Biological Membranes, 2nd ed.; Wiley-Interscience: New York, 1980.

Table 1 – Sample polymerizations of F127-initiated pentablock copolymers and PEGME-initiated diblock copolymers. *-Indicates $\overline{M_n}$ values obtained from manufacturer for the macroinitiator polymers.

Sample ID	Initiator	$\overline{M_n}$ (NMR)	PDI(GPC)	DEAEM %
A	F127	19730	1.20	36.2%
B	F127	15670	1.19	19.6%
C	F127	13890	1.19	9.3%
D	F127	13330	1.18	5.4%
E	F127	12840	1.20	1.9%
F	PEGME	8120	1.08	38.4%
G	PEGME	9351	1.06	46.5%
H	F127	12600*	1.23	0%
I	PEGME	5000*	1.10	0%

Table 2 – Thermodynamic properties of polymer gels obtained from pentablock materials. *-samples contained 2.8% NBCl dye and 25.2% polymer. Numbers in parentheses are the sample standard errors for the measurements.

Sample ID	DEAEM %	T_m (^{o}C)	ΔH (J/g)	ΔS (J/gK)
A	36.2%	7.22 (0.23)	4.60 (0.34)	16.4
B	19.6%	6.91 (0.07)	4.21 (0.07)	15.0
C	9.3%	6.78 (0.16)	5.68 (0.65)	20.3
D	5.4%	6.26 (0.08)	5.52 (0.49)	19.8
E	1.9%	6.77 (0.31)	4.93 (0.11)	17.6
H	0%	9.34 (0.55)	5.11 (0.28)	18.1
H*	0%	9.00 (0.16)	5.28 (0.30)	18.7
A*	36.2%	7.83 (0.21)	3.35 (0.39)	11.9

$$H \left[O-CH_2-CH_2 \right]_n \left[O-CH_2-CH_2-CH \right]_k \left[O-CH_2-CH_2 \right]_n OH \quad + \quad KH$$
$$\underset{CH_3}{}$$

(1)   **(3)**

$$H_3C \left[O-CH_2-CH_2 \right]_m OH \quad + \quad KH$$

(2)   **(3)**

50°C overnight

$$K^+ \left[O-CH_2-CH_2 \right]_n \left[O-CH_2-CH_2-CH \right]_k \left[O-CH_2CH_2 \right]_n O^- \quad K^+$$
$$\underset{CH_3}{}$$

(4)

$$H_3C \left[O-CH_2-CH_2 \right]_m O^- \quad K^+$$

(5)

Scheme 1

Scheme 2

$$K^+ \ C^- \!\!-\!\!-\!\!-\!\! R \!\!-\!\!-\!\!-\!\! C^- \ K^+ \quad + \quad H_3C\!-\!OH \quad \longrightarrow \quad H\!-\!C\!\!-\!\!-\!\!-\!\! R\!\!-\!\!-\!\!-\!\! C\!-\!H$$

(7)   **(9)**   **(11)**

$$R2\!\!-\!\!-\!\! C^- \ K^+ \quad + \quad H_3C\!-\!OH \quad \longrightarrow \quad R2\!\!-\!\!-\!\! C\!-\!H$$

(8)   **(9)**   **(12)**

$$K^+ \ C^- \!\!-\!\!-\!\! R \!\!-\!\!-\!\! C \ K^+ \quad + \quad \text{(benzyl bromide)} \quad \longrightarrow \quad \text{(13)}$$

(7)   **(10)**   **(13)**
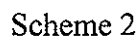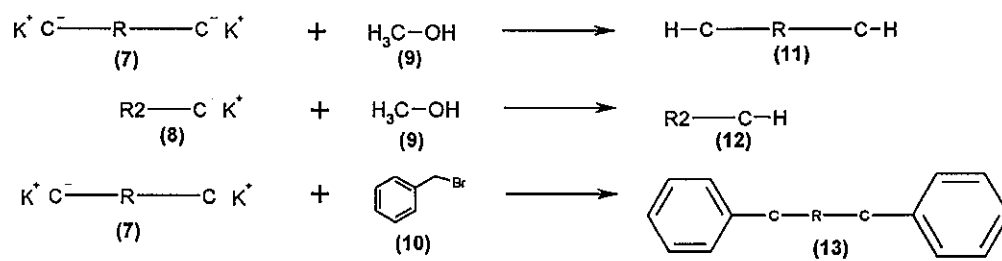
R=PDEAEM-b-PEO-b-PPO-b-PEO-b-PDEAEM living polymer
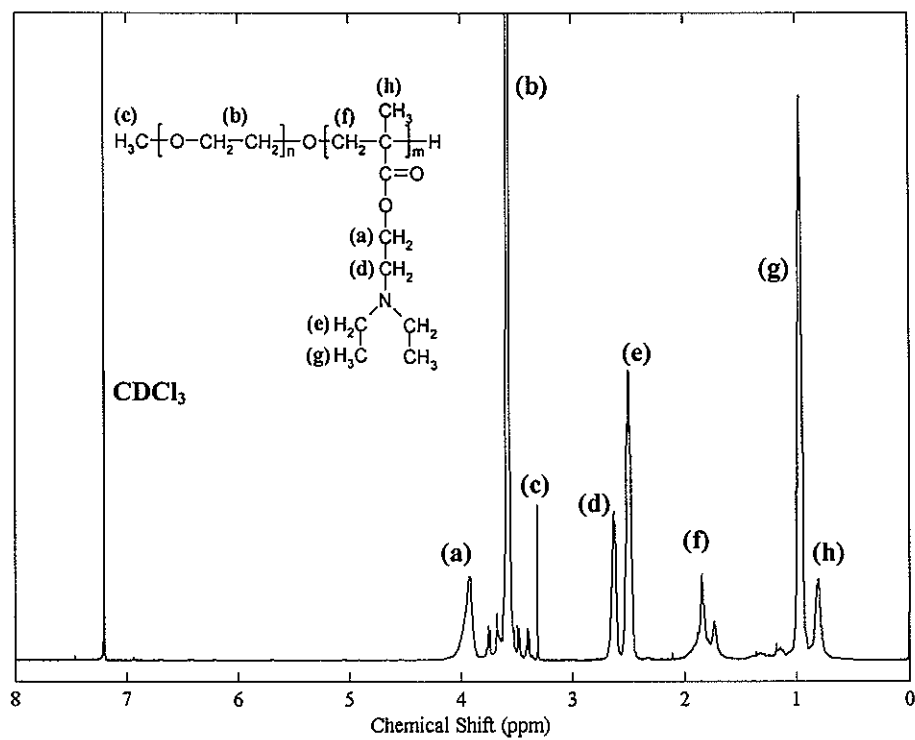R2=PEGME-b-PDEAEM living polymer

Scheme 3

Figure 1. ^{1}H NMR analysis of PEGME-*b*-PDEAEM. Integration of peaks (a), (b), (c), (d) and (e) were used in $\overline{M}_n$ calculations.
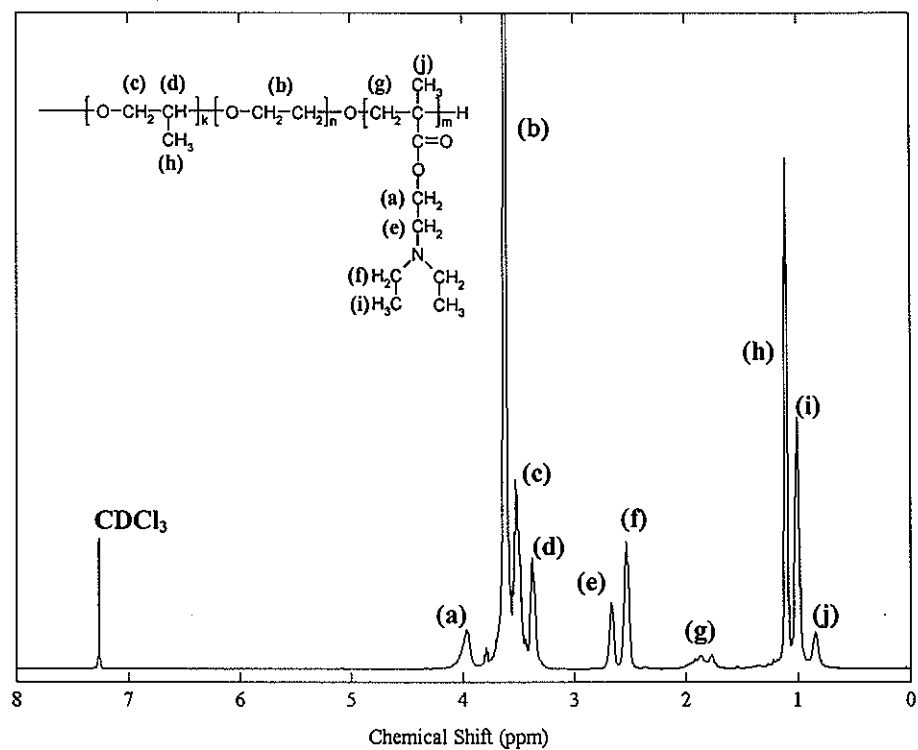
Figure 2. ^{1}H NMR analysis of PDEAEM-*b*-PEO-*b*-PPO-*b*-PEO-*b*-PDEAEM. Integration of peaks (a), (b), (c), (d), (e) and (f) were used in $\overline{M}_n$ calculations.
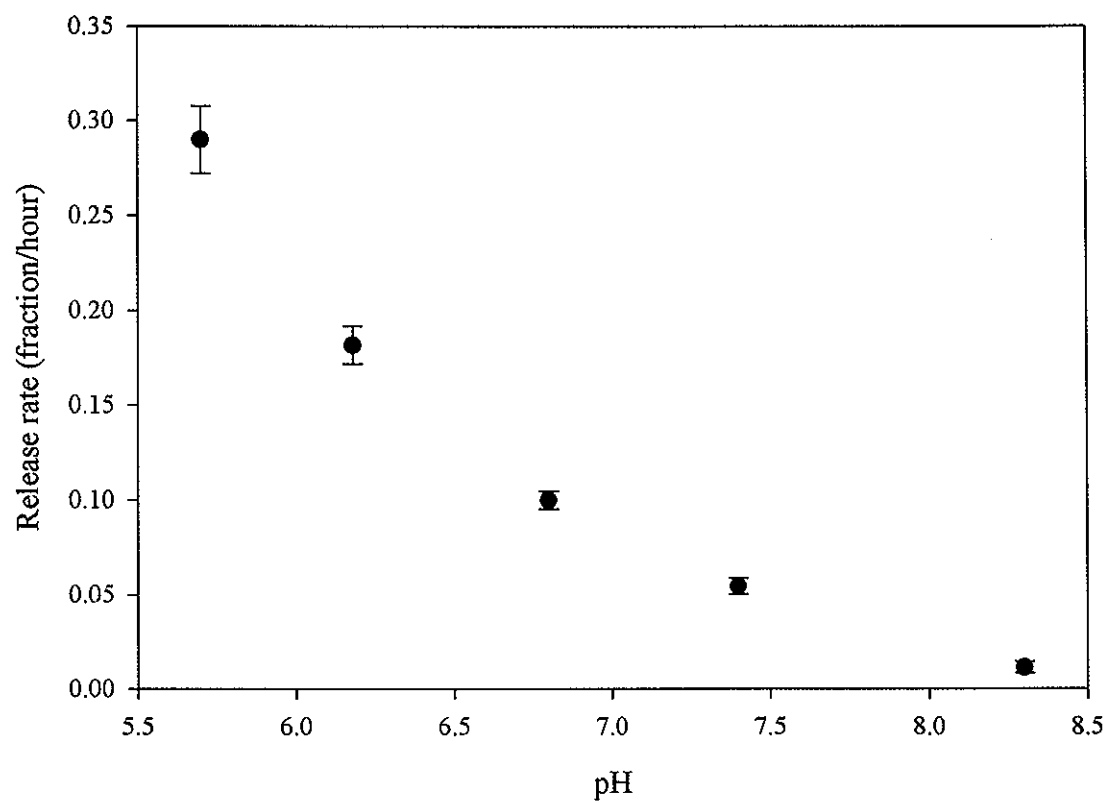
Figure 3. Release of nile blue chloride from PEGME-*b*-PDEAEM diblock copolymer tablets, sample F. Error bars represent standard errors of the parameter estimate of a linear fit to release data. Drug loading is 30mg/cm^3.
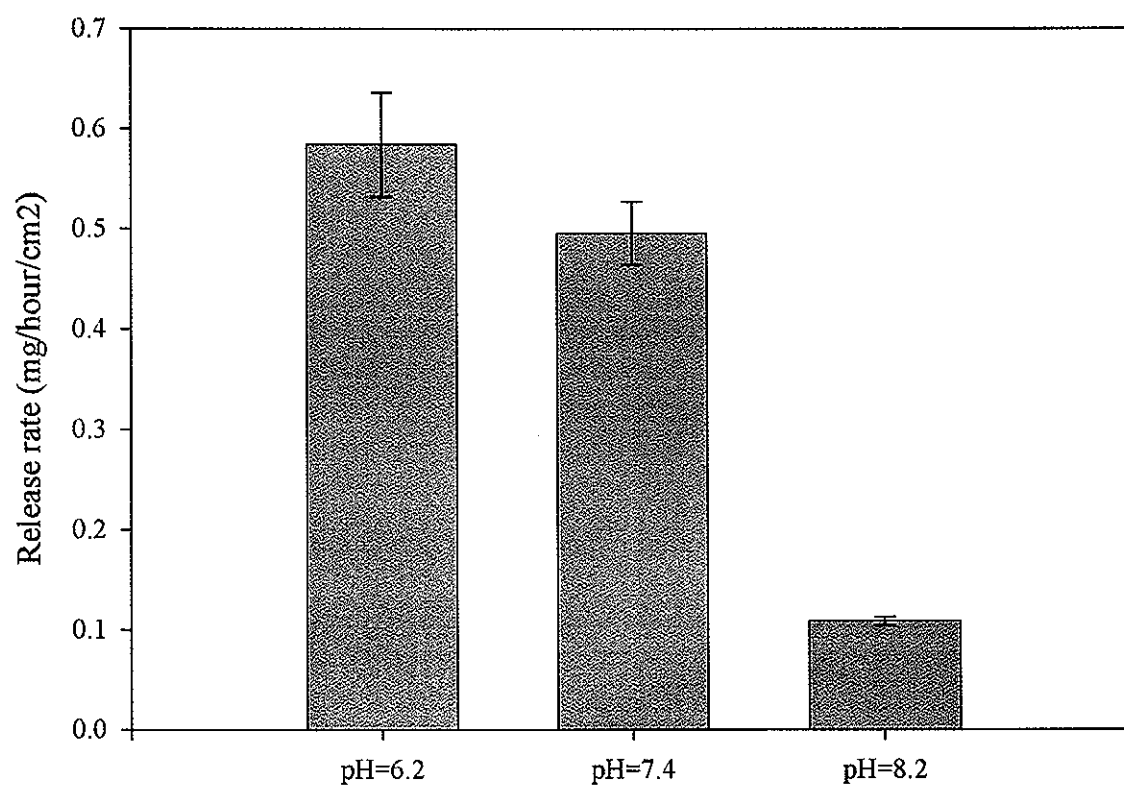
Figure 4. Release of nile blue chloride from PDEAEM-*b*-PEO-*b*-PPO-*b*-PEO-*b*-PDEAEM pentablock copolymer gels, sample A. Error bars represent standard errors of the parameter estimate of a linear fit to release data.
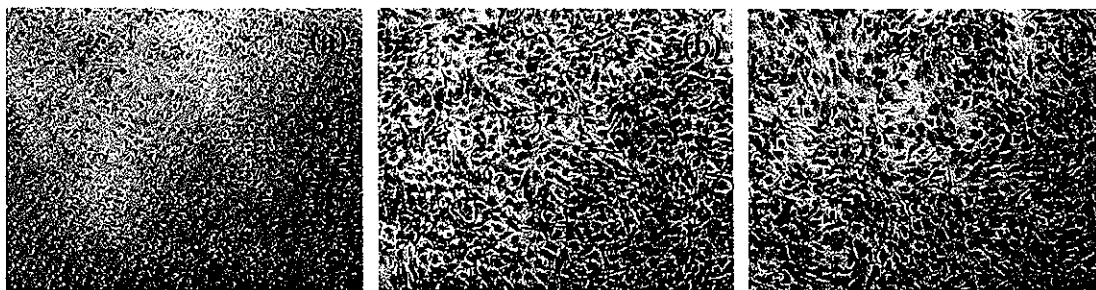
Figure 5. Cytotoxity of (a) positive control, phenol, (b) negative control, growth media, (c) PDEAEM homopolymer, (d) PDEAEM-*b*-PEO-*b*-PPO-*b*-PEO-*b*-PDEAEM, 32% w/w PDEAEM. Polymer and phenol concentrations are all 0.3 mg/L.

CHAPTER 8. Conclusions and Future Recommendations

The breadth of this project has allowed for the exploration of areas, that although only tangentially related in and of themselves, tie the various areas of biomedical engineering, chemical engineering, material science, and polymer chemistry together in such a way that the previous six chapters give a path – from start to finish – of how new ideas are created in the area of polymeric biomaterials. From the exploration of current materials, to the development of test protocols, to the design and synthesis of novel materials, the route that has been taken, at least in retrospect, is made clear.

By beginning with the investigation of current materials, Pluronic® copolymers, we were able to develop a fundamental understanding of how some of the current drug delivery technology works. Models that had not previously been investigated were developed that deconvoluted the effects of diffusion and dissolution in the release of drugs from a potential drug carrier material. The model developed allowed the determination of the magnitude of these two effects, which had not been previously reported. In addition, experimental setups were designed that explore a method for accurately testing the release of entrapped molecules from a class of materials for which very few standard protocols exist. The combination of material dissolution, lack of rigidity and adhesive properties make these materials very difficult to analyze, however the suggestions made in chapter 2 offer experimental researchers an alternative to more inaccurate methods that have been used by many researchers.

In addition to the knowledge gained from the research in chapter 2, the research presented in chapter 3 provided even more insight into both the behavior of a class of

biomaterials and also assisted in understanding the toolbox of analysis techniques at our

disposal for characterizing materials that we would one day synthesize. The research

presented in chapter 3 investigated the effect ionic salts have on the release of entrapped

molecules from Pluronic® gels, specifically on the diffusion coefficient and critical

micellization temperatures. An empirical model was developed that correlates the polymer

and salt concentration of gel formulations to the critical micellization temperature. A

comprehensive model for these predictions, especially for the high polymer concentrations

dealt with in drug delivery, had not previously been reported. In addition to this model, it

was also proven why our group and others had observed no effect on the release rate of

molecules from gels with salts in the gel formulations. The rapid diffusion of salts from the

gels had masked the effect the salts should have on the release rate. We developed a test to

measure the effect of salts on the release rate when the rapid diffusion of salts from the gel at

the interface is arrested. Once this exchange is eliminated, the effect of these ionic species is

very much as would be expected with the addition of salts slowing the release rate of

molecules.

Once there was a sufficient knowledge base regarding Pluronics®, it was time to

begin the synthesis of new materials based on these current materials that would exhibit pH-

sensitivity while retaining the property of thermoreversible gelation. We began investigating

the synthesis of N,N'-diethylaminoethyl methacrylate, DEAEM, with potassium alcoholate

initiators. The specific initiators that was of interest for us were poly(ethylene glycol), or

PEG, based polymers. In addition to the hydroxylated ends, which make them prime

candidates for alcoxide formation, PEG is known to be biocompatible and in many cases

reduces the cytotoxicity of peptides and polymers simply by its addition to these molecules.

The diblock materials of PDEAEM and PEG were terminated with carbon dioxide to form a carboxylic acid endcap, providing the ability to attach this diblock material to biomolecules through amide coupling. The results of this research are presented in chapter 4.

As mentioned above, the PEG additions to the diblock materials were expected to reduce the cytotoxicity of the PDEAEM materials. It was known that PDEAEM itself is rather cytotoxic and has limited use as a biomaterial. However, test procedures needed to be developed to evaluate these novel materials. In conjunction with a group in the chemistry department at Iowa State University, we began a project where we needed to look at materials from a cytotoxic standpoint. The chemistry group had developed a method for making wear resistant polymer composites from a variety of thermoplastics and thermosets. Our research had led us to a bioapplication where high wear and biocompatibility are both very important, acetabular cup prosthetics for total hip replacement operations. Cytotoxicity evaluation tests were developed and materials tested by our collaborators for wear resistance were assayed. In a short time, a composite material had been developed and tested using a variety of biological, mechanical, and microscopic tests. This material, or at least this class of materials, may prove to be an improvement on the current technology used in these types of operations. The results from this project are presented as chapter 5 of this text.

While we were developing the cytotoxicity testing procedures, we were continuing with the synthesis of new polymeric materials. Chapter 6 contains a paper focusing on the development of several materials based on the monomer DEAEM and poly(ethylene glycol) containing monomers. Random copolymers were synthesized with a variety of compositions that contain the monomers DEAEM and poly(ethylene glycol) methyl ether methacrylate, PEGMEM. These copolymers have two distinct properties that make them possible

biomaterials. First, the PDEAEM/PPEGMEM copolymers are water soluble over a wide range of pH conditions, whereas the homopolymer of PDEAEM is not. Water solubility is a key issue in many bioapplications, especially for lower molecular weight polymers. Second, the copolymers are biocompatable, whereas the homopolymer is not. Using similar testing procedures to those presented in chapter 5, we tested the cytotoxicity relative to appropriate controls and the homopolymer PDEAEM. The potential application for this novel material is non-viral gene therapy. Studies which are currently underway are elaborating on the specific application of using these materials as carriers for genetic code transcribed in plasmid-DNA for anti-cancer gene therapy. The material has been shown to complex with pDNA and due to its water solubility and non-cytotoxic nature has the potential for being an ideal gene therapy agent.

Chapter 7 presents the last piece of research included in this dissertation. This is the work that embodies the end goal of the research as a whole, the development of a material that contains a set of desired properties, namely pH-sensitivity and thermodynamic sol-gel and micellization phase transition properties. This material is the first of its kind to incorporate these two extremely useful properties. We synthesized the material using the techniques illustrated in chapters 4 and 6, tested the cytotoxocity using the procedures described in chapters 5 and 6, and measured physical properties and drug release characteristics using tests developed in chapters 2 and 3.

Although the text will end with chapter 8, the advancement of this research will not. Now that the above mentioned techniques and analyses have been developed, there are many complementary and continuing studies that will be performed that will advance many areas of the research summarized here. The random copolymers that are being studied for non-

viral gene therapy will be improved in order to customize their size and nitrogen content to fit specific applications. Receptors may be added to the pendent groups for self-sensing, cell-specific transfection for targeted gene therapy. There are several other classes of block copolymers that can be synthesized using techniques similar to or at least building on those presented in chapters 5 and 7, several of which we are currently investigating. It is hoped that these materials will have some of the properties of the materials in chapter 7, with more dramatic pH-dependence. The pentablock materials presented in chapter 7 are being characterized using more sensitive characterization tools, for example dynamic temperature multi-angle laser light scattering and cryogenic transmission electron microscopy. It is hoped that these tools will give a clearer picture of the nanoscale aggregation behavior of these novel materials. It is exciting to see that this research, as with any good research, will not end with these words but instead will act as the beginning of more and equally exciting research.

Acknowledgements

There are several people that I would like to thank for their assistance and support. First of all I would like to thank Dr. Surya Mallapragada, my supervising professor, who has been an excellent mentor both intentionally and by example. I have learned much from her and am very grateful for this.

Second, I would like to thank my committee members Dr. Valerie Sheares, Dr. Nita Pandit, Dr. R. Dennis Vigil, Dr. Balaji Narasimhan, and Dr. Max Morris. They have all been a great help to me and I thank them for kindly offering their time and in some cases even lab space to help me in my research.

I would like to thank my research group; Anil, Aurelia, Brandon, Cheryl, Jennifer, Mike and Sim-Siong for all the productive and fun cooperation both in and out of the lab. I would also like to express my appreciation to Dr. Sheares graduate students for allowing me to learn from them in their lab this year. I have had the opportunity to work with many undergraduates who have made research more interesting if not more productive. I will not mention them all individually, however I would like to thank two students that are currently working with me; Suzan Cox and Dan Kuster – they are not only exceptional students, but also good friends and will do great things in their lives. I have enjoyed both sharing my knowledge with them and learning many things from them in return.

I would like to thank my family for their support - especially over the last eight years. Of course without the 18 years of support and guidance before that I could not have developed the skills to learn on my own and be a responsible student, so for that I am also grateful.

There are a few individuals that also need to me mentioned. First I want to thank Paul Bloom, who was a wonderful collaborator on chapters 4, 5 and 7. I appreciate all the time he spent teaching a chemical engineer how to be a chemist. I also want to thank Jesse Pikturna for all his help in keeping me motivated and interested in chemical engineering – even though I am still just mixing plastic and salt together.

Finally, I want to thank my wife Yanhui Hu for both her intellectual support and moral support that she has offered so generously. Without that I could not have achieved so much in the last few years – and I certainly would not have enjoyed my time at Iowa State University as much without her in my life.